

Eight new *Arthrinium* species from China

Mei Wang^{1,2,*}, Xiao-Ming Tan^{3,*}, Fang Liu¹, Lei Cai^{1,2}

1 State Key Laboratory of Mycology, Institute of Microbiology, Chinese Academy of Sciences, Beijing 100101, PR China **2** University of Chinese Academy of Sciences, Beijing 100049, PR China **3** College of Navel Orange, Gannan Normal University, Ganzhou, Jiangxi, 341000, PR China

Corresponding author: Lei Cai (cail@im.ac.cn)

Academic editor: P. Cannon | Received 4 February 2018 | Accepted 7 April 2018 | Published 3 May 2018

Citation: Wang M, Tan X-M, Liu F, Cai L (2018) Eight new *Arthrinium* species from China. MycoKeys 34: 1–24. <https://doi.org/10.3897/mycokeys.34.24221>

Abstract

The genus *Arthrinium* includes important plant pathogens, endophytes and saprobes with a wide host range and geographic distribution. In this paper, 74 *Arthrinium* strains isolated from various substrates such as bamboo leaves, tea plants, soil and air from karst caves in China were examined using a multi-locus phylogeny based on a combined dataset of ITS rDNA, TEF1 and TUB2, in conjunction with morphological characters, host association and ecological distribution. Eight new species were described based on their distinct phylogenetic relationships and morphological characters. Our results indicated a high species diversity of *Arthrinium* with wide host ranges, amongst which, Poaceae and Cyperaceae were the major host plant families of *Arthrinium* species.

Keywords

Ascomycota, Morphology, Phylogeny, Systematics, Taxonomy

Introduction

Arthrinium Kunze is an anamorph-typified genus, which has been traditionally linked to the teleomorph-typified genus *Apiospora* Sacc. (Ellis 1971, Seifert et al. 2011). It is strikingly different from other anamorphic genera for the presence of basauxic conidiophores (Hughes 1953, Minter 1985). The traditional generic circumscription of *Arthrinium* was primarily based on morphological characters (e.g. conidial shape, conidiophores, sterile cells and the presence of setae) but has been regarded as too narrow (Ellis 1971,

* These authors contributed equally to this article.

Minter 1985, Crous et al. 2013). It is now recognised that, at the generic level, conidial shape and the presence of setae are not reliable characters to infer phylogenetic relationships (Crous et al. 2013). For example, *Arthrinium* was regarded as being different from *Cordella* Speg. (1886) by the absence of setae amongst the clusters of specialised hyphae and different from *Pteroniconium* Sacc. (1892) by the absence of sporodochia and pseudoparenchyma (Minter 1985). However, both genera have been reduced to the generic synonyms of *Arthrinium*, based on molecular phylogenetic data (Crous et al. 2013).

Arthrinium species are geographically widely distributed in various hosts. Many species of *Arthrinium* are associated with plants as endophytes or saprobes, as well as plant pathogens on some important ornamentals, e.g. *A. phaeospermum* causing culm rot on *Phyllostachys viridis* (Li et al. 2016); *A. arundinis* causing brown culm streak of *Phyllostachys praecox* (Chen et al. 2014). Moreover, *A. phaeospermum* has been reported for causing cutaneous infections of humans (Rai 1989, Zhao et al. 1990, de Hoog et al. 2000, Crous et al. 2013). Many *Arthrinium* species are also known to produce bioactive compounds with pharmacological and medicinal applications, such as *A. arundinis* and *A. saccharicola* isolated from a brown alga *Sargassum* sp., with good antifungal activities against some plant pathogenic fungi (Hong et al. 2015). *Arthrinium saccharicola*, *A. sacchari* and *A. phaeospermum* isolated from *Miscanthus* sp. are known to produce industrially important enzymes (Shrestha et al. 2015).

In this paper, eight new *Arthrinium* species are described and characterised based on morphological characters and phylogeny inferred from the combined ITS rDNA, TEF1 and TUB2 sequences dataset. Comparisons were made with morphologically similar and phylogenetically related species. Fungus-host distribution of *Arthrinium* species are summarised based on data from literature and this study.

Materials and method

Isolates

Diseased and healthy tissues of bamboo leaves and other plant hosts were collected from six provinces or municipalities in China (Chongqing, Guangxi, Guangdong, Guizhou, Jiangxi, Hunan). Tissue pieces (5 mm × 5 mm) were taken from the margin of leaf lesions and the surface sterilised with 75% ethanol for 1 min, 5% NaClO for 30 s, followed by rinsing in sterile distilled water for 1 min. The pieces were dried with sterilised paper towels and then placed on 1/4 PDA (potato dextrose agar) (Cai et al. 2009).

All cultures were preserved in the LC culture collection (personal culture collection of Lei Cai housed in the Institute of Microbiology, Chinese Academy of Sciences). Type specimens were deposited in Mycological Herbarium of the Institute of Microbiology, Chinese Academy of Sciences, Beijing, China (HMAS), with ex-type living cultures deposited in China General Microbiological Culture Collection Center (CG-MCC). Taxonomic information of the new taxa was deposited in MycoBank (www.MycoBank.org; Crous et al. 2004).

Morphology

Cultures were incubated on PDA for 7 d at 25 °C to measure the growth rates and on 2% malt agar with bamboo leaves to enhance sporulation. Morphological descriptions were based on cultures sporulating on MEA (malt extract agar) medium at room temperature (ca. 25 °C). Shape and size of microscopic structures were observed using a light microscope and colonies were assessed according to the colour charts of Rayner (1970). At least 50 conidiogenous cells and conidia were measured to calculate the mean size.

DNA extraction, PCR amplification and sequencing

Fresh fungal mycelia were taken from 7-d-old cultures growing on PDA and ground with the organisation disruptor FastPrep-48. Genomic DNA was extracted following the modified CTAB protocol as described in Guo et al. (2000).

Phylogenetic analyses were conducted using partial sequences of three loci, 5.8S nuclear ribosomal gene with the two flanking transcribed spacers (ITS), part of the translation elongation factor 1-alpha (TEF1) and beta-tubulin (TUB2). The ITS locus was amplified using the primer pair ITS1/ITS4 (Vilgalys and Hester 1990, White et al. 1990); TEF1 using EF1-728F/ EF-2 (O'Donnell et al. 1998, Carbone and Kohn 1999); and TUB2 using T1 (O'Donnell and Cigelnik 1997) and Bt-2b (Glass and Donaldson 1995).

PCR was performed in a 25 ml reaction containing 18.95 µl double distilled water, 2.5 µl 10 × PCR buffer, 0.3 µl dNTP mix (2.5 mM), 1 µl of each primer (10 mM), 1 µl DNA template and 0.25 µl Taq DNA polymerase (Genstar). The annealing temperatures were adjusted to 52 °C for ITS and TUB2, and 56 °C for TEF1. Purification and sequencing of the PCR amplicons were done by SinoGenoMax, Beijing.

Phylogenetic analysis

Sequences generated from the forward and reverse primers were used to obtain consensus sequences using MEGA v. 6.0 (Tamura et al. 2013). The concatenated tree was inferred based ITS, TUB2 and TEF1 sequences (Figure 1) using Bayesian and Maximum-likelihood analyses. Sequences were aligned using an online version of MAFFT v. 7 (available at <http://mafft.cbrc.jp/alignment/server/>). Ambiguous regions were excluded from the analyses and gaps were treated as missing data. Maximum-likelihood (ML) analysis was performed in RAxML v. 7.2.6 (Stamatakis and Alachiotis 2010), employing GTR models of evolution settings of the programme and bootstrap support obtained by running 1000 pseudo replicates. Maximum Likelihood bootstrap values (ML) equal to or greater than 70% are given above each node.

Bayesian analysis was conducted using MrBayes v. 3.2.1 (Ronquist et al. 2012) and the best nucleotide substitution model for each locus was calculated with jModelTest v. 2.1.4 (Posada 2008). Posterior probabilities (PP) (Zhaxybayeva and Gogarten 2002) were de-

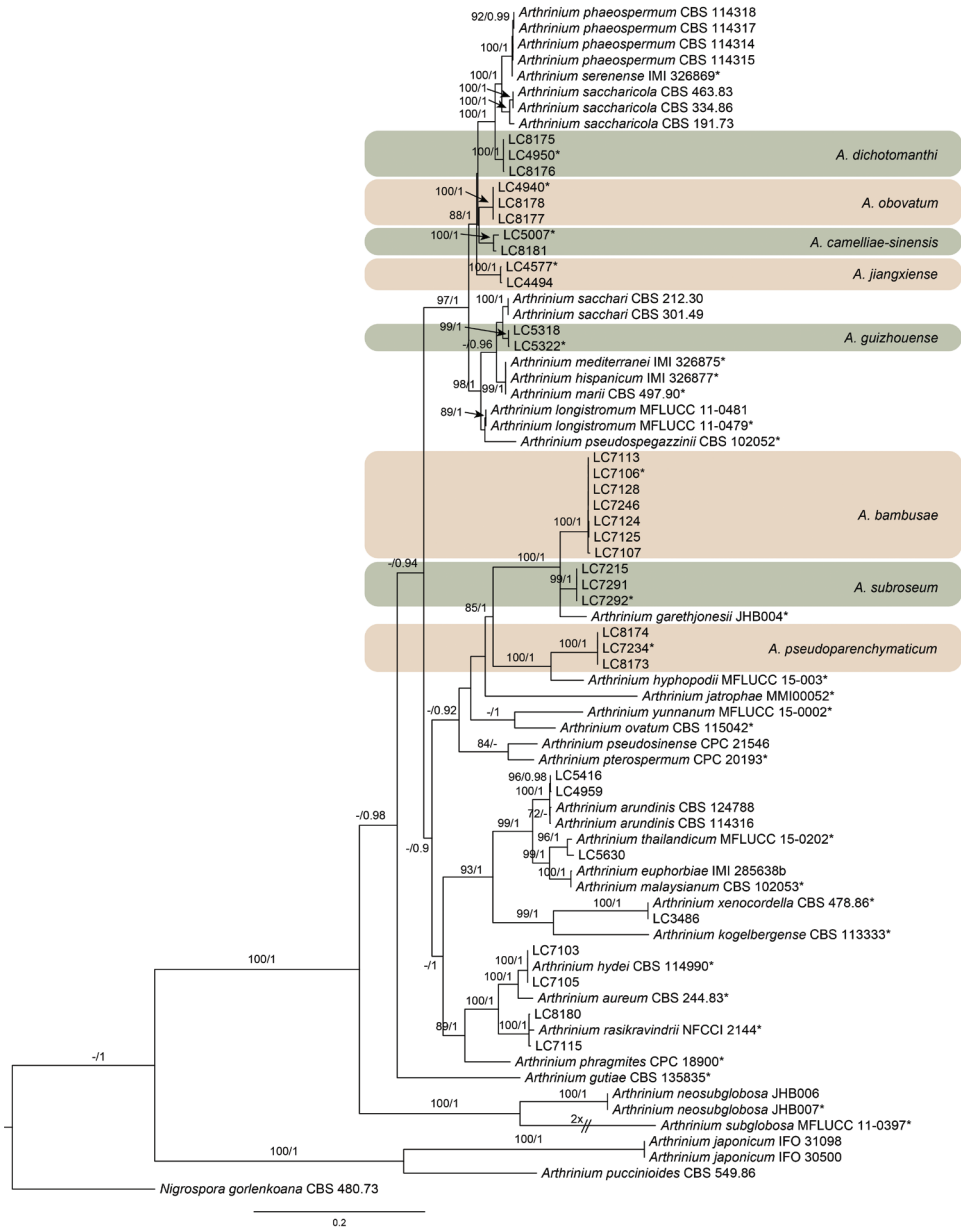


Figure 1. Phylogenetic tree based on the combined ITS, TEF1 and TUB2 sequences alignment generated from a Maximum likelihood phylogenetic analysis. Bootstrap support values (>70%) and posterior probabilities (>0.9) are given at the nodes (ML/PP). The tree is rooted with *Nigrospora gorklenkoana* CBS 480.73. The novel species were highlighted (* indicates the ex-type cultures).

terminated by Markov Chain Monte Carlo sampling (MCMC) under the estimated model of evolution. Four simultaneous Markov chains were run for 10 million generations and trees were sampled every 1000 generations. The run was stopped automatically when the

average standard deviation of split frequencies fell below 0.01. The first 25% trees, which represented the burn-in phase of the analyses, were discarded and the remaining trees were used for calculating PP in the majority rule consensus tree. Sequences generated in this study were deposited in GenBank (Table 1) and the final matrices used for the phylogenetic analyses in TreeBASE (www.treebase.org; accession number: 21341).

Fungus-host distribution of *Arthrinium* species

To determine the distribution of *Arthrinium* species on host/substrate, the number of species occurred on each host (based on family level) was counted based on data from this study, relevant literature and the USDA fungal database (<https://nt.ars-grin.gov/fungalatabases/>). The proportion account for the known 66 species in *Arthrinium* (Index Fungorum) was illustrated in a histogram. Four species with an unknown host range were not included in this analysis.

Results

Phylogeny

The combined ITS, TUB2 and TEF1 dataset contained 75 strains, with *Nigrospora gorlenkoana* CBS 480.73 as the out group. For the Bayesian analyses, the best-fit models TrN+I+G, GTR+I+G, HKY+I+G were selected for ITS, TUB2 and TEF1 loci, respectively. The ML analysis showed the same tree topology as that obtained in the Bayesian analysis. All the *Arthrinium* strains in this study separated into 13 clades, representing five known (*A. arundinis*, *A. hydei*, *A. rasikravindrii*, *A. thailandicum*, *A. xenocordella*) and eight new species (Figure 1). The eight new species clustered in distinct clades with high bootstrap supports (Figure 1). Phylogenetic analyses based on an individual locus were also conducted (not shown) and the generated trees are similar to the one generated from the combined multi-locus dataset (Figure 1).

Host associated with *Arthrinium* species

The histogram in Figure 2 shows that *Arthrinium* species were widely distributed amongst 17 plant families, including Brassicaceae, Bromeliaceae, Cornaceae, Cyperaceae, Euphorbiaceae, Fagaceae, Juncaceae, Lauraceae, Myrsinaceae, Oleaceae, Pinaceae, Poaceae, Restionaceae, Rosaceae, Tiliaceae, Urticaceae and Vitaceae. *Arthrinium* species were also isolated from air, dust, soil and sand. The proportion of species occurring on each host family was assessed (Figure 2). Poaceae and Cyperaceae were the major host families for *Arthrinium*, which accounted for 42.42% and 24.24% of species in *Arthrinium* respectively.

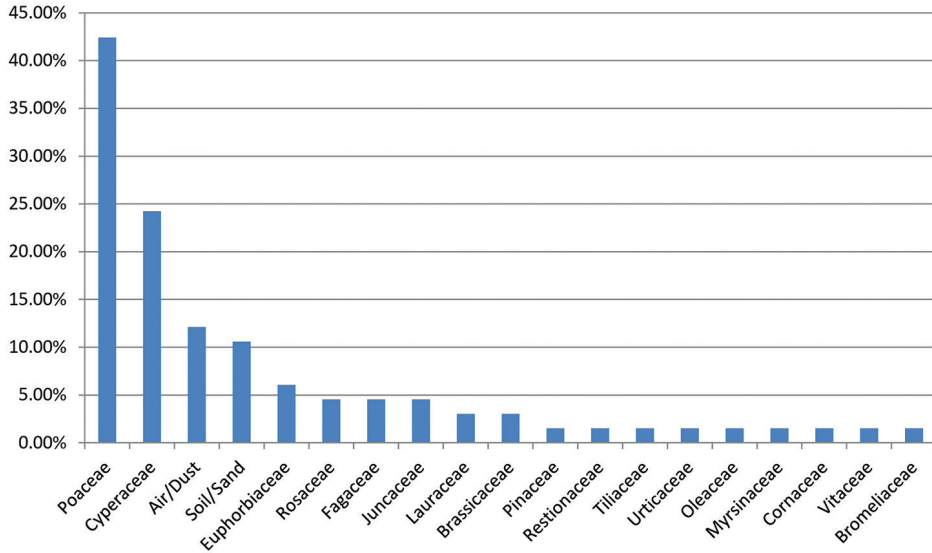


Figure 2. A Histogram to show fungus-host distribution of *Arthrimum* species.

Table 1. Strains included in the phylogenetic analyses.

Species	Strain numbers ¹	Hosts	Countries	GenBank accessions		
				ITS	TUB	TEF
<i>Arthrimum arundinis</i>	CBS 114316	Leaf of <i>Hordeum vulgare</i>	Iran	KF144884	KF144974	KF145016
	CBS 124788	Living leaves of <i>Fagus sylvatica</i>	Switzerland	KF144885	KF144975	KF145017
	LC4477	Unknow host	China	KY494688	KY705159	KY705087
	LC4493	<i>Phyllostachys</i> sp.	China	KY494689	KY806202	KY705088
	LC4650	<i>Osmanthus</i> sp.	China	KY494695	KY705165	KY705094
	LC4951	<i>Dichotomanthus tristaniaecarpa</i>	China	KY494698	KY705168	KY705097
	LC4959	<i>Bothrocaryum controversum</i>	China	KY494699	KY705169	KY705098
	LC5311	Air in karst cave	China	KY494706	KY705175	KY705105
	LC5312	Air in karst cave	China	KY494707	KY705176	KY705106
	LC5332	Air in karst cave	China	KY494710	KY705179	KY705109
	LC5394	Soil in karst cave	China	KY494711	KY705180	KY705110
	LC5416	Water in karst cave	China	KY494712	KY705181	KY705111
	LC7118	Leaf of bamboo	China	KY494723	KY705191	KY705120
	LC7122	Leaf of bamboo	China	KY494726	KY705194	KY705123
	LC7160	Leaf of bamboo	China	KY494738	KY705206	KY705134
	LC7211	Leaf of bamboo	China	KY494739	KY705207	KY705135
	LC7216	Leaf of bamboo	China	KY494741	KY705209	KY705137
	LC7218	Leaf of bamboo	China	KY494742	KY705210	KY705138
	LC7243	Leaf of bamboo	China	KY494744	KY705212	KY705140
	LC7252	Leaf of bamboo	China	KY494747	KY705215	KY705143
LC7277	Leaf of bamboo	China	KY494750	KY705218	KY705146	

Speices	Strain numbers ¹	Hosts	Countries	GenBank accessions		
				ITS	TUB	TEF
<i>A. aureum</i>	CBS 244.83*	Air	Spain	AB220251	KF144981	KF145023
<i>A. bambusae</i>	LC7106* = CGMCC 3.18335	Leaf of bamboo	China	KY494718	KY705186	KY806204
	LC7107	Leaf of bamboo	China	KY494719	KY705187	KY705117
	LC7113	Leaf of bamboo	China	KY494720	KY705188	KY806205
	LC7124	Leaf of bamboo	China	KY494727	KY705195	KY806206
	LC7125	Leaf of bamboo	China	KY494728	KY705196	KY705124
	LC7128	Leaf of bamboo	China	KY494730	KY705198	KY705126
<i>A. camelliae-sinensis</i>	LC5007* = CGMCC 3.18333	<i>Camellia sinensis</i>	China	KY494704	KY705173	KY705103
	LC8181	<i>Brassica capestris</i>	China	KY494761	KY705229	KY705157
<i>A. dichotomanthi</i>	LC4950* = CGMCC 3.18332	<i>Dichotomanthus tristaniaecarpa</i>	China	KY494697	KY705167	KY705096
	LC8175	<i>Dichotomanthus tristaniaecarpa</i>	China	KY494755	KY705223	KY705151
	LC8176	<i>Dichotomanthus tristaniaecarpa</i>	China	KY494756	KY705224	KY705152
<i>A. euphorbiae</i>	IMI 285638b	<i>Bambusa</i> sp.	Bangladesh	AB220241	AB220288	–
<i>A. guizhouense</i>	LC5318	Air in karst cave	China	KY494708	KY705177	KY705107
	LC5322* =CGMCC3.18334	Air in karst cave	China	KY494709	KY705178	KY705108
<i>A. gutiae</i>	CBS 135835	Gut of a grasshopper	India	KR011352	KR011350	KR011351
<i>A. hispanicum</i>	IMI 326877*	Maritime sand	Spain	AB220242	AB220289	–
<i>A. hydei</i>	CBS 114990*	Culms of <i>Bambusa tuldoides</i>	Hong Kong	KF144890	KF144982	KF145024
	LC7103	Leaf of bamboo	China	KY494715	KY705183	KY705114
	LC7105	Leaf of bamboo	China	KY494717	KY705185	KY705116
<i>A. hyphopodii</i>	MFLUCC 15-0003*	Culms of <i>Bambusa tuldoides</i>	Thailand	KR069110	–	–
<i>A. japonicum</i>	IFO 30500	<i>Carex despalata</i> (dead leaf)	Japan	AB220262	AB220309	–
	IFO 31098	<i>Carex despalata</i> (leaf)	Japan	AB220264	AB220311	–
<i>A. Garethjonesii</i>	KUMCC 16-0202	Dead culms of bamboo	China	KY356086	–	–
<i>A. jatrophae</i>	MMI 00052* = MCC 1014	Healthy petiole of <i>Jatropha podagrica</i>	India	JQ246355	–	–
	LC2831	Leaf of bamboo	China	KY494686	KY806201	KY705085
<i>A. jiangxiense</i>	LC4494	<i>Phyllostachys</i> sp.	China	KY494690	KY705160	KY705089
	LC4541	<i>Maesa</i> sp.	China	KY494691	KY705161	KY705090
	LC4547	<i>Machilus</i> sp.	China	KY494692	KY705162	KY705091
	LC4577* = CGMCC 3.18381	<i>Maesa</i> sp.	China	KY494693	KY705163	KY705092
	LC4578	<i>Camellia sinensis</i>	China	KY494694	KY705164	KY705093
	LC4993	<i>Phyllostachys</i> sp.	China	KY494700	KY806203	KY705099
	LC4997	<i>Phyllostachys</i> sp.	China	KY494701	KY705170	KY705100
	LC5001	<i>Phyllostachys</i> sp.	China	KY494702	KY705171	KY705101
	LC5004	<i>Phyllostachys</i> sp.	China	KY494703	KY705172	KY705102
	LC5015	<i>Imperata cylindrica</i>	China	KY494705	KY705174	KY705104

Species	Strain numbers ¹	Hosts	Countries	GenBank accessions		
				ITS	TUB	TEF
<i>A. jiangxiense</i>	LC7104	Leaf of bamboo	China	KY494716	KY705184	KY705115
	LC7154	Leaf of bamboo	China	KY494736	KY705204	KY705132
	LC7156	Leaf of bamboo	China	KY494737	KY705205	KY705133
	LC7275	Leaf of bamboo	China	KY494749	KY705217	KY705145
<i>A. kogelbergense</i>	CBS 113333*	Dead culms of Restionaceae	South Africa	KF144892	KF144984	KF145026
<i>A. longistromum</i>	MFLUCC 11-0481*	Decaying bamboo culms	Thailand	KU940141	–	–
	MFLUCC 11-0479	Decaying bamboo culms	Thailand	KU940142	–	–
<i>A. malaysianum</i>	CBS 102053*	<i>Macaranga bulletii</i> stem colonised by ants	Malaysia	KF144896	KF144988	KF145030
<i>A. marii</i>	CBS 497.90*	Air	Spain	AB220252	KF144993	KF145035
<i>A. mediterranei</i>	IMI 326875*	Air	Spain	AB220243	AB220290	–
<i>A. mytilomorphum</i>	DAOM 214595*	Dead blades of <i>Andropogon</i> sp.	India	KY494685	–	–
<i>A. neosubglobosa</i>	JHB006	Dead culms of bamboo	China	KY356089	–	–
	KUMCC 16-0203	Dead culms of bamboo	China	KY356090	–	–
<i>A. obovatum</i>	LC4940* = CGMCC 3.18331	<i>Lithocarpus</i> sp.	China	KY494696	KY705166	KY705095
	LC8177	<i>Lithocarpus</i> sp.	China	KY494757	KY705225	KY705153
	LC8178	<i>Lithocarpus</i> sp.	China	KY494758	KY705226	KY705154
<i>A. ovatum</i>	CBS 115042*	<i>Arundinaria hindsii</i>	Hong Kong	KF144903	KF144995	KF145037
<i>A. paraphaeospermum</i>	MFLU 16-1974	Dead clumps of <i>Bambusa</i> sp.	Thailand	KX822128	–	–
<i>A. phaeospermum</i>	CBS 114314	Leaf of <i>Hordeum vulgare</i>	Iran	KF144904	KF144996	KF145038
	CBS 114315	Leaf of <i>Hordeum vulgare</i>	Iran	KF144905	KF144997	KF145039
	CBS 114317	Leaf of <i>Hordeum vulgare</i>	Iran	KF144906	KF144998	KF145040
	CBS 114318	Leaf of <i>Hordeum vulgare</i>	Iran	KF144907	KF144999	KF145041
<i>A. phragmites</i>	CPC18900*	Culms of <i>Phragmites australis</i>	Italy	KF144909	KF145001	KF145043
<i>A. pseudoparenchymaticum</i>	LC7234* = CGMCC 3.18336	Leaf of bamboo	China	KY494743	KY705211	KY705139
	LC8173	Leaf of bamboo	China	KY494753	KY705221	KY705149
	LC8174	Leaf of bamboo	China	KY494754	KY705222	KY705150
<i>A. pseudosinense</i>	CPC 21546*	Leaf of bamboo	The Netherlands	KF144910	–	KF145044
<i>A. pseudospegazzinii</i>	CBS 102052*	<i>Macaranga bulletii</i> stem colonised by ants	Malaysia	KF144911	KF145002	KF145045
<i>A. pterospermum</i>	CPC 20193*	Leaf lesion of <i>Machaerina sinclairii</i>	Australia	KF144913	KF145004	KF145046

Species	Strain numbers ¹	Hosts	Countries	GenBank accessions		
				ITS	TUB	TEF
<i>A. puccinioides</i>	CBS 549.86	Leaf of <i>Lepidosperma gladiatum</i>	Germany	AB220253	AB220300	–
<i>A. nasikravindrii</i>	CBS 337.61	<i>Cissus</i> sp.	The Netherlands	KF144914	–	–
	CPC 21602	Rice	Thailand	KF144915	–	–
	MFLUCC 15-0203	Dead bamboo culms	Thailand	KU940143	–	–
	MFLUCC 11-0616	Dead bamboo culms	Thailand	KU940144	–	–
	NFCCI 2144*	Soil	Svalbard	JF326454	–	–
	LC5449	Soil in karst cave	China	KY494713	KY705182	KY705112
	LC7115	Leaf of bamboo	China	KY494721	KY705189	KY705118
	LC7117	Leaf of bamboo	China	KY494722	KY705190	KY705119
	LC7119	Leaf of bamboo	China	KY494724	KY705192	KY705121
	LC7120	Leaf of bamboo	China	KY494725	KY705193	KY705122
	LC7126	Leaf of bamboo	China	KY494729	KY705197	KY705125
	LC7129	Leaf of bamboo	China	KY494731	KY705199	KY705127
	LC7135	Leaf of bamboo	China	KY494732	KY705200	KY705128
	LC7139	Leaf of bamboo	China	KY494733	KY705201	KY705129
	LC7141	Leaf of bamboo	China	KY494734	KY705202	KY705130
	LC7142	Leaf of bamboo	China	KY494735	KY705203	KY705131
	LC7251	Leaf of bamboo	China	KY494746	KY705214	KY705142
	LC7254	Leaf of bamboo	China	KY494748	KY705216	KY705144
LC8179	<i>Brassica capestris</i>	China	KY494759	KY705227	KY705155	
LC8180	<i>Brassica capestris</i>	China	KY494760	KY705228	KY705156	
<i>A. sacchari</i>	CBS 212.30	<i>Phragmites australis</i>	United Kingdom	KF144916	KF145005	KF145047
	CBS 301.49	Bamboo	Indonesia	KF144917	KF145006	KF145048
<i>A. saccharicola</i>	CBS 191.73	Air	The Netherlands	KF144920	KF145009	KF145051
	CBS 334.86	Dead culms of <i>Phragmites australis</i>	France	AB220257	KF145010	KF145052
	CBS 463.83	Dead culms of <i>Phragmites australis</i>	The Netherlands	KF144921	KF145011	KF145053
<i>A. serenense</i>	IMI 326869*	Food, pharmaceutical excipients, atmosphere and home dust	Spain	AB220250	AB220297	–
<i>A. subglobosum</i>	MFLUCC 11-0397*	Dead bamboo culms	Thailand	KR069112	–	–
<i>A. subroseum</i>	LC7215	Leaf of bamboo	China	KY494740	KY705208	KY705136
	LC7291	Leaf of bamboo	China	KY494751	KY705219	KY705147
	LC7292* =CGMCC3.18337	Leaf of bamboo	China	KY494752	KY705220	KY705148
<i>A. thailandicum</i>	MFLUCC 15-0202*	Dead bamboo culms	Thailand	KU940145	–	–
	LC5630	Rotten wood	China	KY494714	KY806200	KY705113

Species	Strain numbers ¹	Hosts	Countries	GenBank accessions		
				ITS	TUB	TEF
<i>A. xenocordella</i>	CBS 478.86*	Soil from roadway	Zimbabwe	KF144925	KF145013	KF145055
	LC3486	<i>Camellia sinensis</i>	China	KY494687	KY705158	KY705086
<i>A. yunnanum</i>	MFLUCC 15-0002*	Decaying bamboo culms	China	KU940147	–	–
<i>N. gorlenkoana</i>	CBS 480.73	<i>Vitis vinifera</i>	Kazakhstan	KX986048	KY019456	KY019420

* = type strains, strains and sequences generated in this study are shown in **bold**.

¹ CBS: Westerdijk Fungal Biodiversity Institute, Utrecht, The Netherlands; CGMCC: China General Microbiological Culture Collection; CPC: Culture collection of Pedro Crous, housed at the Westerdijk Fungal Biodiversity Institute; DAOM: Canadian Collection of Fungal Cultures, Ottawa, Canada; DSM: Deutsche Sammlung von Mikroorganismen und Zellkulturen GmbH, Braunschweig, Germany; IMI: Culture collection of CABI Europe UK Centre, Egham, UK; IFO: Institute for Fermentation, Osaka; LC: Working collection of Lei Cai, housed at CAS, China; MFLUCC: Mae Fah Luang University Culture Collection, Chiang Rai, Thailand; MCC: Microbial Culture Collection of India; NFFCI: National Fungal Culture Collection of India.

Taxonomy

Arthrinium bambusae M. Wang & L. Cai, sp. nov.

Mycobank: MB824906

Figure 3

Type. CHINA, Guangdong Province, on bamboo leaves, 10 Jul. 2016, D.W. Xiao, (holotype: HMAS 247187; culture ex-type: CGMCC 3.18335 = LC7106).

Etymology. Named after the host of the holotype.

Description. Hyphae hyaline, branched, septate, 1.5–5.0 µm diam. Conidiophores reduced to conidiogenous cells. Conidiogenous cells erect, aggregated in clusters on hyphae, hyaline to pale brown, smooth, doliiform to ampulliform, or lageniform, 4.0–12.0 × 3.0–7.0 µm (\bar{x} = 6.6 ± 1.8 × 4.8 ± 0.9, n = 30). Conidia olivaceous to brown, smooth to finely roughened, subglobose to ellipsoid, 11.5–15.5 × 7.0–14.0 µm (\bar{x} = 13.2 ± 0.8 × 11.4 ± 1.2, n = 50).

Culture characteristics. On PDA, colonies flat, spreading, margin circular, with abundant aerial mycelia, surface and reverse white to grey. On MEA, colonies flat, spreading, surface and reverse brown to black.

Additional specimens examined. CHINA, Jiangxi Province, on bamboo leaves, 10 Jul. 2016, Q. Xiong, living culture LC7246; Guangdong Province, on bamboo leaves, 10 Jul. 2016, D.W. Xiao, living culture LC7107; *ibid.* living culture LC7113; *ibid.* living culture LC7124; *ibid.* living culture LC7125; *ibid.* living culture LC7128.

Notes. Seven strains representing *A. bambusae* clustered in a well-supported clade closely related to *A. subroseum* (98% sequence similarity in ITS; 92% in TUB2; 96% in TEF1). *Arthrinium bambusae* differs from *A. subroseum* in the morphology of conidiophore (reduced to conidiogenous cells in *A. bambusae* vs. erect or ascending, clustered in groups in *A. subroseum*). Moreover, *A. bambusae* does not produce pigment on the PDA.

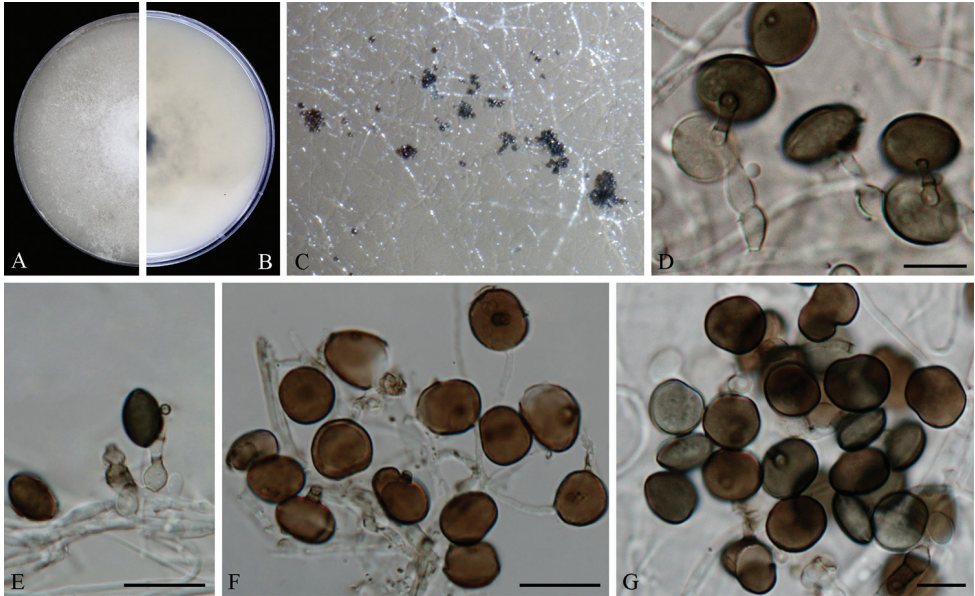


Figure 3. *Arthrinium bambusae* (from ex-holotype strain CGMCC 3.18335) **A–B** 7 d old cultures on PDA **C** Colony on MEA producing conidia masses **D–F** Conidiogenous cells giving rise to conidia **G** Conidia. Scale bars = 10 µm.

***Arthrinium camelliae-sinensis* M. Wang, F. Liu & L. Cai, sp. nov.**

Mycobank: MB824907

Figure 4

Type. CHINA, Jiangxi Province, on *Camellia sinensis*, 22 Apr. 2013, Q. Chen, (holotype: HMAS 247186; culture ex-type: CGMCC 3.18333 = LC5007).

Etymology. Named with the host plant of the type.

Description. Hyphae hyaline, branched, septate, 2.0–4.5 µm diam. Conidiophores reduced to conidiogenous cells. Conidiogenous cells erect, aggregated in clusters, hyaline to pale brown, smooth, doliiform to ampulliform, 4.0–9.5 × 3.0–6.0 µm ($\bar{x} = 6.1 \pm 1.4 \times 4.4 \pm 0.9$, n = 30). Conidia brown to dark brown, smooth, globose to subglobose, 9.0–13.5 × 7.0–12.0 µm ($\bar{x} = 11.1 \pm 0.9 \times 10.1 \pm 1.0$, n = 50).

Culture characteristics. On PDA, colonies flat, margin circular, initially white, becoming greyish on surface, reaching 9 cm in 7 days at 25 °C. On MEA, with sparse aerial mycelia, surface dirty white, reverse pale luteous.

Other specimens. CHINA, Hubei Province, on *Brassica campestris*, 31 Mar. 2016, Y.Z. Zhao, living culture LC8181 = LF1498.

Notes. Two strains representing *A. camelliae-sinensis* clustered in a well-supported clade and appeared closely related to *A. jiangxiense* (97% sequence similarity in ITS; 94% in TUB2; 94% in TEF1) and *A. obovatum* (98% sequence similarity in ITS; 95% in TUB2; 93% in TEF1). While *A. camelliae-sinensis* is distinct from *A. jiangxiense* in its larger conidia (globose or subglobose, 9.0–13.5 × 7.0–12.0 µm in *A. camelliae-sin-*

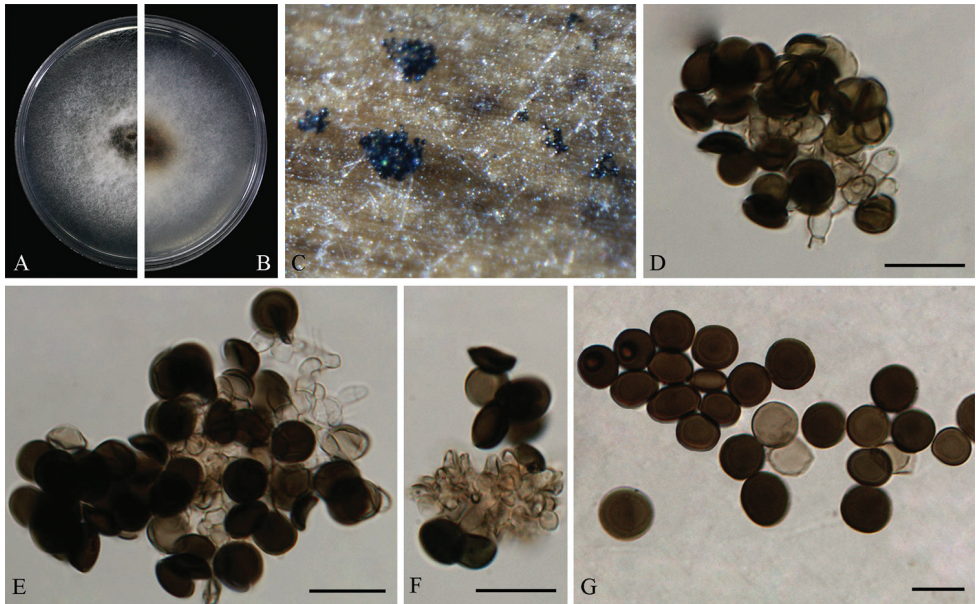


Figure 4. *Arthrinium camelliae-sinensis* (from ex-holotype strain CGMCC 3.18333) **A–B** 7 d old cultures on PDA **C** Colony on MEA with bamboo leaves producing conidia masses **D–F** Conidiogenous cells giving rise to conidia **G** Conidia. Scale bars = 10 µm.

ensis vs. surface view 7.5–10.0 µm diam, side view 4.5–7.0 µm diam in *A. jiangxiense*) and conidiogenous cell arrangement (aggregated irregularly on hyphae vs. scattered on hyphae in *A. jiangxiense*) and distinct from *A. obovatum* in the lack of obovoid conidia (see the note under *A. obovatum*).

***Arthrinium dichotomanthi* M. Wang & L. Cai, sp. nov.**

Mycobank: MB824908

Figure 5

Type. CHINA, Chongqing, on *Dichotomanthus tristaniaecarpa*, 20 Dec. 2012, L. Cai, (holotype: HMAS 247185; culture ex-type: CGMCC 3.18332 = LC4950).

Etymology. Named after the host from which it was isolated.

Description. Hyphae hyaline, branched, septate, 1.5–5.0 µm diam. Conidiophores reduced to conidiogenous cells. Conidiogenous cells erect, aggregated in clusters on hyphae, hyaline to pale brown, smooth, doliiform to clavate or lageniform, 5.5–11.0 × 3.0–5.0 µm ($\bar{x} = 7.9 \pm 1.4 \times 4.0 \pm 0.5$, n = 30). Conidia brown to dark brown, smooth to finely roughened, globose, subglobose to lenticular, with a longitudinal germ slit, 9.0–15.0 × 6.0–12.0 µm ($\bar{x} = 12.0 \pm 1.4 \times 8.5 \pm 1.1$, n = 50).

Culture characteristics. On PDA, colonies umbonate, margin irregular, with sparse aerial mycelia. Colonies creamy-white to greyish without patches reverse, reaching 9 cm in 7 days at 25 °C. On MEA, colonies flat, spreading, surface and reverse pale luteous.

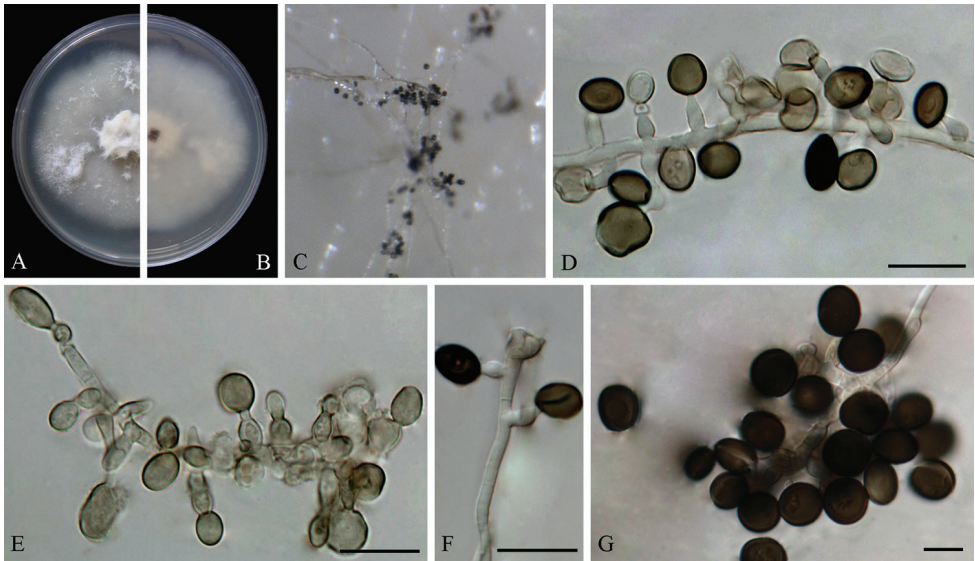


Figure 5. *Arthrini dichotomanthi* (from ex-holotype strain CGMCC 3.18332) **A–B** 7 d old cultures on PDA **C** Colony on MEA producing conidia masses **D–F** Conidiogenous cells giving rise to conidia **G** Conidia. Scale bars = 10 µm.

Other specimens. CHINA, Chongqing, on *Dichotomanthus tristaniaecarpa*, 20 Dec. 2012, L. Cai, living culture LC8175 = WM529; ibid. living culture LC8176 = WM 530.

Notes. Three strains representing *A. dichotomanthi* formed a distinct clade closely related to *A. phaeospermum* (Corda) M.B. Ellis (99% sequence similarity in ITS; 96% in TUB2; 96% in TEF1), *A. serenense* Larrondo & Calvo (99% sequence similarity in ITS; 95% in TUB2) and *A. saccharicola* F. Stevens (99% sequence similarity in ITS; 95% in TUB2; 97% in TEF1). *Arthrini dichotomanthi* differs from *A. phaeospermum* and *A. saccharicola* in its larger conidia (globose or subglobose, 9.0–15.0 × 6.0–12.0 µm in *A. dichotomanthi* vs. surface view (9–)10(–12) µm diam, side view 6–7 µm diam in *A. phaeospermum*, surface view (7–)8–9(–10) µm diam, side view (4–)5(–6) µm diam in *A. saccharicola*) and from *A. serenense* by the absence of odour on the MEA colony (Larrondo 1990).

***Arthrini guizhouense* M. Wang & L. Cai, sp. nov.**

Mycobank: MB824909

Figure 6

Type. CHINA, Guizhou Province, from the air in karst cave, 23 Jul. 2014, Z.F. Zhang, (holotype: HMAS 247188; culture ex-type: CGMCC 3.18334 = LC5322).

Etymology. Named after the province where type was collected, Guizhou province.

Description. Hyphae hyaline, branched, septate, 1.5–5.0 µm diam. Conidiophores reduced to conidiogenous cells. Conidiogenous cells erect, aggregated in clusters on hy-

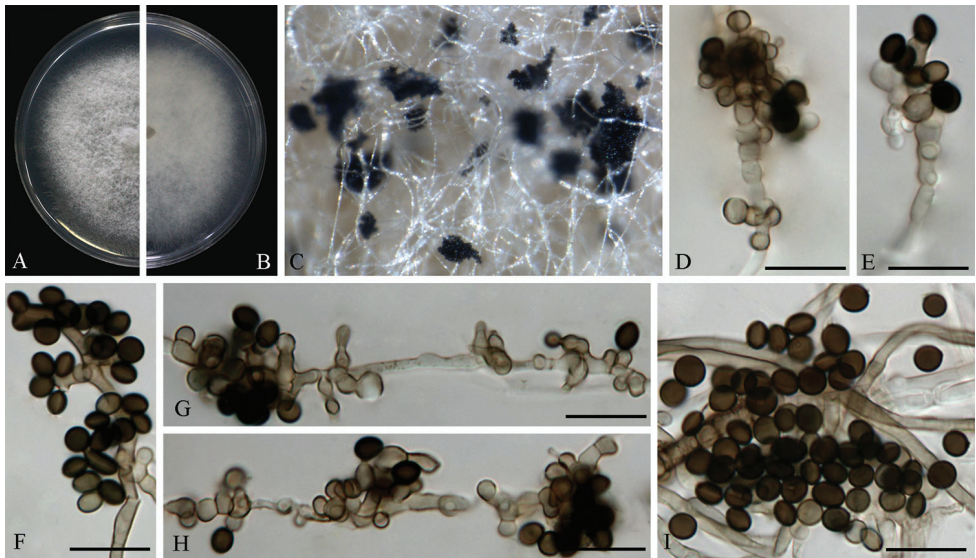


Figure 6. *Arthrinium guizhouense* (from ex-holotype strain CGMCC 3.18334) **A–B** 6 d old cultures on PDA **C** Colony on MEA producing conidia masses **D–H** Conidiogenous cells giving rise to conidia **I** Conidia. Scale bars = 10 µm.

phae, pale brown, smooth, subglobose, ampulliform or doliiform, $3.5\text{--}8.0 \times 3.0\text{--}4.5\ \mu\text{m}$ ($\bar{x} = 5.1 \pm 1.08 \times 3.7 \pm 0.49$, $n = 30$). Conidia dark brown to black, smooth to finely roughened, globose or subglobose, occasionally elongated to ellipsoidal, with a longitudinal, hyaline, thin, germ slit, $5.0\text{--}7.5 \times 4.0\text{--}7.0\ \mu\text{m}$ ($\bar{x} = 6.1 \pm 0.5 \times 5.5 \pm 0.6$, $n = 50$).

Culture characteristics. On PDA, colonies flat, woolly, margin circular, with moderate aerial mycelia, surface initially white, becoming greyish and reverse with black patches, reaching 9 cm in 9 days at 25 °C. On MEA, surface dirty white with patches of olivaceous-grey and reverse greyish.

Other specimens examined. CHINA, Guizhou Province, from the air in karst cave, 23 Jul. 2014, Z.F. Zhang, living culture LC5318.

Notes. *Arthrinium guizhouense* is closely related to *A. sacchari* (Speg.) M.B. Ellis (99% sequence similarity in ITS; 99% in TUB2; 94% in TEF1). Morphologically, *A. guizhouense* and *A. sacchari* are very similar in conidial size, but *A. guizhouensis* produces relatively shorter conidiogenous cells ($3.5\text{--}8.0\ \mu\text{m}$ in *A. guizhouense* vs. $5\text{--}12\ \mu\text{m}$ in *A. sacchari*).

***Arthrinium jiangxiense* M. Wang & L. Cai, sp. nov.**

Mycobank: MB824910

Figure 7

Type. CHINA, Jiangxi Province, on *Maesa* sp., 05 Sept. 2013, Y.H. Gao, (holotype: HMAS 247183; culture ex-type: CGMCC3.18381 = LC4577).

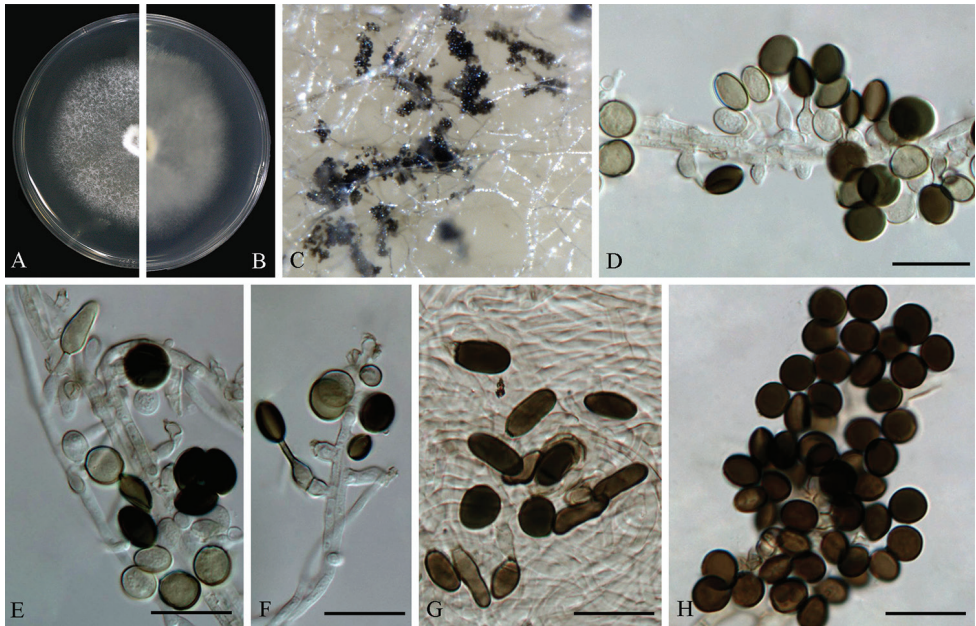


Figure 7. *Arthrinium jiangxiense* (from ex-holotype strain CGMCC 3.18381) **A–B** 5 d old cultures on PDA **C** Colony on MEA producing conidia masses **D–F** Conidiogenous cells giving rise to conidia **G** Elongated conidia **H** Conidia. Scale bars = 10 μm .

Etymology. Named after the province where the most strains of this species were collected, Jiangxi.

Description. Hyphae hyaline, branched, septate, 1.5–5.0 μm diam. Conidiophores reduced to conidiogenous cells. Conidiogenous cells erect, scattered or aggregated in clusters on hyphae, hyaline to pale brown, smooth, ampulliform, 6.0–15.0 \times 2.5–5.0 μm (\bar{x} = 9.7 \pm 2.6 \times 3.7 \pm 0.6, n = 30), apical neck 2.5–6.0 μm long, basal part 3.0–9.0 μm long. Conidia brown, smooth to finely roughened, granular, globose to ellipsoid in surface view, 7.5–10.0 μm diam (\bar{x} = 8.7 \pm 0.6, n = 50), lenticular in side view, with longitudinal, pale germ slit, 4.5–7.0 μm diam (\bar{x} = 5.8 \pm 0.6, n = 50). Sterile cells forming on solitary loci on hyphae, brown, finely roughened, subcylindrical to clavate.

Culture characteristics. On PDA, colonies flat, woolly, margin circular, with sparse aerial mycelia, initially white, becoming greyish due to sporulation, reaching 9 cm in 10 days at 25 $^{\circ}\text{C}$, on MEA, sienna with patches of luteous, reverse luteous to sienna.

Other specimens examined. CHINA, Hunan Province, on bamboo, 22 Sept. 2010, L. Cai, living culture LC2831; Jiangxi Province, on *Phyllostachys* sp., 05 Sept. 2013, Y.H. Gao, living culture LC4494; on *Phyllostachys* sp., 22 Apr. 2013, Q. Chen, living culture LC4993; *ibid.* living culture LC4497; *ibid.* living culture LC5001; *ibid.* living culture LC5004; on *Imperata cylindrical*, 22 Apr. 2013, Q. Chen, living culture LC5015; on *Maesa* sp., 05 Sept. 2013, Y.H. Gao, living culture LC4541; on *Machilus* sp., 05 Sept. 2013, Y.H. Gao, living culture LC4547; on *Camellia sinensis*, 05 Sept. 2013, Y.H. Gao, living culture LC4578; on bamboo, 01 Jul. 2016, J.E. Huang, living

culture LC7104; *ibid.* living culture LC7154; *ibid.* living culture LC7156; *ibid.* living culture LC7275.

Notes. Two strains representing *Arthrinium jiangxiense* clustered in a well-supported clade and appeared closely related to *A. camelliae-sinensis* (97% sequence similarity in ITS; 94% in TUB2; 94% in TEF1). While *A. jiangxiensis* is distinct from *A. camelliae-sinensis* in its smaller conidia (surface view 7.5–10.0 μm diam, side view 4.5–7.0 μm diam in *A. jiangxiensis* vs. globose or subglobose, 9.0–13.5 \times 7.0–12.0 μm in *A. camelliae-sinensis*) and conidiogenous cell arrangements (conidiogenous cells scattered on hyphae vs. aggregated irregularly on hyphae in *A. jiangxiense*).

***Arthrinium obovatum* M. Wang & L. Cai, sp. nov.**

Mycobank: MB824911

Figure 8

Type. CHINA, Chongqing, on *Lithocarpus* sp., 20 Dec. 2012, L. Cai, (holotype: HMAS 247184; culture ex-type: CGMCC 3.18331 = LC4940).

Etymology. Referring to the production of the large obovoid conidia.

Description. Hyphae hyaline to pale brown, branched, septate, 1.5–5.0 μm diam. Conidiophores reduced to conidiogenous cells. Conidiogenous cells erect, aggregated in clusters on hyphae, pale brown, smooth, subcylindrical or clavate, 5.5–13.5 \times 2.5–5.0 μm (\bar{x} = 8.7 \pm 2.4 \times 3.6 \pm 0.6, n = 30). Conidia dark brown,

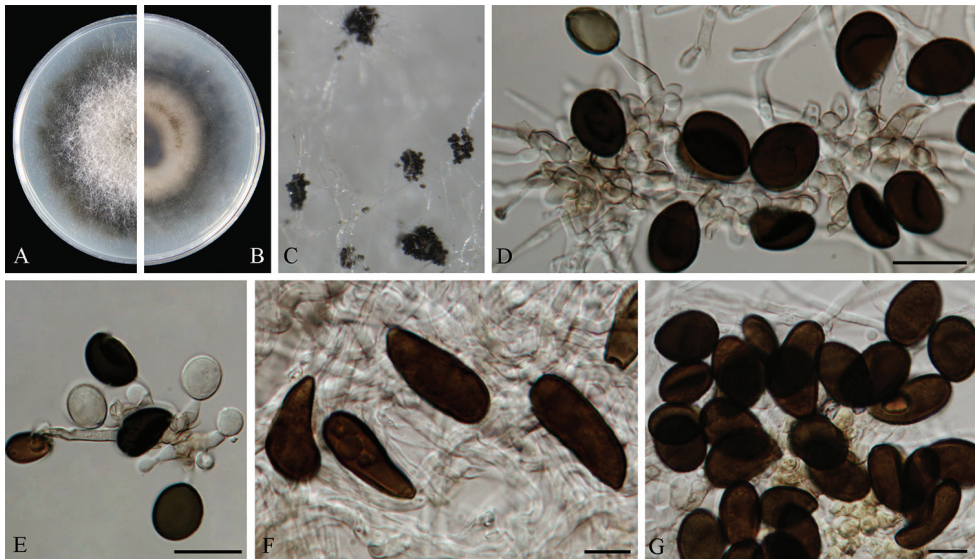


Figure 8. *Arthrinium obovatum* (from ex-holotype strain CGMCC 3.18331) **A–B** 7 d old cultures on PDA **C** Colony on MEA producing conidia masses **D–E** Conidiogenous cells giving rise to conidia **F** Obovoid conidia **G** Globose to subglobose conidia. Scale bars = 10 μm .

roughened, globose to subglobose, 11.0–16.5 μm (\bar{x} = 13.8 \pm 1.5, n = 50) in diam.; obovoid, 16.0–31.0 \times 9.0–16.0 μm (\bar{x} = 23.0 \pm 2.7 \times 12.7 \pm 1.4, n = 50), occasionally elongated to ellipsoidal.

Culture characteristics. On PDA, colonies flat, spreading, margin circular, initially white, becoming olivaceous-grey on surface, reverse smoke-grey with patches of olivaceous grey, reaching 9 cm in 7 days at 25 °C. On MEA, surface olivaceous grey in the central and luteous around, reverse with patches of olivaceous grey.

Other specimens examined. CHINA, Chongqing, on *Lithocarpus* sp., 20 Dec. 2012, L. Cai, living culture LC8177; *ibid.* living culture LC8178.

Notes. *Arthrinium obovatum* is the only species that produces obovoid conidia (Figure. 8F) in this genus, a character distinctly different from other species (Ellis 1965, 1976, Gjaerum 1967, Pollack and Benjamin 1969, Hudson et al. 1976, Calvo and Guarro 1980, Khan and Sullia 1980, Samuels et al. 1981, von Arx 1981, Koskela 1983, Kirk 1986, Larrondo and Calvo 1990, 1992, Müller 1992, Bhat and Kendrick 1993, Hyde et al. 1998, Jones et al. 2009, Singh et al. 2012, Crous et al. 2013, 2015, Sharma et al. 2014, Senanayake et al. 2015, Senanayake et al. 2015, Hyde et al. 2016, Dai et al. 2016a, b).

***Arthrinium pseudoparenchymaticum* M. Wang & L. Cai, sp. nov.**

Mycobank: MB824912

Figure 9

Type. CHINA, Guangdong Province, on bamboo, Jul. 2016, D.W. Xiao, (holotype: HMAS 247189; culture ex-type: CGMCC 3.18336 = LC7234).

Etymology. Referring to the pseudoparenchymatous hyphae.

Description. Hyphae hyaline to pale brown, branched, septate, 1.5–5.0 μm diam., pseudoparenchymatous. Conidiophores aggregated in hyaline to light brown sporodochia, smooth, usually unbranched, up to 40 μm long, 3–6 μm width. Conidiogenous cells hyaline to pale yellow, smooth to finely roughened, subcylindrical to doliiform, 8.0–18.5 \times 3.0–8.5 μm (\bar{x} = 13.7 \pm 3.2 \times 5.4 \pm 1.2, n = 30). Conidia pale to dark brown, smooth, finely guttulate, globose to subglobose, 13.5–27.0 \times 12.0–23.5 μm (\bar{x} = 20.2 \pm 2.5 \times 17.1 \pm 2.4, n = 50). Sometimes lobed or dentate, polygonal or irregular in surface view.

Culture characteristics. On PDA, colonies flat, spreading, margin circular, with moderate aerial mycelia, initially white, becoming grey on surface, reverse smoke-grey without patches, reaching 9 cm in 8 days at 25 °C. On MEA, surface pale luteous to grey with abundant mycelia, reverse greyish without patches.

Other specimens examined. CHINA, Guangdong Province, on bamboo, Jul. 2016, D.W. Xiao, living culture LC8173; *ibid.* living culture LC8174.

Notes. *Arthrinium pseudoparenchymaticum* is closely related to *A. hyphopodii* (94% sequence similarity in ITS), but differs in its much larger conidia (13.5–27.0 \times 12.0–23.5 μm vs. 5–10 \times 4–8 μm), the absence of hyphopodia and the presence of dentate conidia.

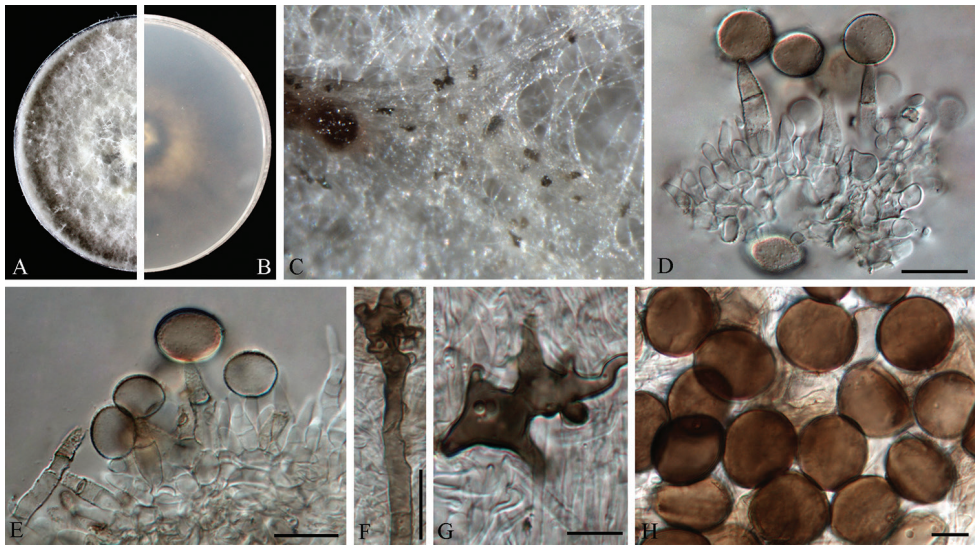


Figure 9. *Arthrinium pseudoparenchymaticum* (from ex-holotype strain CGMCC 3.18336) **A–B** 8 d old cultures on PDA **C** Colony on MEA producing conidia masses **D–E** Conidiogenous cells giving rise to conidia **F–G** Dentate conidia **H** Globose conidia. Scale bars = 10 µm.

***Arthrinium subroseum* M. Wang & L. Cai, sp. nov.**

Mycobank: MB824913

Figure 10

Type. CHINA, Jiangxi Province, on bamboo, 1 Jul. 2016, J.E. Huang, (holotype: HMAS 247190; culture ex-type: CGMCC3.18337 = LC7292).

Etymology. Named after the colour of colony on PDA, pinkish.

Description. Hyphae hyaline to pale brown, branched, septate, 1.5–6.0 µm diam. Conidiophores hyaline to pale brown, smooth, erect or ascending, simple, flexuous, subcylindrical, clustered in groups. Conidiophores aggregated in brown sporodochia, smooth, hyaline to brown, up to 20 µm long, 2–4.5 µm width. Conidiogenous cells pale brown, smooth, doliiiform to subcylindrical, 3.0–6.5 × 2.0–5.0 µm ($\bar{x} = 4.7 \pm 1.2 \times 3.7 \pm 0.9$, n = 30). Conidia pale brown to dark brown, smooth, globose to subglobose or ellipsoidal, 12.0–17.5 × 9.0–16.0 µm ($\bar{x} = 14.9 \pm 1.4 \times 11.8 \pm 1.8$, n = 50).

Culture characteristics. On PDA, colonies flat, spreading, margin circular, with moderate aerial mycelia, initially white, becoming light pink on surface, reverse peach-puff without patches, reaching 10 cm in 8 days at 25 °C. On MEA, surface blackish-green with abundant mycelia, reverse with patches of greyish.

Other specimens. CHINA, Jiangxi Province, on bamboo, 1 Jul. 2016, J.E. Huang, living culture LC7215; *ibid.* living culture LC7291.

Notes. Three strains representing *A. subroseum* clustered in a well-supported clade, closely related to *A. Garethjonesii* (94% sequence similarity in ITS) and *A. bambusae* (98% sequence similarity in ITS; 92% in TUB2; 96% in TEF1). However, *A. subro-*

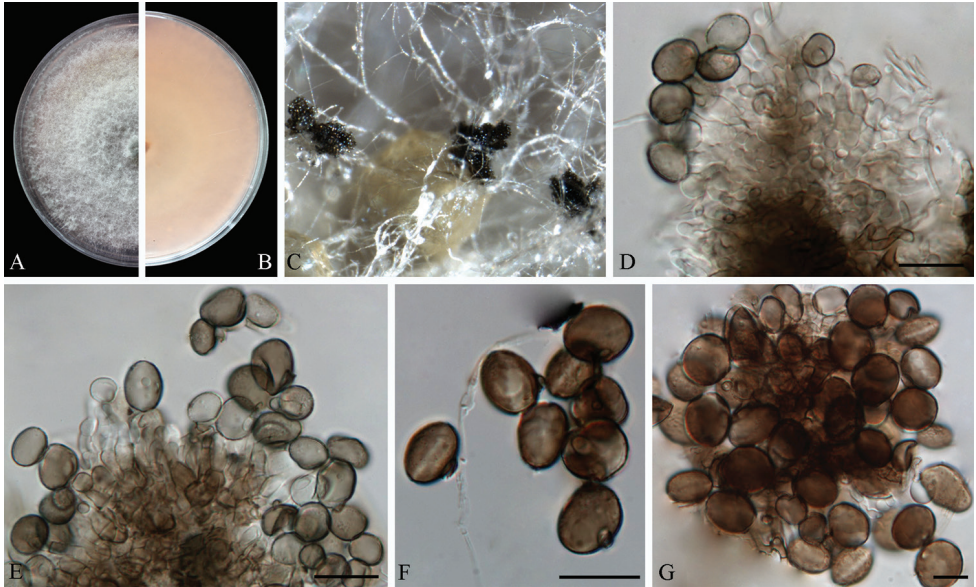


Figure 10. *Arthrinium subroseum* (from ex-holotype strain CGMCC3.18337) **A–B** 10 d old cultures on PDA **C** Colony on MEA producing conidia masses **D–E** Conidiogenous cells giving rise to conidia **F–G** Conidia. Scale bars = 10 µm.

seum differs from *A. bambusae* in the morphology of conidiophores (erect or ascending, clustered in groups in *A. subroseum* vs. reduced to conidiogenous cells in *A. bambusae*). *Arthrinium subroseum* is not morphologically comparable to *A. garethjonesii*, whose asexual morph is undetermined (Dai et al. 2016b).

Discussion

Arthrinium, *Cordella* and *Pteroconium* share similar morphological characters, e.g. basauxillary conidiophores with terminal and intercalary polyblastic conidiogenous cells and brown, unicellular conidia with a pallid germ slit (Ellis 1971, Hyde et al. 1998). Crous et al. (2013) reduced both *Cordella* and *Pteroconium* as generic synonyms of *Arthrinium* based on molecular phylogenetic data and regarded traditionally applied morphological characters in distinguishing these genera as phylogenetically insignificant. This study added eight novel species and our data are in good accordance with that of Crous et al. (2013). For example, *A. pseudoparenchymaticum* is sporodochial and pseudoparenchymatous, which would be classified as *Pteroconium* in the traditional taxonomy. However, the multi-locus (ITS, TEF1 & TUB2) tree (Figure. 1) shows that *A. pseudoparenchymaticum* is phylogenetically distant from *A. pterospermum* (syn. *P. pterospermum*, the type of “*Pteroconium*”).

Currently there are 70 recognised species in *Arthrinium* (Index Fungorum), occurring on a wide variety of both living and decaying plant materials. It is noteworthy that *Arthrinium* species showed distinct preference for growing on two graminaceous families, Poaceae

and Cyperaceae, amongst which, *Bambusa* (Poaceae) and *Carex* (Cyperaceae) are two of the most common host genera for *Arthrinium* species. For example, seven species have been recorded from *Carex* spp., i.e. *A. austriacum* Petr. (1959), *A. caricicola* Kunze (1817), *A. globosum* Koskela (1983), *A. kamtschaticum* Tranzschel & Woron (1914), *A. morthieri* Fuckel (1870), *A. muelleri* Ellis (1976) and *A. naviculare* Rostr. (1886). Bamboo has been widely known as a favourable host for *Arthrinium*, e.g. *A. hyphopodii*, *A. longistromum*, *A. subglobosum*, *A. thailandicum* and *A. yunnanum* (Senanayake et al. 2015, Dai et al. 2016). In this study, three new species (*A. bambusae*, *A. subroseum* and *A. pseudoparenchymaticum*) were also isolated from bamboo. In addition, three species (*A. arundinis*, *A. guizhouense*, and *A. rasikravindrii*) were isolated from air and soil from karst caves, where have been shown to encompass a high fungal diversity (Jiang et al. 2017, Zhang et al. 2017).

In addition to the *Arthrinium* species from China, we also tried to resolve the phylogenetic status of *Arthrinium mytilomorphum* Bhat & W.B. Kendr. (Bhat and Kendrick 1993) in the current study. DNA extraction from the type specimen of *A. mytilomorphum* (DAOM 214595) was prohibited but DAOM provided a DNA sample. Unfortunately, we only managed to obtain an ITS sequence from this DNA sample, while the amplifications of all other protein coding genes were unsuccessful. The ITS phylogenetic tree (not shown here) shows that *A. mytilomorphum* is closely related to *A. subroseum* (99 % sequence similarity in ITS), while the morphology of these two species are very different from each other. Conidia of *A. mytilomorphum* are dark brown, fusiform or navicular, measuring 20–30 × 6–8.5 µm, slightly bowed down and asymmetric (Figure 11), while those of *A. subroseum* are pale brown to dark brown, globose or subglobose, measuring 12–17.5 × 9–16 µm.



Figure 11. *Arthrinium mytilomorphum* (from holotype DAOM 214595) **A–B** Overview of the type specimen **C–F** Conidiogenous cells giving rise to conidia **G** Conidia. Scale bars = 10 µm.

Teleomorph-typified genus *Apiospora* was treated as a synonym of anamorph-typified genus *Arthrinium* on the basis that *Arthrinium* is older and more commonly used in literature (Crous et al. 2013). However, only three of the 58 recorded *Apiospora* species have been properly linked to their known *Arthrinium* counterparts, i.e. *Arthrinium hysterinum* (syn. *Ap. bambusae*) (Sivanesan 1983, Kirk 1986); *Arthrinium arundinis* (syn. *Ap. montagnei*) (Hyde 1998); *Arthrinium sinense* (syn. *Ap. sinensis*) (Réblová et al. 2016). In addition, molecular data of only four *Apiospora* species (*Ap. bambusae*, *Ap. montagnei*, *Ap. setosa* and *Ap. sinensis*) are available, in which only *A. bambusae* and *A. sinensis* have type-derived sequences. A comprehensive taxonomic revision of this taxonomic group awaits fresh collection and epitypification of many *Apiospora* species and, based on which, phylogenetic links with *Arthrinium* species could be established.

Acknowledgments

We thank Peng Zhao, Qian Chen, Yahui Gao and Zhifeng Zhang for providing strains and technical assistance. We kindly appreciated the curator of Agriculture and Agri-Food Canada herbarium and Dr. Wen Chen in Ottawa Research and Development Centre AAFC for providing DNA samples and microscope slides of the type specimen of *Arthrinium mytilomorphum*. This work was financially supported by the National Science Fund for Distinguished Young Scholars of China (NSFC 31725001) and the Frontier Science Research Project of the Chinese Academy of Sciences (QYZDB-SSW-SMC044).

References

- von Arx JA (1981) The genera of fungi sporulating in pure culture (3rd edn). Cramer Vaduz, 424 pp.
- Bhat DJ, Kendrick WB (1993) Twenty-five new conidial fungi from the Western Ghats and the Andaman Islands (India). *Mycotaxon* 49: 19–90.
- Cai L, Hyde KD, Taylor PW, Weir B, Waller J, Abang MM, Zhang JZ, Yang YL, Phoulivong S, Liu ZY, Prihastuti H (2009) A polyphasic approach for studying *Colletotrichum*. *Fungal Diversity* 39: 204.
- Calvo A, Guarro J (1980) *Arthrinium aureum* sp. nov. from Spain. *Transactions of the British Mycological Society* 75: 156–157. [https://doi.org/10.1016/S0007-1536\(80\)80208-7](https://doi.org/10.1016/S0007-1536(80)80208-7)
- Carbone I, Kohn LM (1999) A method for designing primer sets for speciation studies in filamentous ascomycetes. *Mycologia* 91: 553–556. <https://doi.org/10.2307/3761358>
- Chen K, Wu XQ, Huang MX, Han YY (2014) First report of brown culm streak of *Phyllostachys praecox* caused by *Arthrinium arundinis* in Nanjing, China. *Plant Disease* 98: 1274. <https://doi.org/10.1094/PDIS-02-14-0165-PDN>
- Crous PW, Gams W, Stalpers JA, Robert V, Stegehuis G (2004) MycoBank: an online initiative to launch mycology into the 21st century. *Studies in Mycology* 50: 19–22.

- Crous PW, Groenewald JZ (2013) A phylogenetic re-evaluation of *Arthrinium*. IMA fungus 4: 133–154. <https://doi.org/10.5598/imafungus.2013.04.01.13>
- Crous PW, Wingfield MJ, Le Roux JJ, et al. (2015) Fungal planet description sheets: 371–399. Persoonia 35: 264–327. <https://doi.org/10.3767/003158515X690269>
- Dai DQ, Jiang HB, Tang LZ, Bhat DJ (2016b) Two new species of *Arthrinium* (*Apiosporaceae*, *Xylariales*) associated with bamboo from Yunnan, China. Mycosphere 7: 1332–1345. <https://doi.org/10.5943/mycosphere/7/9/7>
- Dai DQ, Phookamsak R, Wijayawardene NN, Li WJ, Bhat DJ, Xu JC, Taylor JE, Hyde KD, Chukeatirote E (2017a) Bambusicolous fungi. Fungal Diversity 82: 1–105. <https://doi.org/10.1007/s13225-016-0367-8>
- Ellis MB (1965) Dematiaceous Hyphomycetes. VI. Mycological Papers 103: 1–46.
- Ellis MB (1971) Dematiaceous Hyphomycetes. Commonwealth Mycological Institute, Kew, 608 pp.
- Ellis MB (1976) More Dematiaceous Hyphomycetes. CAB International Mycological Institute, Kew, 507 pp.
- Farr DE, Rossman AY (2017) Fungal Databases, U.S. National Fungus Collections, ARS, USDA. <https://nt.ars-grin.gov/fungaldatabases/>
- Gjaerum HB (1967) *Arthrinium morthieri*, *A. fuckelii* n. sp., and *A. ushuvaiense*. Nytt magasin for Botanikk 14: 1–6.
- Glass NL, Donaldson GC (1995) Development of primer sets designed for use with the PCR to amplify conserved genes from filamentous ascomycetes. Applied and Environmental Microbiology 61: 1323–1330.
- Guo LD, Hyde KD, Liew ECY (2000) Identification of endophytic fungi from *Livistona chinensis* based on morphology and rDNA sequences. New Phytologist 147: 617–630. <https://doi.org/10.1046/j.1469-8137.2000.00716.x>
- de Hoog GS, Guarro J, Gene J, et al. (2000) Atlas of Clinical Fungi (2nd edn). Centraalbureau voor Schimmelcultures, Utrecht, the Netherlands, 1–1160.
- Hong JH, Jang S, Heo YM, Min M, Lee H, Lee YM, Lee H, Kim JJ (2015) Investigation of marine-derived fungal diversity and their exploitable biological activities. Marine Drugs 13: 4137–4155. <https://doi.org/10.3390/md13074137>
- Hudson HJ, McKenzie EHC, Tommerup IC (1976) Conidial states of *Apiospora* Sacc. Transactions of the British Mycological Society 66: 359–362. [https://doi.org/10.1016/S0007-1536\(76\)80075-7](https://doi.org/10.1016/S0007-1536(76)80075-7)
- Hughes SJ (1953) Conidiophores, conidia, and classification. Canadian Journal of Botany 31: 577–659. <https://doi.org/10.1139/b53-046>
- Hyde KD, Fröhlich J, Taylor JE (1998) Fungi from palms. XXXVI. Reflections on unitunicate ascomycetes with apiospores. Sydowia 50: 21–80.
- Hyde KD, Hongsanan S, Jeewon R, et al. (2016) Fungal diversity notes 367–490: taxonomic and phylogenetic contributions to fungal taxa. Fungal Diversity 80: 1–270. <https://doi.org/10.1007/s13225-016-0373-x>
- Jiang JR, Cai L, Liu F (2017) Oligotrophic fungi from a carbonate cave, with three new species of *Cephalotrichum*. Mycology 8(3): 164–177. <https://doi.org/10.1080/21501203.2017.1366370>

- Jones EBG, Sakayaroj J, Suetrong S, et al. (2009) Classification of marine Ascomycota, anamorphic taxa and Basidiomycota. *Fungal Diversity* 35: 1–187.
- Khan KR, Sullia SB (1980) *Arthrinium phaeospermum* var. *indicum* var. nov., a new market pathogen of cowpea, garden pea and french bean. *Acta Botanica Indica* 8: 103–104.
- Kirk PM (1986) New or interesting microfungi. XV. Miscellaneous hyphomycetes from the British Isles. *Transactions of the British Mycological Society* 86: 409–428. [https://doi.org/10.1016/S0007-1536\(86\)80185-1](https://doi.org/10.1016/S0007-1536(86)80185-1)
- Koskela P (1983) *Arthrinium glabrosom*, a new hyphomycetous species. *Karstenia* 23: 13–14. <https://doi.org/10.29203/ka.1983.218>
- Larrondo JV, Calvo MaA (1990) Two new species of *Arthrinium* from Spain. *Mycologia* 82: 396–398. <https://doi.org/10.2307/3759915>
- Larrondo JV, Calvo MaA (1992) New contributions to the study of the genus *Arthrinium*. *Mycologia* 84: 475–478. <https://doi.org/10.2307/3760203>
- Li BJ, Liu PQ, Jiang Y, Weng QY, Chen QH (2016) First report of culm rot caused by *Arthrinium phaeospermum* on *Phyllostachys viridis* in China. *Plant Disease* 100: 1013. <https://doi.org/10.1094/PDIS-08-15-0901-PDN>
- Minter DW (1985) A re-appraisal of the relationships between *Arthrinium* and other hyphomycetes. *Plant Sciences* 94: 281–308.
- Müller E (1992) A new parasitic species of *Apiospora*. *Boletín de la Sociedad Argentina de Botánica, La Plata* 28: 201–203.
- O'Donnell K, Cigelnik E (1997) Two divergent intragenomic rDNA ITS2 types within a monophyletic lineage of the fungus *Fusarium* are nonorthologous. *Molecular Phylogenetics and Evolution* 7: 103–116. <https://doi.org/10.1006/mpev.1996.0376>
- O'Donnell K, Kistler HC, Cigelnik E, Ploetz RC (1998) Multiple evolutionary origins of the fungus causing Panama disease of banana: concordant evidence from nuclear and mitochondrial gene genealogies. *Proceedings of the National Academy of Sciences* 95: 2044–2049. <https://doi.org/10.1073/pnas.95.5.2044>
- Pollack FG, Benjamin CR (1969) *Arthrinium japonicum* and notes on *Arthrinium kamtschaticum*. *Mycologia* 61: 187–190. <https://doi.org/10.2307/3757360>
- Posada D (2008) jModelTest: phylogenetic model averaging. *Molecular biology and evolution* 25: 1253–1256. <https://doi.org/10.1093/molbev/msn083>
- Rai MK (1989) Mycosis in man due to *Arthrinium phaeospermum* var. *indicum*. First case report: mykose durch *Arthrinium phaeospermum* var. *indicum* beim Menschen. *Erstbericht. Mycoses* 32: 472–475. <https://doi.org/10.1111/j.1439-0507.1989.tb02285.x>
- Rayner RW (1970) *A Mycological Colour Chart*. Commonwealth Mycological Institute, Kew, 34 pp.
- Réblová M, Miller AN, et al. (2016) Recommendations for competing sexual-asexually typified generic names in Sordariomycetes (except *Diaporthales*, *Hypocreales*, and *Magnaporthales*). *IMA Fungus* 7: 131–153. <https://doi.org/10.5598/imafungus.2016.07.01.08>
- Ronquist F, Teslenko M, Van Der Mark P, Ayres DL, Darling A, Höhna S, Larget B, Liu L (2012) MrBayes 3.2: efficient Bayesian phylogenetic inference and model choice across a large model space. *Systematic Biology* 61: 539–542. <https://doi.org/10.1093/sysbio/sys029>

- Samuels GJ, McKenzie EHC, Buchanan DE (1981) Ascomycetes of New Zealand 3. Two new species of *Apiospora* and their *Arthrinium anamorphs* on bamboo. *New Zealand Journal of Botany* 19: 137–149. <https://doi.org/10.1080/0028825X.1981.10425113>
- Seifert K, Morgan-Jones G, Gams W, Kendrick B (2011) The genera of hyphomycetes. CBS Biodiversity Series 9, Utrecht, the Netherlands, 1–997.
- Senanayake IC, Maharachchikumbura SS, Hyde KD, Bhat JD, Jones EG, McKenzie EH, Dai DQ, Daranagama DA, Dayarathne MC, Goonasekara ID, Konta S (2015) Towards unraveling relationships in *Xylariomycetidae* (Sordariomycetes). *Fungal Diversity* 73: 73–144. <https://doi.org/10.1007/s13225-015-0340-y>
- Sharma R, Kulkarni G, Sonawane MS, Shouche YS (2014) A new endophytic species of *Arthrinium* (Apiosporaceae) from *Jatropha podagrica*. *Mycoscience* 55: 118–123. <https://doi.org/10.1016/j.myc.2013.06.004>
- Shrestha P, Ibáñez AB, Bauer S, Glassman SI, Szaro TM, Bruns TD, Taylor JW (2015) Fungi isolated from *Miscanthus* and sugarcane: biomass conversion, fungal enzymes, and hydrolysis of plant cell wall polymers. *Biotechnology for Biofuels* 8: 1. <https://doi.org/10.1186/s13068-015-0221-3>
- Singh SM, Yadav LS, Singh PN, Hepat R, Sharma R, Singh SK (2012) *Arthrinium rasikravindrii* sp. nov. from Svalbard, Norway. *Mycotaxon* 122: 449–460. <https://doi.org/10.5248/122.449>
- Sivanesan A (1983) Studies on ascomycetes. *Transactions of the British Mycological Society* 81: 313–332. [https://doi.org/10.1016/S0007-1536\(83\)80084-9](https://doi.org/10.1016/S0007-1536(83)80084-9)
- Stamatakis A, Alachiotis N (2010) Time and memory efficient likelihood-based tree searches on phylogenomic alignments with missing data. *Bioinformatics* 26: 132–139. <https://doi.org/10.1093/bioinformatics/btq205>
- Tamura K, Stecher G, Peterson D, Filipinski A, Kumar S (2013) MEGA6: molecular evolutionary genetics analysis version 6.0. *Molecular Biology and Evolution* 30: 2725–2729. <https://doi.org/10.1093/molbev/mst197>
- Vilgalys R, Hester M (1990) Rapid genetic identification and mapping of enzymatically amplified ribosomal DNA from several *Cryptococcus* species. *Journal of Bacteriology* 172: 4238–4246. <https://doi.org/10.1128/jb.172.8.4238-4246.1990>
- White TJ, Bruns T, Lee SJ, Taylor JL (1990) Amplification and direct sequencing of fungal ribosomal RNA genes for phylogenetics. *PCR protocols: a guide to methods and applications* 18(1): 315–322. <https://doi.org/10.1016/B978-0-12-372180-8.50042-1>
- Zhang ZF, Liu F, Zhou X, Liu XZ, Liu SJ, Cai L (2017) Culturable mycobiota from Karst caves in China, with descriptions of 20 new species. *Persoonia* 39(1): 1–31. <https://doi.org/10.3767/persoonia.2017.39.01>
- Zhao YM, Deng CR, Chen X (1990) *Arthrinium phaeospermum* causing dermatomycosis, a new record of China. *Acta Mycologica Sinica* 9: 232–235.
- Zhaxybayeva O, Gogarten JP (2002) Bootstrap, Bayesian probability and maximum likelihood mapping: exploring new tools for comparative genome analyses. *BMC Genomics* 3: 4. <https://doi.org/10.1186/1471-2164-3-4>

***Architrypethelium murisporum* (Ascomycota, Trypetheliaceae), a remarkable new lichen species from Thailand challenging ascospore septation as an indicator of phylogenetic relationships**

Theerapat Luangsaphabool¹, H. Thorsten Lumbsch²,
Jittra Piapukiew³, Ek Sangvichien¹

1 Department of Biology, Faculty of Science, Ramkhamhaeng University, Bangkok, Thailand **2** Science & Education, The Field Museum, Chicago, Illinois, USA **3** Department of Botany, Faculty of Science, Chulalongkorn University, Bangkok, Thailand

Corresponding author: H. Thorsten Lumbsch (tlumbsch@fieldmuseum.org)

Academic editor: P. Divakar | Received 23 January 2018 | Accepted 21 April 2018 | Published 10 May 2018

Citation: Luangsaphabool T, Lumbsch HT, Piapukiew J, Sangvichien E (2018) *Architrypethelium murisporum* (Ascomycota, Trypetheliaceae), a remarkable new lichen species from Thailand challenging ascospore septation as an indicator of phylogenetic relationships. MycoKeys 34: 25–34. <https://doi.org/10.3897/mycokeys.25.23836>

Abstract

Architrypethelium murisporum Luangsaphabool, Lumbsch & Sangvichien is described for a crustose lichen occurring in dry evergreen forest in Thailand. It is characterised by a green to yellow-green corticated thallus, perithecia fused in black pseudostromata with white rim surrounding the ostiole and small, hyaline and muriform ascospores. Currently, all species in the genus *Architrypethelium* have transversely septate ascospores, hence the discovery of this new species indicates that ascospore septation is variable within the genus, similar to numerous other groups of lichen-forming ascomycetes. Phylogenetic analyses of two loci (mtSSU and nuLSU) supported the position of the new species within *Architrypethelium*. This is the first report of the genus in Southeast Asia.

Keywords

Lichens, taxonomy, phylogeny, tropical diversity, Southeast Asia, Trypetheliales

Introduction

The genus *Architrypethelium* Aptroot (Ascomycota, Dothideomycetes, Trypetheliales) includes crustose lichens with perithecioid ascomata growing on tree bark in the tropics (Aptroot 1991, Aptroot et al. 2008, Aptroot and Lücking 2016). The genus accommodates species with a corticate thallus, solitary or aggregate ascomata with apical or eccentric ostioles, a clear or interspersed hymenium and hyaline or brown, 3–5 septate, transversely septate ascospores (Aptroot et al. 2008, Aptroot and Lücking 2016). Although, *Architrypethelium* is morphologically similar to *Astrothelium* species, the two genera have been shown to be distantly related. The latter genus fell into two clades (Lücking et al. 2016) with one being a sister group to *Architrypethelium*. Phenotypically *Architrypethelium* differs from *Astrothelium* in having predominantly large ascospore without diamond-shaped lumina when mature (Aptroot 1991, Aptroot et al. 2008, Nelsen et al. 2014, Aptroot and Lücking 2016, Lücking et al. 2016b). Another genus with muriform ascospores is *Aptrootia*, which also shares an astrothelioid stage in the young ascospores (Lücking et al. 2016) and the genus formed a sister-group to a clade including *Architrypethelium* and *Astrothelium* p.pt. further calling the generic delimitation in the family in question. Morphologically, *Aptrootia* differs from *Astrothelium* in having dark brown ascospores with a hard outer shell (Lücking et al. 2016). While most genera in Trypetheliaceae, such as *Astrothelium* s.str., *Bathelium*, *Polymeridium* and *Viridothelium* include species with various ascospore types (Hyde et al. 2013, Nelsen et al. 2014, Aptroot and Lücking 2016, Lücking et al. 2016b), the species of *Architrypethelium* shared a similar ascospore morphology (Nelsen et al. 2014, Lücking et al. 2016b).

Previously, three species were accepted in *Architrypethelium* (Aptroot 1991, Aptroot et al. 2008). Recently, the numbers of species increased with the description of two new species and two combinations into the genus (Aptroot and Lücking 2016, Flakus et al. 2016, Lücking et al. 2016a). Currently, seven species are accepted in *Architrypethelium*, viz. *Architrypethelium columbianum* (Nyl.) Aptroot & Lücking, *Architrypethelium grande* (Kremp.) Aptroot & Lücking, *Architrypethelium hyalinum* Aptroot, *Architrypethelium lauropaluanum* Lücking, Nelsen & Marcelli, *Architrypethelium nitens* (Fée) Aptroot, *Architrypethelium penuriixanthum* Flakus & Aptroot, and *Architrypethelium uberinum* (Fée) Aptroot (Aptroot 1991, Aptroot et al. 2008, Aptroot and Lücking 2016, Flakus et al. 2016, Lücking et al. 2016a). All species are known from the Neotropics, except *A. uberinum*, which is also known from Oceania (Aptroot and Lücking 2016, Flakus et al. 2016, Lücking et al. 2016a), suggesting a pantropical distribution (Aptroot and Lücking 2016). Until now, the genus *Architrypethelium* has not been known from southeast Asia. Here we describe a new species from Thailand, which has a rich pyrenocarpous lichen flora (Buaruang et al. 2017), with muriform ascospores, confirming its presence in southeast Asia. Further, we provide phylogenetic evidence to support its placement in the genus *Architrypethelium* and hence demonstrating that the ascospore septation is also variable in this genus.

Material and methods

Specimen collection and phenotypical studies

The material of the new species was found in a dry evergreen forest of the north-eastern region in Thailand. Morphology was studied using an Olympus SZ11 dissecting microscope and free hand sections were mounted in distilled water and studied using an Olympus BX53 compound microscope with differential interference contrast (DIC) (Olympus U-DICT), connected to a Canon EOS650 digital camera. Secondary metabolites were studied using thin-layer chromatography (TLC) with standard solvent A (Orange et al. 2001, Lumbsch 2002).

Molecular data

Genomic DNA of the holotype was extracted from the dried lichen thallus using the CTAB method with chloroform precipitation (Cubero and Crespo 2002). DNA amplification was performed for mitochondrial small subunit ribosomal DNA (mtSSU) and nuclear large subunit ribosomal DNA (nuLSU) using primer pairs mrSSU1 (Zoller et al. 1999) with MSU7 (Zhou and Stanosz 2001) and LR0R with LR3 (Vilgalys and Hester 1990), respectively. PCR reaction mixture was prepared in a total volume of 50 µl, consisting of 5 µl of 10× *Pfu* Buffer with MgSO₄, 2mM of dNTP mix, 20 µM of each primer, 1.25 U of *Pfu* DNA Polymerase (Thermo Fisher Scientific Inc.) and 5 µl of 1/10 dilution of DNA solution. PCR was performed using a thermal cycler Life ECO (Hangzhou Bioer Technology Co., China) as follows: initial denaturation for 1 min at 94 °C and 38 cycles of 94 °C for 1 min, 52 °C for 45 s (LR0R/LR3) and 53 °C for 45 s (mrSSU1/MSU7), followed by an extension at 72 °C for 1 min and a final extension at 72 °C for 5 min. DNA purification and sequencing methods followed Luangsuphabool et al. (2016).

Phylogenetic analysis

The new sequences were aligned with other species of *Architrypethelium* and other Trypetheliaceae from GenBank (Table 1). *Aptrootia* and *Astrothelium* s. lat. have been shown to be the sister groups to *Architrypethelium* (Lücking et al. 2016b) and two taxa of *Bathelium madreporiforme* were used as the outgroup. The DNA datasets (mtSSU and nuLSU) were aligned separately using MUSCLE (Edgar 2004) and improved manually using MEGA v.7 (Kumar et al. 2016). The nucleotide substitution model for maximum likelihood (ML) and Bayesian inference (BI) analyses was chosen using jModelTest v.2.1.4 (Darriba et al. 2012) with the Akaike Information Criterion (AIC). The ML tree was performed on the CIPRES supercomputer using the programme RAxML-HPC2 v.8.2.10 on XSEDE (Miller et al. 2010) and bootstrap values were estimated with 1000 pseudo-

Table 1. Species, location, voucher information and GenBank accession numbers for samples used in this study. Newly obtained sequences in bold and missing data are indicated by [-].

Species	Isolate	Country	Voucher information	GenBank accession No.	
				mtSSU	nuLSU
<i>Aptrootia elatior</i>	MPN560B	New Zealand	<i>Knight</i> O61815 (OTA)	KM453821	KM453754
<i>A. robusta</i>	MPN235B	Australia	<i>Lumbsch</i> 20012 (F)	KM453822	KM453755
<i>A. terricola</i>	DNA1501	Costa Rica	<i>Lücking</i> 17211 (F)	DQ328995	KM453756
<i>Architrypethelium lauropaluanum</i>	MPN48	Peru	<i>Nelsen</i> Cit1P (F)	KX215566	KX215605
<i>A. nitens</i>	MPN257	Panama	<i>Lücking</i> 27038 (F)	KM453823	KM453757
<i>A. uberinum</i>	MPN489	Brazil	<i>Nelsen</i> s. n. (F)	[-]	KM453758
<i>A. murisporum</i>	UBN215	Thailand	<i>Luangsaphabool</i> 031332 (RAMK)	LC361339	LC361340
<i>Astrothelium endochryseum</i>	MPN436	Brazil	<i>Lücking</i> 31088 (F)	KM453837	KM453772
<i>A. subendochryseum</i>	MPN202B	El Salvador	<i>Lücking</i> 28121 (F)	[-]	KX215659
<i>A. scorizum</i>	MPN336	Brazil	<i>Lücking</i> 29814 (F)	KM453872	KM453808
<i>A. obtectum</i>	MPN422	Brazil	<i>Lücking</i> 31242 (F)	KM453832	KM453767
<i>A. laevithallinum</i>	MPN442	Brazil	<i>Lücking</i> 31061 (F)	KM453836	KM453771
<i>A. subinterjectum</i>	MPN157	Brazil	<i>Nelsen</i> B15 (F)	KX215583	KX215660
<i>Bathelium madreporiforme</i>	NAN95	Thailand	<i>Luangsaphabool</i> 027903 (RAMK)	LC128029	LC127414
<i>B. madreporiforme</i>	UBN147	Thailand	<i>Luangsaphabool</i> 027904 (RAMK)	LC128028	LC127413

replicates. Bayesian inference analysis and posterior probabilities were calculated using MrBayes v.3.2.1 (Ronquist and Huelsenbeck 2003) with the Markov chain Monte Carlo (MCMC) algorithm. Four chains and two independent runs were carried out with 10 million generations. Every 100th tree was saved into a file and aborting the analysis was set at the mean standard deviation < 0.01. Tree topology of both ML and BI analyses was illustrated using FigTree v.1.4.2 ([http:// tree.bio.ed.ac.uk/software/figtree/](http://tree.bio.ed.ac.uk/software/figtree/)).

Results and discussion

Two new DNA sequences of mtSSU and nuLSU were generated for this study (Table 1). The alignment matrix contained 609 unambiguously aligned nucleotide position characters, including 200 mtSSU and 409 nuLSU positions. The GTR+I+G model was chosen as the best-fit model for phylogenetic analyses. The topology of single locus analyses did not show any conflicts and hence the combined data set was used for the analysis. The posterior probabilities of the BI analysis together with the ML bootstrap values are both shown in the ML tree (Fig. 1).

The tree topology supported the fact that the new species is part of the genus *Architrypethelium* with strong support values (Fig. 1). Although the morphological characters of the new species would place it in the genus *Astrothelium* (Fig. 2), the shape of ascospore lumina is somewhat different from *Astrothelium* in having rounded-shaped

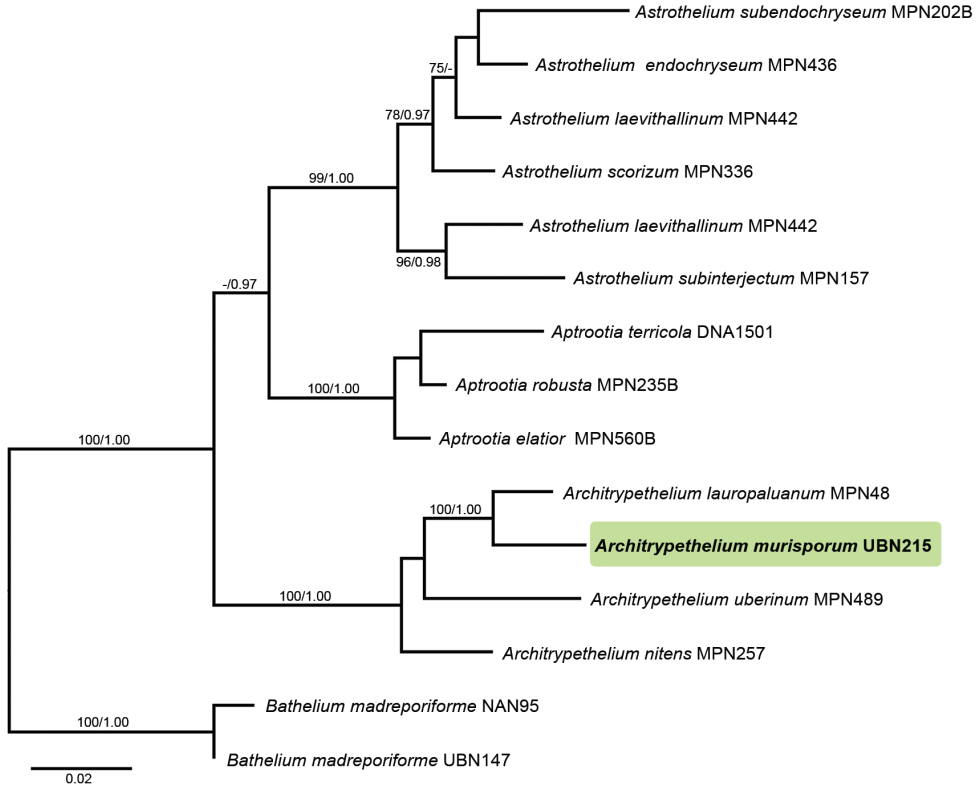


Figure 1. Phylogenetic relationships of *Architrypethelium* and sister genera based on a combined data set of two DNA loci (mtSSU and nuLSU rDNA). Bootstrap values $\geq 70\%$ and posterior probabilities ≥ 0.95 are shown at above and below branches.

lumina (Fig. 2C) (Aptroot and Lücking 2016). This new species seems to be closer related to species with hyaline ascospore (*Architrypethelium lauropaluanum*) than brown ascospores (*A. nitens* and *A. uberinum*) (Aptroot 1991, Aptroot et al. 2008, Lücking et al. 2016a). So far, all species in *Architrypethelium* had large, transversely septate ascospores (Aptroot and Lücking 2016). However, our new species has small, muriform ascospores (Fig. 2B–C). The ascospore ontogeny in the new species resembles that of *Architrypethelium* spp. (Sweetwood et al. 2012), but continues septation to form muriform spores and the endospore is reduced when mature.

The variation of ascospore size and septation in *Architrypethelium* is not surprising given the variation of ascospores in other genera of Trypetheliaceae. This phenomenon is also commonly found in many genera in families of non-lichenised ascomycetes, viz. Lophiostomataceae and Melanommataceae (Mugambi and Huhndorf 2009) and lichenised families, such as Graphidaceae and Pyrenulaceae (Lücking 2009, Aptroot 2012, Weerakoon et al. 2012, Aptroot and Lücking 2016, Gueidan et al. 2016), which supports the fact that ascospore characters are often poor predictors of phylogenetic relationships (Nelsen et al. 2014, Lücking et al. 2016b).

Taxonomic treatment

Architrypethelium murisporum Luangsaphabool, Lumbsch & Sangvichien, sp. nov.

MycoBank: MB823970

Figure 2

Type. THAILAND. Ubon Ratchathani Province: Na Pho Klang, Khong Chiam District, 15°31'N, 105°35'E, ca. 130 m alt., dry evergreen forest, on tree bark, 27 November 2012, *T. Luangsaphabool* RAMK 031332 (holotype: RAMK).

Diagnosis. Characterised within the genus by having small, hyaline and muriform ascospores.

Etymology. The specific epithet refers to the muriform ascospore character of the new species.

Description. Thallus crustose, corticate, thick, green to yellow-green, smooth to uneven, with cortex 40–125 µm thick, medulla 20–75 µm thick, prothallus black. Algae trentepohlioid, cells 18–65 µm wide. Ascomata perithecia, pyriform, black, 0.45–0.60 mm diam., erupent to prominent, fused into a pseudostroma, not covered by thallus. Ascoma wall carbonised, up to ca. 145 µm thick. Ostiole apical, black, not shared, with a white annulus surrounding the ostiolar region. Pseudostroma forming raised black lines, irregular in shape or forming a partial network on the thallus. Hamathecium hyaline, not interspersed with droplets or granules, consisting of branched and anastomosing paraphyses, 1.5–2.5 µm thick. Asci clavate to cylindrical, 150–200 × 32–50 µm. Ascospores 8 per ascus, hyaline, muriform with 6–9 transverse and 1–2 longitudinal septa per tier near centre of spore in optical section, narrowly ellipsoid, 35–50 × 13–15.5 µm. Pycnidia not observed.

Secondary chemistry. Thallus UV–, K–, C–, KC–, PD–; pseudostroma UV–, K–, C–, KC–, PD–. TLC: no substances detected.

Distribution and ecology. The new species was found in north-eastern Thailand, growing in a dry evergreen forest on tree bark. It is only known from the type locality.

Notes. *Architrypethelium murisporum* is morphologically similar to *Astrothelium keralense* (Upreti & Ajay Singh) Aptroot & Lücking and *A. variatum* (Nyl.) Aptroot & Lücking in having hyaline, small and muriform ascospores, but differs in having ascomata fused into a pseudostroma and not covered by the thallus (ascomata solitary, covered by the thallus in *A. keralense* and ascomata covered by thallus except ostiole regions in *A. variatum*), narrowly ellipsoid ascospores (fusiform in both *Astrothelium* spp.). Also the ascospore size (35–50 × 13–15.5 µm) differs from *A. keralense* (50–60 × 15–20 µm) and *A. variatum* (24–35 × 11–13 µm). The placement of the new species in *Architrypethelium* is supported by molecular evidence (Fig 1), but it is unlikely to be confused with any of the currently accepted species in that genus due to the differences in ascospore size and septation (Aptroot et al. 2008, Aptroot and Lücking 2016, Flakus et al. 2016, Lücking et al. 2016a). The new taxon has muriform and relatively small ascospores (ca. 50 µm, long) (Fig 2), whereas other *Architrypethelium* species have transversely septate ascospores (3–5 septate), that are longer than 90 µm (Aptroot 1991, Aptroot et al. 2008, Aptroot and Lücking 2016, Flakus et al. 2016, Lücking et al. 2016a).

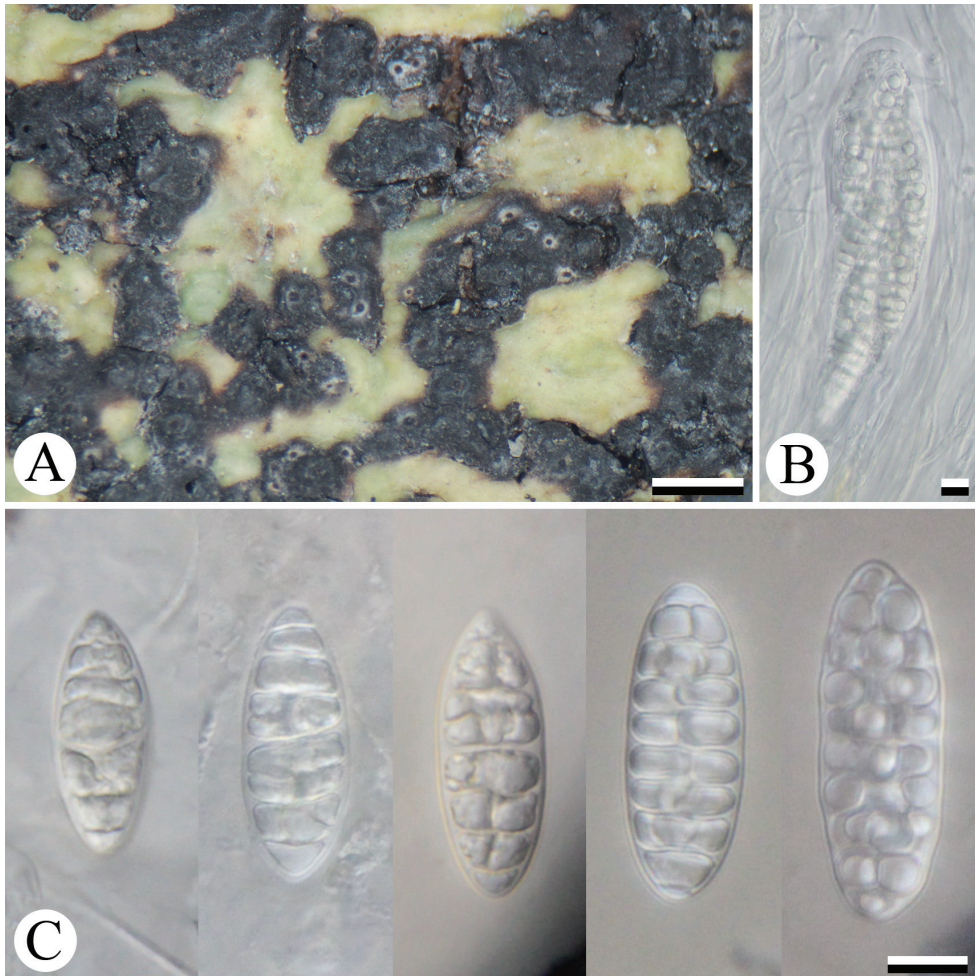


Figure 2. Morphological characters of *Architrypethelium murisporum* (holotype): **A** thallus and pseudostromata with ascomata **B** ascus with ascospores and **C** ascospores. Scale bars: 1 mm (**A**); 10 μ m (**B–C**).

Acknowledgements

This study was financially supported by the Royal Thai Government through Ramkhamhaeng University. We would like to thank Kansri Boonpragob and Kajonsak Vongshewarat for their helpful suggestions and Montri Sanglarpharoenkit for their assistance during fieldwork.

References

Aptroot A (1991) A monograph of the Pyrenulaceae (excluding *Anthracothecium* and *Pyrenula*) and the Requiennellaceae, with notes on the Pleomassariaceae, the Trypetheliaceae, and

- Mycomicrothelia* (lichenized and non-lichenized ascomycetes). *Bibliotheca Lichenologica* 44: 1–178.
- Aptroot A (2012) A world key to the species of *Anthracotheceium* and *Pyrenula*. *Lichenologist* 44: 5–53. <https://doi.org/10.1017/S0024282911000624>
- Aptroot A, Lücking R (2016) A revisionary synopsis of the Trypetheliaceae (Ascomycota: Trypetheliales). *Lichenologist* 48: 763–982. <https://doi.org/10.1017/S0024282916000487>
- Aptroot A, Lücking R, Sipman HJM, Umaña L, Chaves JL (2008) Pyrenocarpous lichens with bitunicate asci. A first assessment of the lichen biodiversity inventory in Costa Rica. *Bibliotheca Lichenologica* 97: 1–162.
- Buaruang K, Boonpragob K, Mongkolsuk P, Sangvichien E, Vongshewarat K, Polyiam W, Rangsiruji A, Saipunkaew W, Naksuwankul K, Kalb K, Parnmen S, Kraichak E, Phraphuchamnonng P, Meesim P, Luangsaphabool T, Nirongbut P, Poengsungnoen V, Duangphui N, Sodamuk M, Phokaeo S, Molsil M, Aptroot A, Kalb K, Lücking R, Lumbsch HT (2017) A new checklist of lichenized fungi occurring in Thailand. *Myckeys* 23: 1–91. <https://doi.org/10.3897/mycokeys.23.12666>
- Cubero OF, Crespo A (2002) Isolation of nucleic acids from lichens. In: Kranner I, Beckett R, Varma A (Eds) *Protocols in Lichenology*. Springer-Verlag Berlin Heidelberg, 381–391. https://doi.org/10.1007/978-3-642-56359-1_23
- Darriba D, Taboada GL, Doallo R, Posada D (2012) jModelTest 2: more models, new heuristics and parallel computing. *Nature Methods* 9: 772. <https://doi.org/10.1038/nmeth.2109>
- Edgar RC (2004) MUSCLE: multiple sequence alignment with high accuracy and high throughput. *Nucleic Acids Research* 32: 1792–1797. <https://doi.org/10.1093/nar/gkh340>
- Flakus A, Kukwa M, Aptroot A (2016) Trypetheliaceae of Bolivia: an updated checklist with descriptions of twenty-four new species. *Lichenologist* 48: 661–692. <https://doi.org/10.1017/S0024282915000559>
- Gueidan C, Aptroot A, Cáceres MEDS, Binh NQ (2016) Molecular phylogeny of the tropical lichen family Pyrenulaceae: contribution from dried herbarium specimens and FTA card samples. *Mycological Progress* 15: 7. <https://doi.org/10.1007/s11557-015-1154-8>
- Hyde KD, Jones EBG, Liu J-K, Ariyawansa H, Boehm E, Boonmee S, Braun U, Chomnunti P, Crous PW, Dai D-Q, Diederich P, Dissanayake A, Doilom M, Doveri F, Hongsanan S, Jayawardena R, Lawrey JD, Li Y-M, Liu Y-X, Lücking R, Monkai J, Muggia L, Nelsen MP, Pang K-L, Phookamsak R, Senanayake IC, Shearer CA, Suetrong S, Tanaka K, Thambugala KM, Wijayawardene NN, Wikee S, Wu H-X, Zhang Y, Aguirre-Hudson B, Alias SA, Aptroot A, Bahkali AH, Bezerra JL, Bhat DJ, Camporesi E, Chukeatirote E, Gueidan C, Hawksworth DL, Hirayama K, Hoog SD, Kang J-C, Knudsen K, Li W-J, Li X-H, Liu Z-Y, Mapook A, McKenzie EHC, Miller AN, Mortimer PE, Phillips AJL, Raja HA, Scheuer C, Schumm F, Taylor JE, Tian Q, Tibpromma S, Wanasinghe DN, Wang Y, Xu J-C, Yacharoen S, Yan J-Y, Zhang M (2013) Families of Dothideomycetes. *Fungal Diversity* 63: 1–313. <https://doi.org/10.1007/s13225-013-0263-4>
- Kumar S, Stecher G, Tamura K (2016) MEGA7: Molecular Evolutionary Genetics Analysis Version 7.0 for Bigger Datasets. *Molecular Biology and Evolution* 33: 1870–1874. <https://doi.org/10.1093/molbev/msw054>

- Luangsaphabool T, Lumbsch HT, Aptroot A, Piapukiew J, Sangvichien E (2016) Five new species and one new record of *Astrothelium* (Trypetheliaceae, Ascomycota) from Thailand. *Lichenologist* 48: 727–737. <https://doi.org/10.1017/S0024282916000499>
- Lücking R (2009) The taxonomy of the genus *Graphis sensu* Staiger (Ascomycota: Ostropales: Graphidaceae). *Lichenologist* 41: 319–362. <https://doi.org/10.1017/S0024282909008524>
- Lücking R, Nelsen MP, Aptroot A, Benatti MN, Binh NQ, Gueidan C, Gutiérrez MC, Jungbluth P, Lumbsch HT, Marcelli MP, Moncada B, Naksuwankul K, Orozco T, Salazar-Allen N, Upreti DK (2016a) A pot-pourri of new species of Trypetheliaceae resulting from molecular phylogenetic studies. *Lichenologist* 48: 639–660. <https://doi.org/10.1017/S0024282916000475>
- Lücking R, Nelsen MP, Aptroot A, Klee RB, Bawingan PA, Benatti MN, Binh NQ, Bungartz F, Cáceres MES, Canèz LS, Chaves JL, Ertz D, Esquivel RE, Ferraro LI, Grijalva A, Gueidan C, Hernández JE, Knight A, Lumbsch HT, Marcelli MP, Mercado-Díaz JA, Moncada B, Morales EA, Naksuwankul K, Orozco T, Parnmen S, Rivas Plata E, Salazar-Allen N, Spielmann AA, Ventura N (2016b) A phylogenetic framework for reassessing generic concepts and species delimitation in the lichenized family Trypetheliaceae (Ascomycota: Dothideomycetes). *Lichenologist* 48: 739–762. <https://doi.org/10.1017/S0024282916000505>
- Lumbsch HT (2002) Analysis of phenolic products in lichens for identification and taxonomy. In: Kranner I, Beckett R, Varma A (Eds) *Protocols in Lichenology*. Springer-Verlag Berlin Heidelberg, 281–295. https://doi.org/10.1007/978-3-642-56359-1_17
- Miller M, Pfeiffer W, Schwartz T (2010) Creating the CIPRES Science Gateway for inference of large phylogenetic trees. *Proceedings of the Gateway Computing Environments Workshop (GCE)*, New Orleans, LA, USA, 1–8. <https://doi.org/10.1109/GCE.2010.5676129>
- Mugambi GK, Huhndorf SM (2009) Molecular phylogenetics of Pleosporales: Melanommataceae and Lophiostomataceae re-circumscribed (Pleosporomycetidae, Dothideomycetes, Ascomycota). *Studies in Mycology* 64: 103–121. <https://doi.org/10.3114/sim.2009.64.05>
- Nelsen MP, Lücking R, Aptroot A, Andrew CJ, Cáceres M, Plata ER, Gueidan C, Canèz LdS, Knight A, Ludwig LR, Mercado-Díaz JA, Parnmen S, Lumbsch HT (2014) Elucidating phylogenetic relationships and genus-level classification within the fungal family Trypetheliaceae (Ascomycota: Dothideomycetes). *Taxon* 63: 974–992. <https://doi.org/10.12705/635.9>
- Orange A, James PW, White FJ (2001) *Microchemical methods for the identification of lichens*. British Lichen Society, London, 101 pp.
- Ronquist F, Huelsenbeck JP (2003) MrBayes 3: Bayesian phylogenetic inference under mixed models. *Bioinformatics* 19: 1572–1574. <https://doi.org/10.1093/bioinformatics/btg180>
- Sweetwood G, Lücking R, Nelsen MP, Aptroot A (2012) Ascospore ontogeny and discharge in megalosporous Trypetheliaceae and Graphidaceae (Ascomycota: Dothideomycetes and Lecanoromycetes) suggest phylogenetic relationships and ecological constraints. *Lichenologist* 44: 277–296. <https://doi.org/10.1017/S0024282911000740>
- Vilgalys R, Hester M (1990) Rapid genetic identification and mapping of enzymatically amplified ribosomal DNA from several *Cryptococcus* species. *Journal of Bacteriology* 172: 4238–4246. <https://doi.org/10.1128/jb.172.8.4238-4246.1990>

- Weerakoon G, Aptroot A, Lumbsch HT, Wolseley PA, Wijeyaratne SC, Gueidan C (2012) New molecular data on Pyrenulaceae from Sri Lanka reveal two well-supported groups within this family. *Lichenologist* 44: 639–647. <https://doi:10.1017/S0024282912000333>
- Zhou S, Stanosz GR (2001) Primers for amplification of mtSSU rDNA, and a phylogenetic study of *Botryosphaeria* and associated nanomorphic fungi. *Mycological Research* 105: 1033–1044. <https://doi.org/10.1017/S0953756201004592>
- Zoller S, Scheidegger C, Sperisen C (1999) PCR primers for the amplification of mitochondrial small subunit ribosomal DNA of lichen-forming ascomycetes. *Lichenologist* 31: 511–516. <https://doi.org/10.1006/lich.1999.0220>

Diversity of polypores in the Dominican Republic: *Pseudowrightoporia dominicana* sp. nov. (Hericiaceae, Russulales)

Alfredo Vizzini¹, Claudio Angelini^{2,3}, Cristiano Losi⁴, Enrico Ercole¹

1 Department of Life Sciences and Systems Biology, University of Torino, Viale P.A. Mattioli 25, I-10125, Torino, Italy **2** Herbario Jardín Botánico Nacional Dr. Rafael Ma. Moscoso, Apartado 21-9, Santo Domingo, Dominican Republic **3** Via Cappuccini 78, I-33170 Pordenone (PN), Italy **4** Canaregio, 3608 – I-30121 Venezia, Italy

Corresponding author: Alfredo Vizzini (alfredo.vizzini@unito.it)

Academic editor: M. P. Martín | Received 29 March 2018 | Accepted 24 April 2018 | Published 16 May 2018

Citation: Vizzini A, Angelini C, Losi C, Ercole E (2018) Diversity of polypores in the Dominican Republic: *Pseudowrightoporia dominicana* sp. nov. (Hericiaceae, Russulales). MycoKeys 34: 35–45. <https://doi.org/10.3897/mycokeys.34.25371>

Abstract

The new species *Pseudowrightoporia dominicana* is described from the Dominican Republic based on morphological and molecular data (nrITS and nrLSU sequence analyses). It is mainly characterised by pileate basidiomata with a bright pinkish context and a di-trimitic hyphal system. Phylogenetically, it is sister to the African species *P. gillesii* and to the Asiatic *P. japonica*.

Keywords

Basidiomycota, Agaricomycetes, Caribbean Islands, Polypores, Phylogeny, Taxonomy

Introduction

The genus *Wrightoporia* Pouzar, typified with *W. lenta* (Overh. & J. Lowe) Pouzar (Pouzar 1966), is traditionally characterised by resupinate to pileate basidiomata, annual to perennial habit, small to medium pores and cottony to hard texture. Hyphal system monomitic to di-trimitic, generative hyphae clamped or rarely with simple septa, skeletal hyphae dextrinoid, partially dextrinoid (only in the tubes) or not dextrinoid. Basidiospores small, cylindrical to globose, smooth to finely asperulate, amyloid

(Ryvarden 1982, 2016; David and Raichenberg 1987, Stalpers 1996, Núñez and Ryvarden 2001, Hattori 2008). To date, there are 52 species transferred to or described in the genus (Index Fungorum 2018). This genus belongs to the Hericiaceae, in the Russulales (Larsson and Larsson 2003, Chen et al. 2016).

Chen et al. (2016), on the basis of combined nrITS/nrLSU phylogenetic analyses and morphological data, indicated that the genus *Wrightoporia*, as currently circumscribed, is strongly polyphyletic and recognised six clades in *Wrightoporia* s.l. Consequently, species previously treated in *Wrightoporia* were transferred to *Amylonotus* Ryvarden, *Amylosporus* Ryvarden and to the three new genera *Larssoniporia* Y.C. Dai, Jia J. Chen & B.K. Cui, *Pseudowrightoporia* Y.C. Dai, Jia J. Chen & B.K. Cui and *Wrightoporiopsis* Y.C. Dai, Jia J. Chen & B.K. Cui. In particular, the genus *Pseudowrightoporia* was established by Chen et al. (2016) to accommodate *Wrightoporia cylindrospora* Ryvarden (the generic type), *W. japonica* Núñez & Ryvarden, *Pseudowrightopora crassihypha* Y.C. Dai, Jia J. Chen & B.K. Cui, *P. hamata* Y.C. Dai, Jia J. Chen & B.K. Cui and *P. oblongispora* Y.C. Dai, Jia J. Chen & B.K. Cui, species causing white rot and mostly characterised by soft corky to corky basidiomes, shining pores, dimitic hyphal structure with clamped generative hyphae and skeletal hyphae, ellipsoid, finely asperulate and amyloid basidiospores and a subtropical to tropical distribution. Based only on these morphological characteristics, the following species were transferred to *Pseudowrightoporia*: *Wrightoporia africana* Johans. & Ryvarden, *W. aurantipora* T. Hatt., *W. gillesii* A. David & Rajchenb., *W. solomonensis* (Corner) T. Hatt. and *W. straminea* T. Hatt.

During the species diversity study of wood-inhabiting macromycetes in the Dominican Republic, a pileate *Pseudowrightoporia* was discovered. The aim of this investigation was to identify and to analyse the *Pseudowrightoporia* specimens using both morphological and molecular techniques.

Materials and methods

Morphology

Photographs of fresh basidiomata were taken *in situ* by a Nikon Coolpix 8400 digital camera and then dried, while the photos of the microscopical structures were obtained through a Olympus BH-2 light microscope and a Nikon D7100 digital camera. For microscopical analysis, tiny fragments from dried material were mounted in Melzer's anionic reagent for testing amyloid and dextrinoid reactions of spores and other microscopical elements. All microscopic measurements were carried out with a $\times 1000$ oil immersion objective. Basidiospores were measured from hymenophores of mature basidiomes, dimensions are given as: (minimum–) average minus standard deviation – average – average plus standard deviation (–maximum) of length \times (minimum–) average minus standard deviation – average – average plus standard deviation (–maximum) of width; Q = (minimum–) average minus standard deviation – average – average plus

standard deviation (–maximum) of the length/width ratio. Spore statistics were produced using R version 3.4.4 (R Core Team 2018). Herbarium acronyms follow Thiers (2018, continuously updated) with the exception of ANGE that refers to the personal herbarium of C. Angelini.

DNA extraction, PCR amplification and DNA sequencing

Genomic DNA was isolated from 10 mg of a dried voucher specimen (JBSD 127410), using the DNeasy Plant Mini Kit (Qiagen, Milan) according to the manufacturer's instructions. Primers LR0R/LR6 (Vilgalys and Hester 1990, Vilgalys lab. <http://www.botany.duke.edu/fungi/mycolab>) were used for the nrLSU (28S) DNA amplification and universal primers ITS1F/ITS4 for the ITS region amplification (White et al. 1990, Gardes and Bruns 1993). Amplification reactions were performed in a PE9700 thermal cycler (Perkin-Elmer, Applied Biosystems, Norwalk) in 25 ml reaction mixtures using the following final concentrations or total amounts: 5 ng DNA, 1 × PCR buffer (20 mM Tris/HCl pH 8.4, 50 mM KCl), 1 mM of each primer, 2.5 mM MgCl₂, 0.25 mM of each dNTP, 0.5 unit of Taq polymerase (Promega, Madison). The PCR programme was as follows: 3 min at 95 °C for 1 cycle; 30 s at 94 °C, 45 s at 50 °C, 2 min at 72 °C for 35 cycles, 10 min at 72 °C for 1 cycle. PCR products were resolved on a 1% agarose gel and visualised by staining with ethidium bromide. The PCR products were purified with the AMPure XP kit (Beckman Coulter, Pasadena) and sequenced by MACROGEN (Seoul). The sequences were submitted to GenBank (<http://www.ncbi.nlm.nih.gov/genbank/>) and their accession numbers are reported in Figs 1–2.

Sequence alignment, dataset assembly and phylogenetic analysis

Sequences were checked and assembled with Geneious 5.3 (Drummond et al. 2010) and compared to those available in the GenBank database (<http://www.ncbi.nlm.nih.gov/Genbank/>) using the BLASTN algorithm (Altschul et al. 1990). Based on BLASTN results, sequences were selected according to the recent monographic work on *Wrightoporia* s.l. by Chen et al. (2016).

Two phylogenetic analyses were performed: the first, based on a combined nrITS and nrLSU sequences dataset, to focus on the phylogenetic position of the new species in the Russulales (Russuloid clade); the second, based only on a nrITS dataset was restricted to the taxa closely related to *P. dominicana* according with the previous combined data analysis. Alignments were generated for each nrITS and nrLSU dataset using MAFFT (Katoh et al. 2002) with default conditions for gap openings and gap extension penalties. The two alignments were imported into MEGA 6 (Tamura et al. 2013) for manual adjustment. The best-fit substitution model for each single alignment was estimated by both the Akaike information criterion (AIC) and the Bayesian information criterion (BIC) with jModelTest 2 (Darriba et al. 2012). The GTR + G

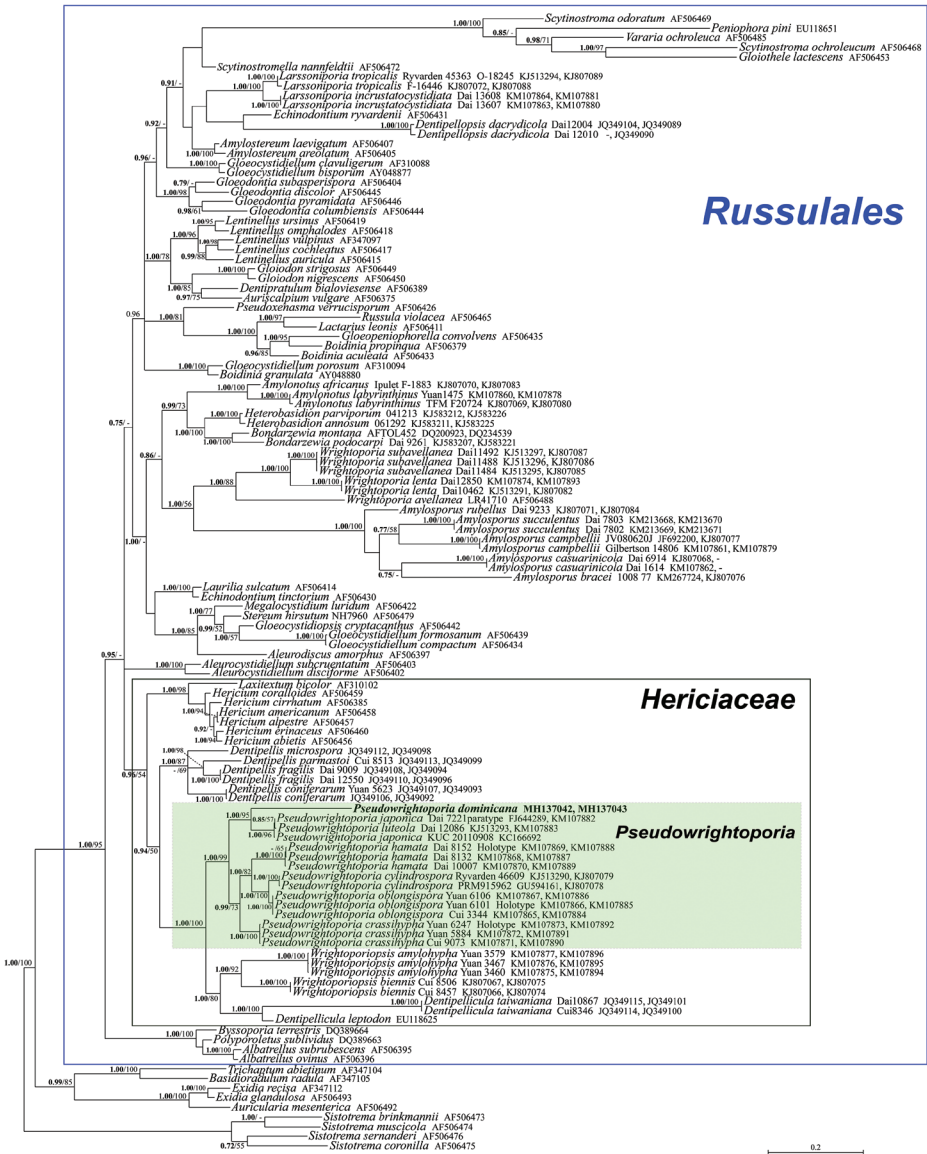


Figure 1. Bayesian phylogram obtained from the combined nrITS-nrLSU sequence alignment of *Russulales* taxa selected according to Chen et al. (2016). *Sistotrema brinkmannii*, *S. coronilla*, *S. muscicola* and *S. sernanderi* were used as outgroup taxa. Values for clades that are supported in either the Bayesian (posterior probabilities, BPP) and Maximum likelihood (ML bootstrap percentage, MLB) analyses are indicated. BPP values (in bold) above 0.70 and MLB values above 50% are given above/below branches. The newly sequenced collection is in bold.

model was chosen for both the nrITS and nrLSU alignments. The sequences of *Sistotrema brinkmannii*, *S. coronilla*, *S. muscicola* and *S. sernanderi* were used as outgroup taxa (Larsson and Larsson 2003, Chen et al. 2016) in the combined analysis; *Dentipel-*

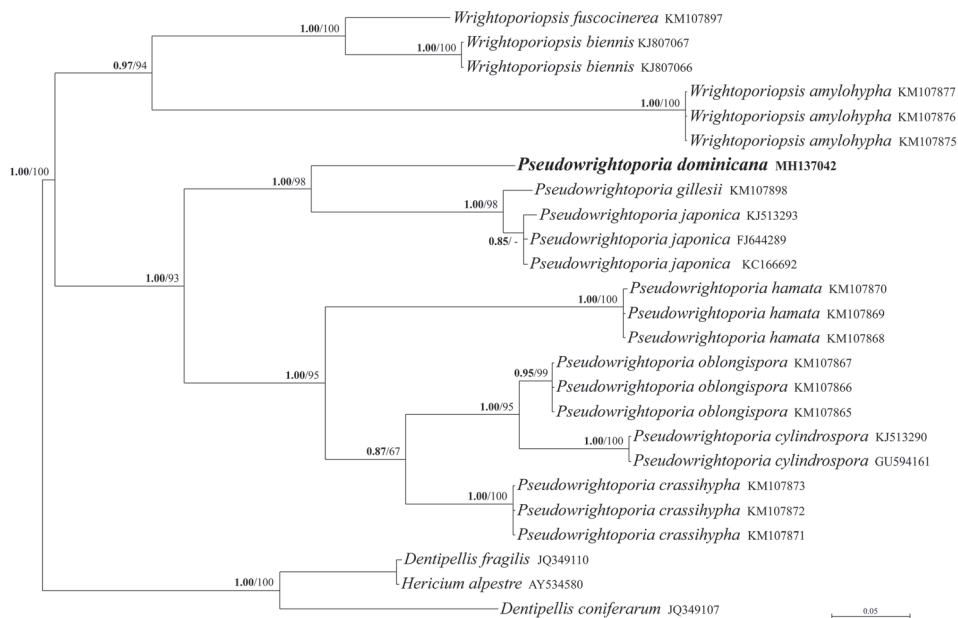


Figure 2. Bayesian phylogram obtained from the nrITS sequence alignment of *Pseudowrightoporia* and *Wrightoporiopsis* species. *Dentipellis coniferarum*, *D. fragilis* and *Hericium alpestre* were used as outgroup taxa. Values for clades that are supported in either the Bayesian (posterior probabilities, BPP) and maximum likelihood (ML bootstrap percentage, MLB) analyses are indicated. BPP values (in bold) above 0.70 and MLB values above 50% are given above/below branches. The newly sequenced collection is in bold.

lis coniferarum, *D. fragilis* and *Hericium alpestre* were selected as outgroup taxa in the nrITS analysis. The ITS dataset was not partitioned into ITS1, 5.8S and ITS2 subsets. Phylogenetic hypotheses were constructed under Bayesian inference (BI) and Maximum likelihood (ML) criteria. The BI was performed with MrBayes 3.2.6 (Ronquist et al. 2012) with one cold and three incrementally heated simultaneous Monte Carlo Markov chains (MCMC) run for 10 million generations, under the selected evolutionary model. Two simultaneous runs were performed independently. Trees were sampled every 1,000 generations, resulting in overall sampling of 10,001 trees per single run; the first 2,500 trees (25%) were discarded as burn-in. For the remaining trees of the two independent runs, a majority rule consensus tree showing all compatible partitions was computed to obtain estimates for Bayesian posterior probabilities (BPP). ML estimation was performed through RAxML 7.3.2 (Stamatakis 2006) with 1,000 bootstrap replicates using the GTRGAMMA algorithm to perform a tree inference and search for a good topology. Support values from bootstrapping runs (MLB) were mapped on the globally best tree using the “-f a” option of RAxML and “-x 12345” as a random seed to invoke the novel rapid bootstrapping algorithm. BI and ML analyses were run on the CIPRES Science Gateway web server (Miller et al. 2010). Only BPP and MLB values over 0.70 and 50%, respectively, are reported in the resulting trees (Figs 1–2). Branch lengths were estimated as mean values over the sampled trees.

Results

The combined nrITS and nrLSU data matrix comprised 118 sequences (including 117 from GenBank) and includes 2132 positions. The nrITS data matrix comprises a total of 25 sequences (including 24 from GenBank) and includes 687 positions. As both Bayesian and Maximum likelihood analyses produced comparable topologies, only the Bayesian trees with both BPP and MLB values are shown (Figs 1–2). In the combined two-gene phylogeny of Russulales taxa (Fig. 1), the new species falls, as an independent phylogenetic branch, in the Hericiaceae within the *Pseudowrightoporia* cluster. *Pseudowrightoporia dominicana* is sister (BPP = 1.00, MLB = 95) to *P. japonica*. *Pseudowrightoporia* is shown to be sister (BPP = 1.00, MLB = 100) to a well-supported clade (BPP = 1.00, MLB = 80) consisting of *Wrightoporiopsis* and *Dentipellicula*, as previously highlighted by Chen et al. (2016). The small ITS analysis restricted to species of *Pseudowrightoporia* and *Wrightoporiopsis* (Fig. 2) supports *P. dominicana* as a new species and indicates *P. gillesii* and *P. japonica* as its phylogenetically closest species.

Taxonomy

Pseudowrightoporia dominicana Angelini, Losi & Vizzini, sp. nov.

Mycobank MB824844

Fig. 3

Holotype. Dominican Republic. La Vega (Province), Jarabacoa (Municipality), Montaña (Locality), 19°06'39"N, 70°37'57"W, on an unidentified live trunk of a deciduous tree, in a mixed mountain forest with several broadleaved species and pines (*Pinus occidentalis*), 17 December 2016, Claudio Angelini, (JBSD 127410, isotype ANGE 789).

Etymology. The epithet refers to the country, The Dominican Republic, where this species was found.

Basidiomata annual, pileate, sessile, single or in small clusters, fibrous-tough (Fig. 3a and b). Pileus broadly attached to dimidiate, up to 25 mm wide and 15 mm deep, 5–10 mm thick; upper surface white to cream with pinkish tint, velutinate to glabrous, azonate, smooth; margin rounded, even or slightly lobed; pore surface concolorous with the pileus surface, pores round to angular, at first cupulate, 6–8 per mm, dissepiments thick and entire; tube layer 2–4 mm thick, whitish to cream; context pinkish (Fig. 3c), homogenous, tough-fibrous, up to 6 mm thick. Hyphal system di-trimitic; generative hyphae clamped, hyaline, thin-walled, 2.2–4.8 µm wide; skeletal hyphae thick-walled, rarely branched, 2.4–5.6 µm wide, dextrinoid especially in the trama (Fig. 3d); contextual binding hyphae thick-walled, short-branched, 1.6–2.4 µm wide, weakly dextrinoid (Fig. 3e). Cystidia none. Basidia densely united, clavate, 4-sterigmate, 8–12 × 4–5 µm. Basidiospores (2.6–)2.98–3.2–3.43(–3.6) ×

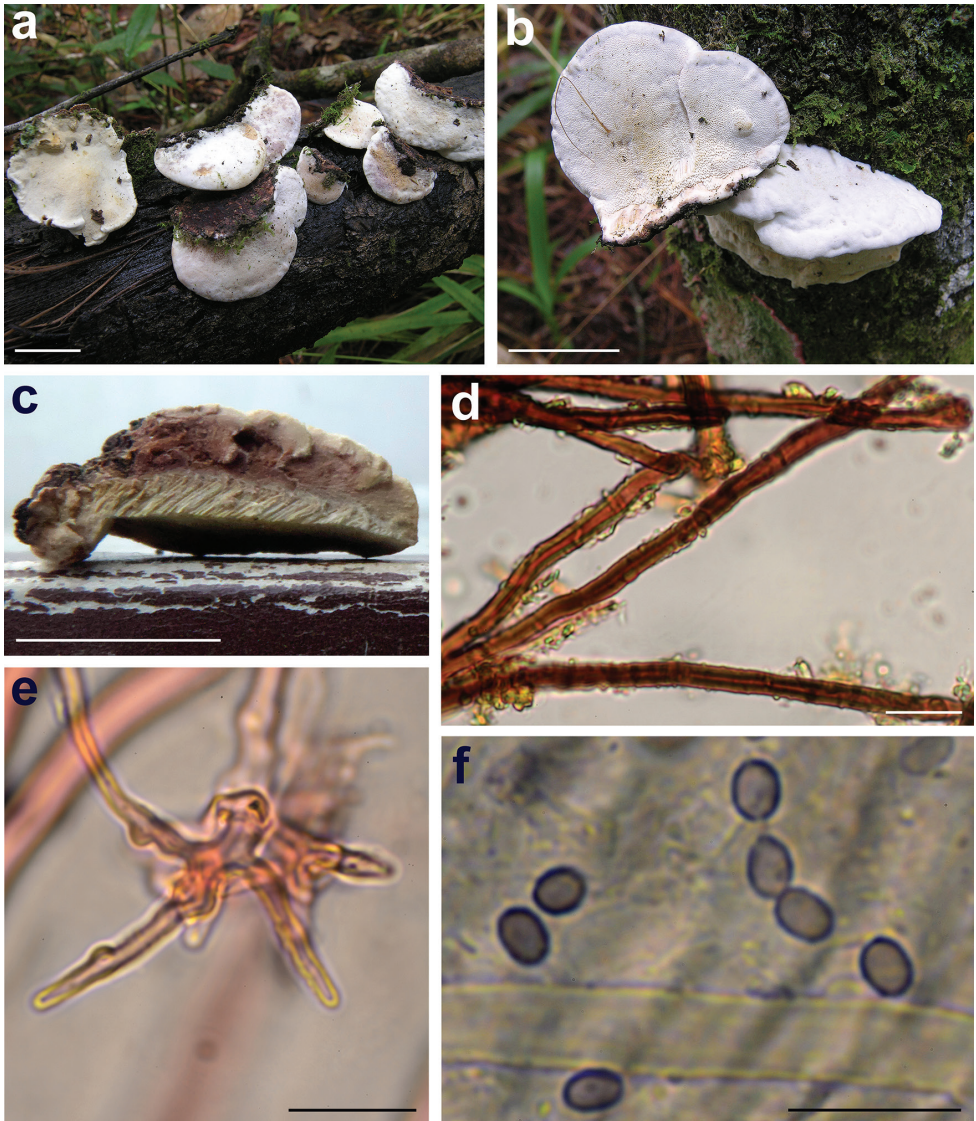


Figure 3. *Pseudowrightoporia dominicana* (JBSD 127410) **a, b** fresh basidiomes in situ **c** cut side of the basidiome **d** dextrinoid skeletal hyphae **e** binding hypha **f** amyloid spores. Microscopical elements observed in Melzer's anionic reagent. Scale bars: 10 mm (**a–c**); 10 μ m (**d–f**).

(1.8–)1.96–2.2–2.44(–2.8) μ m ($n = 40$), $Q = (1.14–)1.28–1.44–1.6(–1.89)$, broadly ellipsoid to ellipsoid, finely asperulate, thin- to slightly thick-walled, distinctly amyloid (Fig. 3f).

Habit, habitat and distribution. Pileate, gregarious on a live trunk of deciduous tree, so far known only from the type locality.

Discussion

All the phylogenetic analyses show *P. dominicana* to be a distinct lineage in the genus *Pseudowrightporia* (Figs 1–2). The new species displays a unique combination of outstanding characters such as pileate basidiomes, pink context, very small spores and di-trimitic hyphal system (Fig. 3). In particular, the presence of binding hyphae (only in the context) is quite unusual in *Pseudowrightporia* as well as in the other genera of *Wrightporia* s.l. (Ryvarden 1982, 1987, 2000, 2016; David and Rajchenberg 1987, Dai 1995, Núñez and Ryvarden 2001, Dai and Cui 2006, Hattori 2008, Chen and Cui 2012, 2014; Chen and Yu 2012, Jang et al. 2013, Westphalen et al. 2014, Chen et al. 2016, Drechsler-Santos et al. 2016, Campi et al. 2017); binding hyphae have so far been reported only in *P. aurantipora* (Hattori 2008), *W. brunneo-ochracea* A. David & Rajchenb. (David and Rajchenberg 1985), *W. trimitica* (Corner) Stalpers (Corner 1989, Stalpers 1996) and *Larssoniporia tropicalis* (Cooke) Y.C. Dai, Jia J. Chen & B.K. Cui, (Núñez and Ryvarden 2001).

Pseudowrightporia gillesii and *P. japonica* are the species phylogenetically most closely related to *P. dominicana* (Figs 1–2). *Pseudowrightporia gillesii*, originally described from Africa (Gabon), is characterised by an effused-reflexed basidiome, chestnut ochraceous context, dimitic context, skeletal hyphae dextrinoid only in the pore mouths and presence of lageniform to mucronate cystidiola (David and Rajchenberg 1987). *Pseudowrightporia japonica* (= *Wrightporia luteola* B.K. Cui & Y.C. Dai according with Jang et al. 2013 and Chen et al. 2016) shows a basidiome shape ranging from pileate (and then with a zoned pileus) to resupinate, a pore surface cream to wood-coloured, a dimitic hyphal system and more elongated spores, up to $4 \times 2.6 \mu\text{m}$ (Núñez and Ryvarden 1999, 2001; Jang et al. 2013).

Amongst the morphologically most similar species to *P. dominicana*, *Wrightporia dimidiata* A. David & Rajchenb. from Asia (Singapore) is distinguished by a hymenophore with 3–4 pores per mm, dimitic hyphal system, spores measuring $3.5\text{--}4 \times 3 \mu\text{m}$ and presence of cystidiola, gloeocystidia and gloeopleurous hyphae (David and Rajchenberg 1987). From above, the new species may resemble the pileate basidiomes of *Wrightporia cremea* Ryvarden from Brazil, but the latter has larger pores (3–4 per mm) and spores (subglobose, $3\text{--}4 \mu\text{m}$ in diam.), dimitic hyphal system, in addition to a cream to pale ochre context (Ryvarden 1987, 2017 and pers. comm.). Finally, *P. aurantipora* from Japan, *W. brunneo-ochracea* from Guadeloupe, *W. trimitica* from Malaya and the pantropical *W. tropicalis* share with *P. dominicana* the presence of binding hyphae, but *P. aurantipora* differs in having resupinate basidiomes with light orange to brown orange 4–6/mm pores, context orange without pinkish hues, tramal skeletal hyphae strongly covered with granules near the tip and longer spores, $3\text{--}4.2 \times 2\text{--}3 \mu\text{m}$ (Hattori 2008); *W. brunneo-ochracea* differs in having effused-reflexed basidiomes with ochraceous, irregular to angular pores, 3–4 per mm, a thin ochraceous context, non-dextrinoid skeletal hyphae and narrower spores, $3\text{--}3.5 \times 2 \mu\text{m}$ (David and Rajchenberg 1985, Ryvarden 2016); *W. trimitica* has dimidiate basidiomes, with a short resupinate foot, ochraceous to wood-coloured pores and up to $4 \mu\text{m}$ long spores (Corner 1989, Stalpers 1996); *Larssoniporia*

tropicalis has resupinate, applanate to pulvinate, widely effused, grey to black perennial and very woody basidiomes, grey to brown pore surface, thick-walled and heavily enrusted cystidia, blunt at the apex, presence of gloecystidia and subglobose spores 3–4 × 2–3 µm (Ryvarden and Johansen 1980, Núñez and Ryvarden 2001, Ryvarden 2016).

Acknowledgements

We are grateful to Leif Ryvarden (University of Oslo) for his valuable comments and suggestions on the new species and to D. Jean Lodge (USDA Forest Service, Luquillo, Puerto Rico) for improving the English text. We also wish to thank Ricardo G. García, Francisco Jiménez, Brígido Peguero, Yuley E. Piñeyro and Alberto Veloz (Jardín Botánico Nacional Dr. Rafael M. Moscoso, Santo Domingo, Dominican Republic) for their interest and encouragement to study the fungi of the Dominican Republic and for their active cooperation in putting at our disposal herbarium material of this institution.

References

- Altschul SF, Gish W, Miller W, Myers EW, Lipman DJ (1990) Basic local alignment search tool. *Journal of Molecular Biology* 215: 403–410. [http://dx.doi.org/10.1016/S0022-2836\(05\)80360-2](http://dx.doi.org/10.1016/S0022-2836(05)80360-2)
- Campi M, Maubet Y, Grassi E, Robledo GL (2017) *Amylosporus guaraniticus* sp. nov. (Wrightporiaceae, Russulales) a new neotropical species from Paraguay. *Mycosphere* 8(6): 1060–1070. <https://doi.org/10.5943/mycosphere/8/6/6>
- Chen JJ, Cui BK (2012) Studies on *Wrightporia* from China 2. A new species and three new records from South China. *Mycotaxon* 21: 333–343. <https://doi.org/10.5248/121.333>
- Chen JJ, Cui BK (2014) Studies on *Wrightporia* from China 3. *Wrightporia subavellanea* sp. nov. based on morphological characters and rDNA sequence data. *Phytotaxa* 175: 225–234. <http://dx.doi.org/10.11646/phytotaxa.175.4.4>
- Chen JJ, Yu HY (2012) Studies on the genus of *Wrightporia* from China 1. A new species described from Hunan Province, South China. *Mycotaxon* 120: 295–300. <http://dx.doi.org/10.5248/120.295>
- Chen JJ, Cui BK, Dai YC (2016) Global diversity and molecular systematics of *Wrightporia* s.l. (Russulales, Basidiomycota). *Persoonia* 37: 21–36. <https://doi.org/10.3767/003158516X689666>
- Corner EJJ (1989) Ad Polyporaceas V. *Beihefte zur Nova Hedwigia* 96: 1–218.
- Cui BK, Dai YC (2006) *Wrightporia* (Basidiomycota, Aphyllophorales) in China. *Nova Hedwigia* 83: 159–166. <https://doi.org/10.1127/0029-5035/2006/0083-0159>
- Dai YC (1995) A new species of *Wrightporia* (Basidiomycetes) from China. *Karstenia* 35: 85–89. <https://doi.org/10.29203/ka.1995.312>
- Dai YC, Cui BK (2006) Two new species of *Wrightporia* (Basidiomycota, Aphyllophorales) from southern China. *Mycotaxon* 96: 199–206.

- Darriba D, Taboada GL, Doallo R, Posada D (2012) jModelTest 2: more models, new heuristics and parallel computing. *Nature Methods* 9(8): 772. <https://doi.org/10.1038/nmeth.2109>
- David A, Rajchenberg M (1985) Pore fungi from French Antilles and Guiana. *Mycotaxon*. 22(2): 285–325.
- David A, Rajchenberg M (1987) A reevaluation of *Wrightoporia* and *Amylonotus* (Aphyllophorales, Polyporaceae). *Canadian Journal of Botany* 65: 202–209. <https://doi.org/10.1139/b87-027>
- Drechsler-Santos ER, Salvador-Montoya CA, Ryvarden L (2016) Studies in neotropical polypores 41. A new species of *Amylosporopus* from Caatinga dry woodlands, Brazil. *Synopsis Fungorum* 35: 4–8.
- Drummond AJ, Ashton B, Cheung M, Heled J, Kearse M, Moir R, Stones-Havas S, Thierer T, Wilson A (2010) Geneious v5.3. Available from <http://www.geneious.com/>
- Gardes M, Bruns TD (1993) ITS primers with enhanced specificity for basidiomycetes – application to the identification of mycorrhizae and rusts. *Molecular Ecology* 2: 113–118. <https://doi.org/10.1111/j.1365-294x.1993.tb00005.x>
- Index Fungorum (2018) <http://www.indexfungorum.org> [Accessed 25 March 2018]
- Hattori T (2008) *Wrightoporia* (Basidiomycota, Hericiales) species and their allies collected in Japan. *Mycoscience* 49: 56–65. <https://doi.org/10.1007/s10267-007-0389-x>
- Katoh K, Misawa K, Kuma K, Miyata T (2002) MAFFT: a novel method for rapid multiple sequence alignment based on fast Fourier transform. *Nucleic Acids Research* 30: 3059–3066. <https://doi.org/10.1093/nar/gkf436>
- Jang Y, Lee SW, Lim YW, Lee JS, Hattori T, Kim J-J (2013) The genus *Wrightoporia* in Korea. *Mycotaxon* 123: 335–341. <https://doi.org/10.5248/123.335>
- Larsson E, Larsson KH (2003) Phylogenetic relationships of russuloid basidiomycetes with emphasis on aphyllophorean taxa. *Mycologia* 95: 1037–1065. <https://doi.org/10.2307/3761912>
- Miller MA, Pfeiffer W, Schwartz T (2010) Creating the CIPRES Science Gateway for inference of large phylogenetic trees. *Proceedings of the Gateway Computing Environments Workshop (GCE)*, 14 November 2010, New Orleans, LA, 1–8. <https://doi.org/10.1109/gce.2010.5676129>
- Núñez M, Ryvarden L (1999) New and interesting polypores from Japan. *Fungal Diversity* 3: 107–121.
- Núñez M, Ryvarden L (2001) East Asian Polypores 2. *Synopsis Fungorum* 14: 170–522.
- Pouzar Z (1966) Studies in the taxonomy of the polypores I. *Česká Mykologie* 20: 171–177. <https://doi.org/10.1007/BF02854587>
- R Core Team (2018) R: a language and environment for statistical computing, version 3.4.4. <http://www.R-project.org>
- Ronquist F, Teslenko M, van der Mark P, Ayres DL, Darling A, Höhna S, Larget B, Liu L, Suchard MA, Huelsenbeck JP (2012) MrBayes 3.2: efficient Bayesian phylogenetic inference and model choice across a large model space. *Systematic Biology* 61: 539–542. <https://doi.org/10.1093/sysbio/sys029>
- Ryvarden L (1982) Synopsis of the genus *Wrightoporia*. *Nordic Journal of Botany* 2: 145–149. <https://doi.org/10.1111/j.1756-1051.1982.tb01174.x>

- Ryvarden L (1987) New and noteworthy polypores from tropical America. *Mycotaxon* 28(2): 525–541.
- Ryvarden L (2000) Studies in neotropical polypores 7. *Wrightoporia* (Hericiaceae, Basidiomycetes) in tropical America. *Karstenia* 40: 153–158. <https://doi.org/10.29203/ka.2000.366>
- Ryvarden L (2016) Neotropical polypores Part 3. Polyporaceae, *Obba-Wrightoporia*. *Synopsis Fungorum* 46: 445–613.
- Ryvarden L, Johansen I (1980) A preliminary polypore flora of East Africa. Oslo, Fungiflora.
- Stalpers JA (1996) The aphyllophoraceous fungi II. Keys to the species of the Hericiales. *Studies in Mycology* 40: 1–185.
- Stamatakis A (2006) RAxML-VI-HPC: Maximum likelihood-based phylogenetic analyses with thousands of taxa and mixed models. *Bioinformatics* 22: 2688–2690. <https://doi.org/10.1093/bioinformatics/btl446>
- Tamura K, Stecher G, Peterson D, Filipski A, Kumar S (2013) MEGA 6: molecular evolutionary genetics analysis version 6.0. *Molecular Biology and Evolution* 30(12): 2725–2729. <https://doi.org/10.1093/molbev/mst197>
- Thiers B (2018, continuously updated) Index Herbariorum: A global directory of public herbaria and associated staff. New York Botanical Garden's Virtual Herbarium. <http://sweetgum.nybg.org/science/ih/> [Accessed 25 March 2018]
- Vilgalys R, Hester M (1990) Rapid genetic identification and mapping of enzymatically amplified ribosomal DNA from several *Cryptococcus* species. *Journal of Bacteriology* 172: 4238–4246. <https://doi.org/10.1128/jb.172.8.4238-4246.1990>
- Westphalen MC, Reck MA, da Silveira RMB (2014) Studies on *Wrightoporia* (Basidiomycota) from southern Brazil. *Phytotaxa* 166(1): 94–100. <https://doi.org/10.11646/phytotaxa.166.1.7>
- White TJ, Bruns T, Lee S, Taylor JW (1990) Amplification and direct sequencing of fungal ribosomal RNA genes for phylogenetics. In: Innis MA, Gelfand DH, Sninsky JJ, White TJ (Eds) *PCR protocols: a guide to methods and applications*. Academic Press Inc., New York, 315–322. <https://doi.org/10.1016/b978-0-12-372180-8.50042-1>

Two novel species of *Neoaquastroma* (Parabambusicolaceae, Pleosporales) with their phoma-like asexual morphs

Chayanard Phukhamsakda^{1,2}, Darbhe J. Bhat³, Sinang Hongsanan¹,
Jian-Chu Xu^{2,4,5}, Marc Stadler⁶, Kevin D. Hyde^{1,2}

1 Center of Excellence in Fungal Research, Mae Fah Luang University, Chiang Rai 57100, Thailand **2** Key Laboratory for Plant Diversity and Biogeography of East Asia, Kunming Institute of Botany, Chinese Academy of Science, Kunming 650201, Yunnan, China **3** Formerly, Department of Botany, Goa University, Goa, India; No. 128/1-J, Azad Housing Society, Curca, Goa Velha, India **4** Germplasm Bank of Wild Species, Kunming Institute of Botany, Chinese Academy of Science, Kunming 650201, Yunnan, China **5** Centre of Mountain Ecosystem Studies, Kunming Institute of Botany, Chinese Academy of Sciences, Kunming 650201, Yunnan, China **6** Department of Microbial Drugs, Helmholtz Centre for Infection Research, Braunschweig, Germany

Corresponding author: Kevin D. Hyde (kdhyde3@gmail.com)

Academic editor: G. Mugambi | Received 20 March 2018 | Accepted 7 May 2018 | Published 23 May 2018

Citation: Phukhamsakda C, Bhat DJ, Hongsanan S, Xu J-C, Stadler M, Hyde KD (2018) Two novel species of *Neoaquastroma* (Parabambusicolaceae, Pleosporales) with their phoma-like asexual morphs. MycoKeys 34: 47–62. <https://doi.org/10.3897/mycokeys.34.25124>

Abstract

The monotypic genus *Neoaquastroma* (Parabambusicolaceae, Pleosporales) was introduced for a microfungus isolated from a collection of dried stems of a dicotyledonous plant in Thailand. In this paper, we introduce two novel species, *N. baubiniaae* and *N. krabiense*, in this genus. Their asexual morphs comprise conidiomata with aseptate and hyaline conidia. *Neoaquastroma baubiniaae* has ascomata, asci and ascospores that are smaller than those of *N. krabiense*. Descriptions and illustrations of *N. baubiniaae* and *N. krabiense* are provided and the two species compared with the type species of the genus, *N. guttulatum*. Evidence for the introduction of the new taxa is also provided from phylogenetic analysis of a combined dataset of partial LSU, SSU, ITS and *tefl* sequence data. The phylogenetic analysis revealed a distinct lineage for *N. baubiniaae* and *N. krabiense* within the family Parabambusicolaceae.

Keywords

Dothideomycetes, holomorph, Massarineae, saprotrophs, Southeast Asia

Introduction

Thailand is a highly biodiverse country in the tropics with hot and humid climate (MacKinnon et al. 1986, Marod and Kutintara 2012). Although the fungal diversity in Thailand has been relatively well-studied (Rostrup 1902, Schumacher 1982, Hyde 1989, Jones 2000, Jones et al. 2006, Suetrong et al. 2009), the number of species being discovered is steadily growing due to increasing activities in studying microfungi in a large variety of terrestrial and aquatic ecosystems (Mapook et al. 2016, Phukhamsakda et al. 2016, Dai et al. 2017, Doilom et al. 2017, Phukhamsakda et al. 2017).

The family Parabambusicolaceae was introduced for a distinct phylogenetic lineage in the suborder Massarineae (Pleosporales) (Tanaka et al. 2015). Species of Parabambusicolaceae are characterised by pseudothecioid ascomata with or without stromatic tissues, papillate to apapillate ostioles, clavate to fusiform asci and hyaline or brown phragmospores (Liu et al. 2015, Tanaka et al. 2015, Li et al. 2016, Wanasinghe et al. 2017). The asexual morphs are sporodochial or *Monodictys*-like (Tanaka et al. 2015, Ariyawansa et al. 2015). Currently, there are seven known genera in this family; *Aquastroma*, *Monodictys*-like spp., *Multilocularia*, *Multiseptospora*, *Neoaquastroma*, *Parabambusicola* (with *P. bambusina* as generic type) and *Pseudomonodictys* (Tanaka and Harada 2003, Wijayawardene et al. 2017, 2018). The genus *Neoaquastroma* Wanas., E.B.G. Jones & K.D. Hyde, has been introduced from a dead twig of a herbaceous plant collected in Northern Thailand and been typified with *N. guttulatum* Wanas., E.B.G. Jones & K.D. Hyde (Wanasinghe et al. 2017). The genus is characterised by immersed, glabrous pseudothecia, short, papillate, fissitunicate, clavate asci and ellipsoidal to sub-fusiform, multi-septate hyaline phragmospores, surrounded by a mucilaginous sheath (Wanasinghe et al. 2017). Molecular phylogenetic analysis using ribosomal DNA (LSU, SSU and ITS) and translation elongation factor 1- α (*tef1*) sequence data support it as a distinct genus in Parabambusicolaceae.

The purpose of this study is to describe two new species of *Neoaquastroma* from collections of dicotyledonous plants in Thailand. Phylogenetic analysis of combined of LSU, SSU, ITS and *tef1* sequence data are provided.

Materials and methods

Sample collection, morphological study and isolation

Fresh specimens were collected from northern and southern part of Thailand during 2015–2017. The specimens were packed into brown paper bags for transport to the laboratory. Pure cultures were obtained from single ascospores on malt extract agar (MEA; 62 g/l) in distilled water following the method of Chomnunti et al. (2014). Cultures were incubated at 25 °C for up to 8 weeks. Induction of asexual reproduction has been adapted from Tanaka and Harada (2003) by placing agar squares with mycelia on water agar placed with sterile rice straw pieces. The plates were incubated at room tempera-

ture (25 °C) with the standard light cycles, 12 hrs in the light followed by 12 hrs in the dark for about eight weeks until the fructifications were produced. Type specimens are deposited in Mae Fah Luang University (MFLU) herbarium and isotypes are deposited at the Kunming Institute of Botany, Academia Sinica Herbarium (HKAS), China. Ex-type living cultures are deposited at the Mae Fah Luang Culture Collection (MFLUCC) and duplicates at the International Collection of Microorganisms and Plants (ICMP), New Zealand. Faces of fungi numbers (Jayasiri et al. 2015) and MycoBank number (<http://www.Mycobank.org>) are provided. Samples were examined under a Nikon ECLIPSE 80i compound microscope and photographed with a Canon 600D digital camera fitted to the microscope. Measurements were made using Tarosoft (R) Image Frame Work programme and photo-plates were made by using Adobe Photoshop CS6 Extended version 10.0 software (Adobe Systems, United States).

DNA extraction, amplification and sequencing

DNA was extracted from mycelium by using Biospin Fungus Genomic DNA Extraction Kit (BioFlux) (Hangzhou, P. R. China) and gene extraction kit (Bio Basic Inc., Canada). PCR amplification was carried out using primers LROR/LR5 for the nuclear ribosomal large subunit 28S rDNA gene (LSU), NS1/NS4 for the nuclear ribosomal small subunit 18S rDNA gene (SSU) and ITS5/ITS4 for internal transcribed spacer rDNA region (ITS1, 5.8S rDNA and ITS2); partial fragments of the translation elongation factor 1-alpha (*tefl*) gene region was amplified using primers EF1-983F and EF1-2218R (Vilgalys and Hester 1990, White et al. 1990, Carbone and Kohn 1999). Primer sequences are available at the WASABI database at the AFTOL website (aftol.org). Amplification reactions for LSU, SSU and ITS followed Phukhamsakda et al. (2016). The PCR thermal cycle programme for EF1-983F and EF1-2218R (Carbone and Kohn 1999) for translation elongation factor 1-alpha (*tefl*) was set for denaturation at 96 °C for 2 min, followed by 40 cycles of denaturation at 96 °C for 45 sec, annealing at 54 °C for 30 sec and extension at 72 °C for 1.30 min, with a final extension step at 72 °C for 5 min. Genomic DNA and PCR amplification products were checked on 1% agarose gel. PCR products were purified as described in Wendt et al. (2017), sequences were generated by Shanghai Sangon Biological Engineering Technology & Services Co. (Shanghai, P.R. China) and sequencing services at Helmholtz Centre For Infection Research (HZI, Braunschweig, Germany).

Sequence alignment and phylogenetic analysis

SeqMan v. 7.0.0 (DNASTAR, Madison, WI) was used to assemble consensus sequences. Sequences of closely related strains were retrieved using BLAST searches against GenBank (<http://www.ncbi.nlm.nih.gov>). We also included the strains from Wanasinthe et al. (2017) and these are listed in Table 1. Sequences were aligned with MAFFT

Table 1. Taxa used in the phylogenetic analysis and their corresponding culture collections, and accession numbers used in this study.

Taxon	Culture accession number(s) ^{1,2}	GenBank accession numbers				References
		LSU	SSU	ITS	<i>tefl</i>	
<i>Aquastroma magniostiolata</i>	CBS 139680^T = MAFF 243824	AB807510	AB797220	LC014540	AB808486	Tanaka et al. 2015
<i>Aquilomyces patris</i>	CBS 135661^T	KP184041	KP184077	KP184002	–	Knapp et al. 2015
<i>Aquilomyces rebunensis</i>	CBS 139684^T	AB807542	AB797252	AB809630	AB808518	Tanaka et al. 2015
<i>Bambusicola massarina</i>	MFLUCC 11-0389^T	JX442037	JX442041	NR_121548	–	Dai et al. 2012
<i>Clypeolocus akitaensis</i>	CBS 139681^T	AB807543	AB797253	AB809631	AB808519	Tanaka et al. 2015
<i>Corynespora cassicola</i>	CBS 100822^T	GU301808	GU296144	–	GU349052	Schoch et al. 2009
<i>Corynespora smithii</i>	CABI 5649b	GU323201	–	FJ852597	GU349018	Schoch et al. 2009
<i>Falciformispora lignatilis</i>	BCC 21117	GU371826	GU371834	KF432942	GU371819	Schoch et al. 2009
<i>Falciformispora senegalensis</i>	CBS 196.79^T	KF015631	KF015636	KF015673	KF015687	Ahmed et al. 2014
<i>Falciformispora tompkinsii</i>	CBS 200.79^T	KF015625	KF015639	NR_132041	KF015685	Ahmed et al. 2014
<i>Helicascus elaterascus</i>	A22-5A = HKUCC 7769	AY787934	AF053727	–	–	Tanaka et al. 2015
<i>Massarina eburnea</i>	CBS 473.64	GU301840	GU296170	–	GU349040	Zhang et al. 2009
<i>Monodictys</i> sp.	KH 331 = MAFF 243826	AB807553	AB797263	–	AB808529	Tanaka et al. 2015
<i>Monodictys</i> sp.	JO 10 = MAFF 243825	AB807552	AB797262	–	AB808528	Tanaka et al. 2015
<i>Morosphaeria ramunculicola</i>	BCC 18404	GQ925853	GQ925838	–	–	Suetrong et al. 2009
<i>Morosphaeria velatipora</i>	BCC 17059^T	GQ925852	GQ925841	–	–	Suetrong et al. 2010
<i>Multilocularia bambusae</i>	MFLUCC 11-0180^T	KU693438	KU693442	KU693446	–	Li et al. 2016
<i>Multiseptospora thailandica</i>	MFLUCC 11-0183^T	KP744490	KP753955	KP744447	–	Liu et al. 2015
<i>Multiseptospora thailandica</i>	MFLUCC 11-0204	KU693440	KU693444	KU693447	KU705659	Liu et al. 2015
<i>Multiseptospora thailandica</i>	MFLUCC 12-0006	KU693441	KU693445	KU693448	KU705660	Liu et al. 2015
<i>Multiseptospora thysanolaenae</i>	MFLUCC 11-0238^T	KU693439	KU693443	–	KU705658	Li et al. 2016
<i>Neoaquastroma baubinae</i>	MFLUCC 16-0398^T	MH023319	MH023315	MH025952	MH028247	This study

Taxon	Culture accession number(s) ^{1,2}	GenBank accession numbers				References
		LSU	SSU	ITS	<i>tefl</i>	
<i>Neoaquastroma baubinia</i>	MFLUCC 17-2205	MH023320	MH023316	MH025953	MH028248	This study
<i>Neoaquastroma krabiense</i>	MFLUCC 16-0419^T	MH023321	MH023317	MH025954	MH028249	This study
<i>Neoaquastroma guttulatam</i>	MFLUCC 14-0917^T	KX949740	KX949741	KX949739	KX949742	Wanasinghe et al. 2017
<i>Palmascoma gregariascomum</i>	MFLUCC 11-0175^T	KP744495	KP753958	KP744452	–	Liu et al. 2015
<i>Parabambusicola bambusina</i>	KH 139 = MAFF 243823	AB807537	AB797247	LC014579	AB808512	Tanaka et al. 2015
<i>Parabambusicola bambusina</i>	H 4321 = MAFF 239462	AB807536	AB797246	LC014578	AB808511	Tanaka et al. 2015
<i>Parabambusicola bambusina</i>	KT 2637 = MAFF 243822	AB807538	AB797248	LC014580	AB808513	Tanaka et al. 2015
<i>Pseudomonodictys tectonae</i>	MFLUCC 12-0552	KT285573	KT285574	–	KT285571	Ariyawansa et al. 2015
<i>Stagonospora pseudocaricis</i>	CBS 135132	KF251762	–	KF251259	–	Quaedvlieg et al. 2013
<i>Trematosphaeria pertusa</i>	CBS 122368^{ET}	FJ201990	FJ201991	NR_132040	KF015701	Zhang et al. 2008

¹ Abbreviations: **BCC**: BIOTEC Culture Collection, Bangkok, Thailand; **CABI**: Centre for Agriculture and Biosciences International, Egham, UK; **CBS**: CBS-KNAW Collections, Westerdijk Fungal Biodiversity Institute, Utrecht, The Netherlands; **CPC**: Culture collection of Pedro Crous, housed at CBS; **HKUCC**: The University of Hong Kong Culture Collection; **HHUF**: Herbarium of Hirosaki University, Fungi; **JCM**: The Japan Collection of Microorganisms, Japan; **JK**: J. Kohlmeyer; **JO**: J. Onodera; **KH**: K. Hirayama; **KT**: K. Tanaka; **MAFF**: Ministry of Agriculture, Forestry and Fisheries, Japan; **MFLU**: Mae Fah Luang University herbarium, **MFLUCC**: Mae Fah Luang University Culture Collection, Chiang Rai, Thailand.

² Status of the strains: (T) ex-type, (ET) ex-epitype. The strains generated in this study are given in bold.

version 7.220 (Katoh et al. 2013) online sequence alignment tools (mafft.cbrc.jp/alignment/server), with minimal adjustment of the ambiguous nucleotides by visual examination and manually corrected in AliView programme (Larsson 2014). Leading or trailing gaps exceeding from primer binding site were trimmed from the alignments prior to tree building and alignment gaps were treated as missing data. The concatenation of the multigene alignment was created in MEGA 6 (Tamura et al. 2013).

Maximum likelihood analyses (ML), including 1,000 bootstrap replicates, was performed using RAxML (Stamatakis 2014) as implemented in raxmlGUI version v.1.3.1 (Silvestro and Michalak 2011). The search strategy was set to rapid bootstrapping. The analysis was carried out with the general time reversible (GTR) model for nucleotide substitution and a discrete gamma-distributed with four rate categories (O'Meara et al. 2006, Stamatakis et al. 2008). The bootstrap replicates were summarised on to the best scoring tree.

The best fitting substitution model for each single gene partition and the concatenated data set was determined in MrModeltest 2.3 (Nylander 2004) for Bayesian

inference posterior probabilities (PP). In our analysis, GTR+I+G model was used for each partition. The Bayesian inference posterior probabilities (PP) distribution (Zhaxybayeva and Gogarten 2002) was estimated by Markov Chain Monte Carlo sampling (MCMC) in MrBayes v. 3.2.2 (Huelsenbeck and Ronquist 2001). Six simultaneous Markov chains were run for 1,000,000 generations and trees were sampled every 100th generation, thus 10,000 trees were obtained. The suitable burn-in phases were determined by traces inspected in Tracer version 1.6 (Rambaut et al. 2014). Based on the tracer analysis, the first 1,000 trees representing 10% of burn-in phase of the analyses were discarded. While the remaining trees were used for calculating posterior probabilities in the majority rule consensus tree (critical value for the topological convergence diagnostic set to 0.01).

Phylogenetic trees and data files were visualised in FigTree v. 1.4 (Rambaut and Drummond 2008). The phylogram with bootstrap values and/or posterior probabilities on the branches are presented in Fig. 1 by using graphical options available in Adobe Illustrator CS v. 6. All sequences generated in this study were submitted to GenBank. The finalised alignment and tree were deposited in TreeBASE, submission ID: 22419 (<http://www.treebase.org/>). Maximum likelihood bootstrap values equal to or greater than 70% with Bayesian Posterior Probabilities (PP) equal or greater than 0.90 are presented below or above each node (Fig. 1).

Results

Phylogenetic analyses

The phylogenetic tree included 32 taxa representing six families from the suborder Masarineae. The phylogenetic trees from each individual data sets were initially generated, these were not significantly different (data not shown) and therefore combined data sets were performed. The combined dataset consisting 3,554 nucleotide characters, of which 1,001 characters corresponded to LSU, 1,038 characters to SSU, 508 characters to ITS and 929 characters to *tefl*. *Corynespora smithii* (CABI 5649b) and *C. cassicola* (CBS 100822) are used as outgroup taxa. An insertion in the SSU rDNA region of isolates *Aquilomyces rebunensis* Tanaka & K. Hiray. (CBS 139684), *Clypeoloculus aki-taensis* Tanaka & K. Hiray. (CBS 139681) and *Trematosphaeria pertusa* Fuckel (CBS 122368) were excluded from the analysis prior to tree building. The best scoring tree from maximum likelihood analysis was selected with a final likelihood value of – In: 23014.934293 and the result is presented in Fig. 1. Phylogenetic trees obtained from maximum likelihood and Bayesian analyses yielded trees with similar overall topology as that of previous work (Tanaka et al. 2015, Liu et al. 2015, Wanasinghe et al. 2017).

In this study, the family Parabambusicolaceae received high support in the phylogenetic analysis. While within the family, the taxa are separated into three subclades (Fig. 1). *Parabambusicola bambusina*, the generic type, clustered with *Multiseptospora* with high support. However, *M. thysanolaenae* (MFLUCC 11-0202) formed a sister

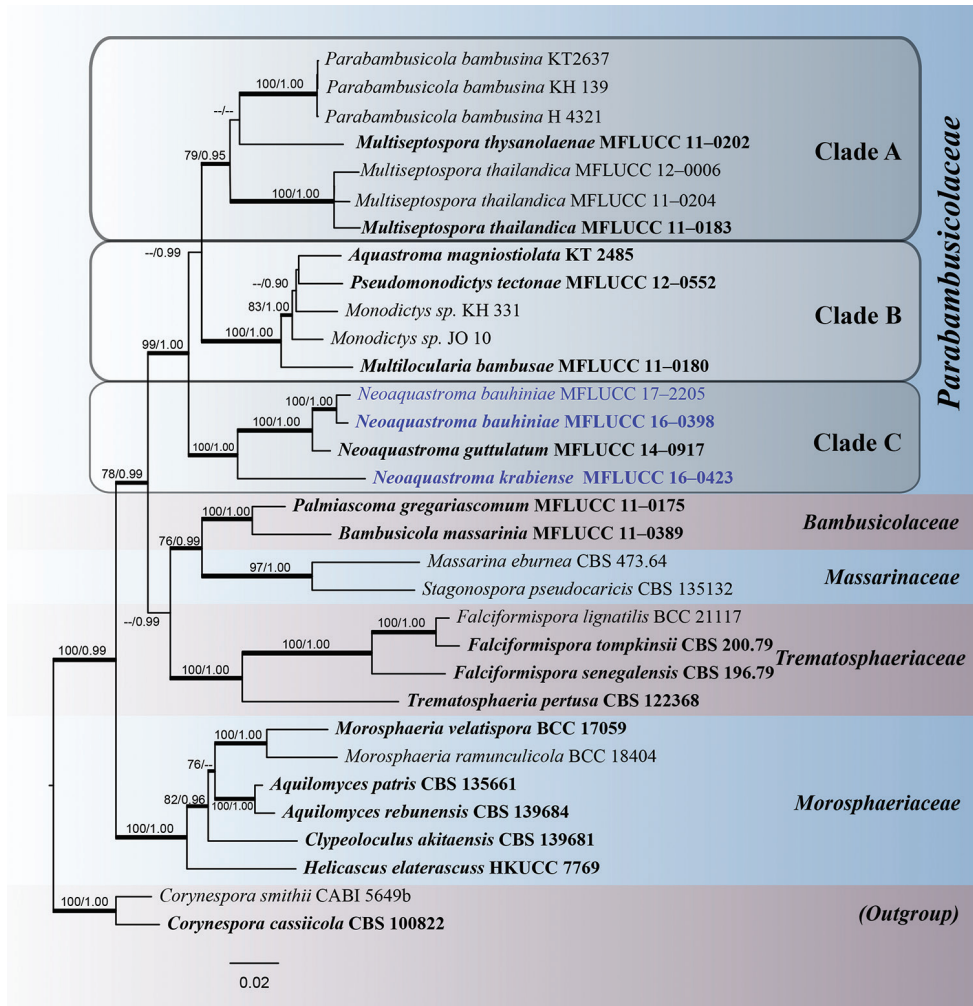


Figure 1. The best scoring RAxML tree based on a combined partial LSU, SSU, ITS and *tefl* gene datasets. Bootstrap values (BS) from maximum likelihood (ML, left) of more than 70% BS and Bayesian posterior probabilities (PP, right) greater than 0.90 are given above or below the nodes. The tree is rooted with *Corynespora smithii* (CABI 5649b) and *C. cassicola* (CBS 100822) in Corynesporaceae. The species, determined in this study, are indicated in blue. The ex-type and references strains are indicated in bold. Hyphens (-) represent support values less than 70% BS/0.90 PP. Thick branches represent significant support values from all analyses (BS ≥ 70%/PP ≥ 0.95).

taxon with *Parabambusicola bambusina* (Clade A). *Aquastroma magniostiolata* (CBS 139680) and *Multilocularia bambusae* (MFLUCC 11-0180) formed a clade with the hyphomycetes strains of *Monodictys* spp. and *Pseudomonodictys tectonae* (MFLUCC 12-0552) with high support in all computational methods (Clade B). *Neoaquastroma* formed a basal clade (Clade C), with *N. baubiniiae* (MFLUCC 16-0398, 17-2205) and *N. krabiense* (MFLUCC 16-0423) clustered with the type species *N. guttatum*, with

strong support (100% ML /1.00 PP). We describe the new taxa based on agreement in support for all computational methods (Jeewon and Hyde 2016). The new sequence data is deposited in GenBank (Table 1).

Taxonomy

Neoaquastroma baubiniaie C. Phukhams. & K.D. Hyde, sp. nov.

MycoBank: MB824673

Facesoffungi number: FoF04371

Figure 2

Etymology. Name refers the host from which this fungus was isolated.

Type material. THAILAND. Phrae Province: Song District, on dead twigs of *Bauhinia variegata* L. (Fabaceae), 25 July 2015, C. Phukhamsakda, S1-11, MFLU 17-0002 (**holotype**), MFLUCC 16-0398 = ICMP 21572 (**ex-type living culture**).

Description. *Saprobic* on dead twigs of *Bauhinia variegata* L. *Sexual morph.* *Ascomata* 113–190 μm high \times 170–307 μm diam. (\bar{x} = 160 \times 260 μm , n = 10), semi-immersed to immersed, solitary, scattered, subglobose to compressed, coriaceous, brown to dark brown, rough-walled, with short hyphae projecting from peridium, ostiolate. *Ostiole* 33 \times 85 μm diam., centrally located, papillate, periphysoid. *Peridium* 8–25 μm wide (\bar{x} = 17, n = 30), with cells 3–8 μm wide, composed of 3 layers of reddish-brown to dark brown, cells of *textura angularis*, inner layer composed of hyaline gelatinous cells. *Hamathecium* composed of numerous, dense, long, 1–2.4 μm (\bar{x} = 1.7 μm , n = 50), narrow, filiform, transversely septate, branched, anastomosing, cellular pseudoparaphyses. *Asci* 53–116 \times 26–43 μm (\bar{x} = 98 \times 37 μm , n = 30), 8-spored, bitunicate, fissitunicate, obovoid to oblong, with furcate pedicel, with ocular chamber visible when immature. *Ascospores* 37–46 \times 9–16 μm (\bar{x} = 43 \times 13 μm , n = 50), bi-seriate or overlapping, broad fusiform, narrow towards the apex, initially hyaline, becoming brown to dark brown at maturity, 4–7-transversely euseptate, constricted at the septa, with cell above central septum wider, rough-walled, indentations present, surrounded by 7–12 μm wide, mucilaginous sheath. *Asexual morph* coelomycetous. Pycnidia produced on mycelium in water agar. *Conidiomata* 33–49 μm high \times 92–108 μm wide diam., pycnidial, dark brown to black, covered by dense vegetative hyphae, globose, in agar immersed to superficial, uniloculate, solitary to scattered, ostiolate. *Conidiomatal wall* thin, brown to black-walled with cells of *textura angularis*. *Conidiophores* reduced to conidiogenous cells. *Conidiogenous cells* 3–4 \times 2–3.5 μm , enteroblastic, phialidic, integrated, oblong, hyaline, formed from the inner layer of pycnidium wall. *Conidia* 2–4 \times 1.5–2 μm (\bar{x} = 3 \times 1.7 μm , n = 100), broad-oblong to oval, hyaline, aseptate, smooth-walled.

Culture characteristics. Colonies on MEA, reaching 50 mm diam. after 4 weeks at 25 °C. Culture dark olive-green with black centre, with dense mycelia, circular, flat, umbonate, rough surface, dull, fimbriate, radially furrowed, covered with white aerial

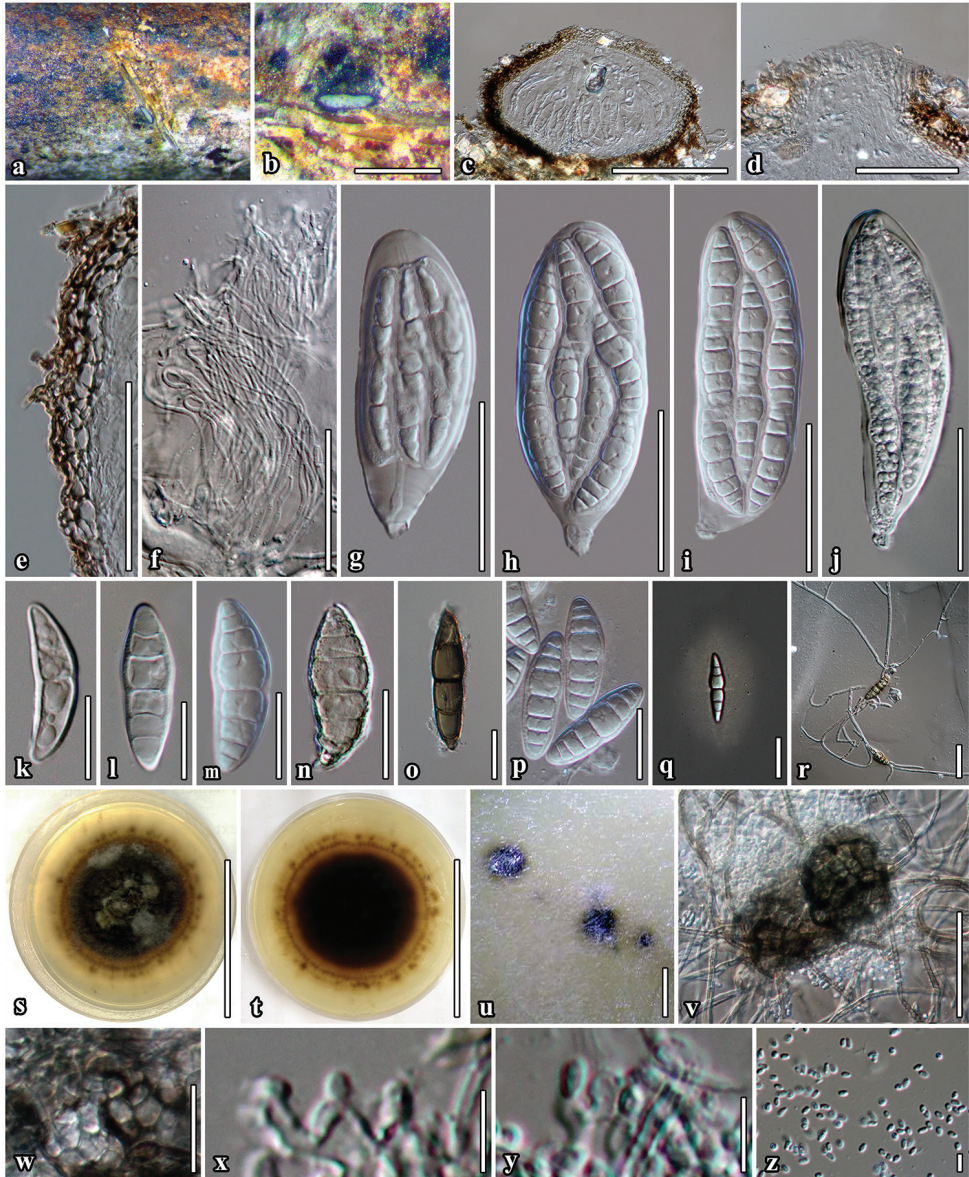


Figure 2. *Neoaquastroma baubinia* (MFLU 17-0002, holotype) **a** Appearance of ascomata on host surface **b** Close up of ascoma **c** Section of ascoma **d** Ostiolar canal **e** Section of partial peridium layer **f** Pseudoparaphyses **g-j** Development state of asci **j** Asci produced in culture **k-p** Development state of ascospores; (**n, o** Senescent spores **m, p** ascospores in 5% of KOH reagent); **q** Ascospores stained with India ink, sheath surrounding the entire ascospore **r** Germinated ascospore **s, t** Culture character on MEA **u** Conidiomata forming on agar on rice straw media after 8 weeks **v** Immature conidiomata **w** Conidiomatal wall **x, y** Conidiogenous cells and developing conidia **z** Conidia **j, m** Asci and ascospore in culture (on rice straw). Scale bars: 500 μm (**b**); 100 μm (**c, v**); 50 μm (**d-j**); 20 μm (**k-r, w**); 5 μm (**x-z**).

mycelium; mycelium strongly radiating into agar, yellow pigment diffusing in the agar; reverse black with radiating brown mycelium. Sexual and asexual morphs formed in culture. Morphology of sexual phase similar to those on substrate.

Additional material examined. THAILAND, Phrae Province, Song District, on dead twigs of *Bauhinia variegata* L. (Fabaceae), 25 July 2015, C Phukhamsakda, S1-11 (**isotype in HKAS**, under the code of HKAS 99513); *ibid.*, on dead twigs of *Bauhinia purpurea* L. (Fabaceae), 5 May 2016, C Phukhamsakda, S1_03_16, ex-paratype living culture, MFLUCC 17-2205.

Distribution. Phrae Province, Thailand.

Notes. *Neoaquastroma baubiniaie* is similar to *N. krabiense*, but the ascomata, asci and ascospores are smaller and the species also has a thinner peridium with 4–7 septate hyaline ascospores. Thus, *Neoaquastroma baubiniaie* is introduced as a second species in *Neoaquastroma* based on its unique morphology coupled with high support values from the phylogenetic analysis (100% ML/1.00 PP, Fig. 1). Tanaka et al. (2015) only described the asexual morph in *Parabambusicola* to produce spermatia. We now obtained a single spore isolate which produces both sexual and asexual morphs in culture. The asexual morph of *Neoaquastroma baubiniaie* produced pycnidial conidiomata with hyaline conidia (Fig. 2, u–z).

***Neoaquastroma krabiense* C. Phukhams. & K.D. Hyde, sp. nov.**

Mycobank: MB824674

Facesoffungi number: FoF04372

Figure 3

Etymology. Name refers the location where this fungus was collected.

Type material. THAILAND, Krabi Province: Meuang district, on dead twigs of *Barringtonia acutangula* (Lecythidaceae), 16 December 2015, C. Phukhamsakda, Kr015, MFLU 17-0003 (**holotype**), MFLUCC 16-0419 = ICMP 21572 (**ex-type living culture**).

Description. *Saprobic* on dead twigs of *Barringtonia acutangula* (L.) Gaertn. *Sexual morph.* *Ascomata* 404–498 µm high × 290–319 µm diam. (\bar{x} = 426 × 300 µm, n = 10), immersed in bark, solitary, scattered or sometimes gregarious, compressed globose, with a flattened base, coriaceous, black to dark brown, smooth, papillate, ostiolate. *Ostirole* 137–146 µm high × 117–154 µm diam. (\bar{x} = 143 × 137 µm, n = 10), centrally located, oblong, filled with hyaline periphysoid. *Peridium* 45–73 µm wide (\bar{x} = 56, n = 30), cell width 3–12 (\bar{x} = 8 µm, n = 40) composed of 6–10(–13 at base) layers of blackish-brown to dark brown, with cells of *textura angularis*, outer layer heavily pigmented, inner layer composed of hyaline gelatinous cells. *Hamathecium* composed of numerous, dense, long, 1.6–2.4 µm (\bar{x} = 2 µm, n = 50), broad, filiform, transversely septate, branched, anastomosing, cellular pseudoparaphyses. *Asci* 95–169 × 29–45 µm (\bar{x} = 135 × 35 µm, n = 25), 8-spored, bitunicate, fisitunicate, obovoid to clavate, with furcate pedicel, ocular chamber clearly visible when immature. *Ascospores* 50–64 × 9–18 µm (\bar{x}

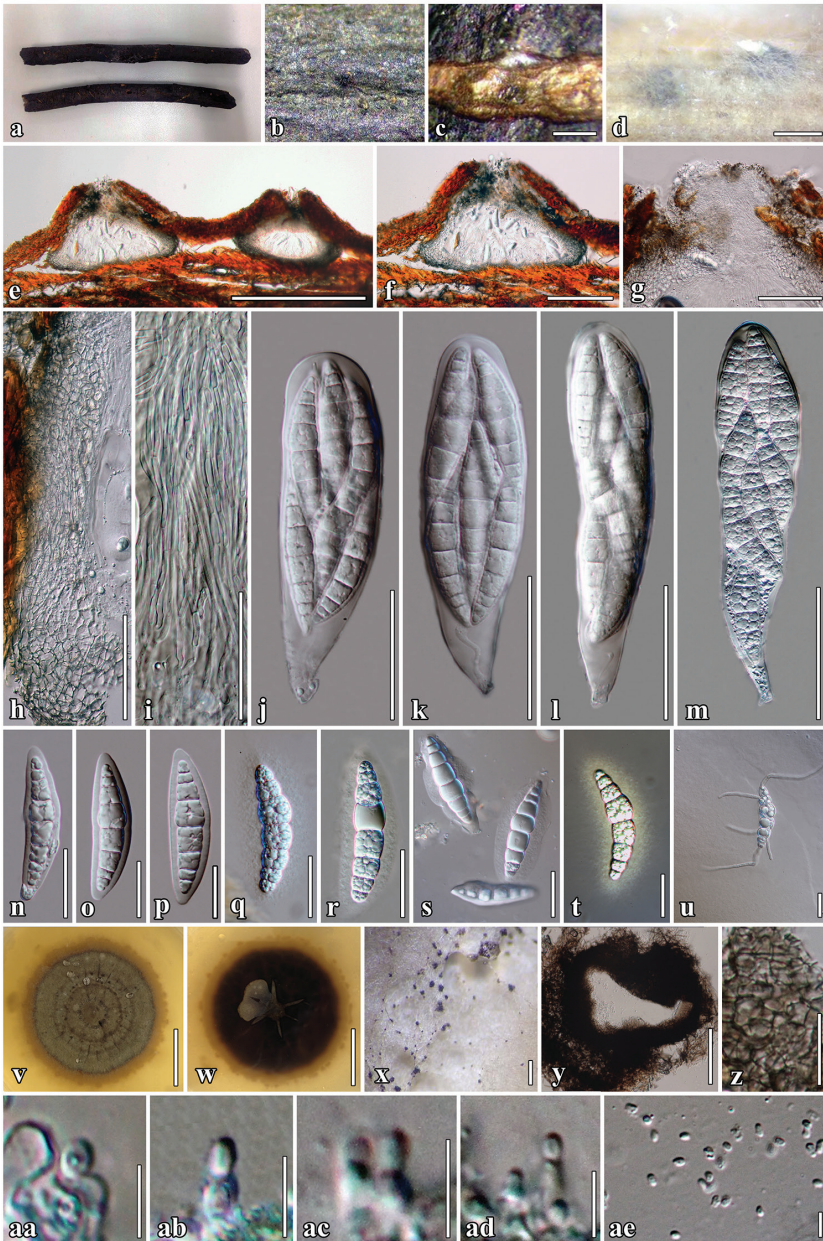


Figure 3. *Neoaquastroma krabiense* (MFLU 17-0003, holotype) **a** *Barringtonia acutangula* (L.) Gaertn specimens **b** Appearance of ascomata on host surface **c** Close up of ascomata **d** Ascomata forming on rice straw on WA after 8 weeks **e, f** Section of ascoma **g** Ostiolar canal **h** Section of partial peridium layer **i** Hyaline pseudoparaphyses **j-m** Asci **n-s** Hyaline ascospores with visible mucilaginous sheath **q** Ascospores stained in Indian ink to show sheath **u** Germinated ascospore **v, w** Culture characteristics on MEA **x, y** Conidiomata forming in culture after 8 weeks **z** Conidiomatal wall **aa-ad** Conidiogenous cells and developing conidia **ae** Conidia **n-p** Ascospores in 5% of KOH reagent **m, r** Asci and ascospore in culture (on rice straw). Scale bars: 500 μ m (**c-e**); 200 μ m (**f, x**); 50 μ m (**g-m, y**), 20 μ m (**n-u, z**); 5 μ m (**aa-af**); 20 mm (**v-w**).

= $57 \times 13 \mu\text{m}$, $n = 50$), bi-seriate or overlapping, fusiform, narrow towards the apex, hyaline, 5–8-transversely septate, constricted at the septa, cell above central septum slightly wider, rough-walled, indentations present when mature, granulate when stained with India ink, surrounded by 3–9 μm wide, mucilaginous sheath. *Asexual morph* coelomycetous, formed on rice straw agar. *Conidiomata* 84–90 μm high \times 73–89 μm wide., pycnidial, uniloculate, confluent or scattered, superficial, covered with dense vegetative hyphae, globose, dark brown to black. *Conidiomatal wall* thin, brown to black-walled cells of *textura angularis*. *Conidiophores* reduced to conidiogenous cells. *Conidiogenous cells* 3–5 \times 1.5–4 μm , enteroblastic, phialidic, integrated, broad-cylindrical to oblong, hyaline, formed from the inner layer of pycnidium wall. *Conidia* 2–4 \times 1.5–2.5 μm ($\bar{x} = 3 \times 2 \mu\text{m}$, $n = 60$), ellipsoidal to oblong, hyaline, aseptate, smooth-walled.

Culture characteristics. Colonies on MEA, reaching 50 mm diam. after four weeks at 25 °C. Culture grey, becoming dark-olive brown after four weeks, of dense mycelia, colonies circular, flat, umbonate, raised from the agar in the centre, surface rough, dull, covered with aerial mycelium, white mycelium radiating into the agar, pale orange pigment diffusing in the agar; reverse black, dense, circular, with irregular, fimbriate margin. Sexual and asexual morphs formed in culture. Morphology of sexual phase similar to those on the substrates.

Additional material examined. THAILAND, Krabi Province, Meuang district, on dead twigs of *Barringtonia acutangula* (Lecythidaceae), 16 December 2015, C. Phukhamsakda, Kr015, (**isotype in HKAS**, under the code of HKAS 99512).

Distribution. Krabi Province, Thailand

Notes. *Neoaquastroma krabiense* was collected in the southern part of Thailand on dead twigs of *Barringtonia acutangula*. It is placed in *Neoaquastroma* based on its morphology of both sexual and asexual morph and close phylogenetic affinity to other species of *Neoaquastroma*. *Neoaquastroma krabiense* is distinct in that it has a flattened ascomata base and larger and more slender asci and ascospores than *N. guttulatatum* and *N. baubiniaie*. The species formed an asexual morph in culture (Fig. 3, m) as pycnidial conidiomata with hyaline conidia (Fig. 3, x-ae).

Discussion

In the present study, we introduce two new species of *Neoaquastroma*, as *N. baubiniaie* and *N. krabiense*. The descriptions were made from fungi isolated from dicotyledonous plants in Thailand. The new species are introduced based on multi-locus phylogeny coupled with morphology that support their placement within Parabambusicolaceae.

Parabambusicolaceae is typified with *Parabambusicola* Tanaka & K. Hiray. The type of the genus was described originally as *Massarina bambusina* Teng (Teng, 1936) from bamboo. The family is characterised by ascomata surrounded by stromatic tissues and multiseptate, clavate to fusiform and hyaline ascospores (Tanaka and Harada 2003, Tanaka et al. 2015). The asexual morph in Parabambusicolaceae can be coelomycetous or hyphomycetous. Sporodochia or pycnidia with hyaline conidia are formed in

Parabambusicola and *Neoaquastroma* (Tanaka et al. 2015, this study), while hyphomyceteous structures are known from *Pseudomonodictys* and *Monodictys* spp. (Ariyawansa et al. 2015, Tanaka et al. 2015).

Neoaquastroma was introduced as a distinct genus in Parabambusicolaceae, with *N. guttulatum* as the type species (Wanasinghe et al. 2017). The genus resembles *Parabambusicola* and *Multiseptospora*, but form distinct lineages in phylogenetic studies (Liu et al. 2015, Tanaka et al. 2015, Wanasinghe et al. 2017). *Parabambusicola* and *Neoaquastroma* are similar in their morphology. The differentiation between *Multiseptospora*, *Neoaquastroma* and *Parabambusicola* is predominantly based on the morphology of ascospores, particularly with the size and number of septa.

In the phylogenetic analyses of Wanasinghe et al. (2017), Parabambusicolaceae clustered into three clades, where *Neoaquastroma guttulatum* (MFLUCC 14-0917) clustered with *Aquastroma magniostiolata* (KT 2485), *Multilocularia bambusae* (MFLUCC 11-0180), *Monodictys* sp. (JO 10, KH 331) and *Pseudomonodictys tectonae* (MFLUCC 12-0552) with high statistical support. In this study, *Neoaquastroma* forms a separate clade, sister to *Multiseptospora* and *Parabambusicola*. This is probably due to limited taxon sampling.

Acknowledgements

The authors would like to thank the Royal Golden Jubilee PhD Program under Thailand Research Fund (RGJ) and the German Academic Exchange Service (DAAD) for a joint TRF-DAAD (PPP 2017–2018) academic exchange grant to K.D. Hyde and M. Stadler and the RGJ for a personal grant to C. Phukhamsakda (The scholarship no. PHD/0020/2557 to study towards a PhD). Dr. Shaun Pennycook for checking and suggesting Latin names of the new taxa. Dr. Rajesh Jeewon for his suggestions on the phylogenetic analysis.

References

- Ahmed SA, Van De Sande WW, Stevens DA, Fahal A, Van Diepeningen AD, Menken SB, de Hoog GS (2014) Revision of agents of black-grain eumycetoma in the order Pleosporales. *Persoonia* 33: 141–154. <http://doi.org/10.3767/003158514X684744>
- Ariyawansa HA, Hyde KD, Jayasiri SC, Buyck B, Chethana T, Dai DQ, Dai YC, Daranagama DA, Jayawardena RS, Luecking R, Ghobad-Nejhad M (2015) Fungal diversity notes 111–252 – taxonomic and phylogenetic contributions to fungal taxa. *Fungal Diversity* 75(1): 27–274. <http://dx.doi.org/10.1007/s13225-015-0346-5>
- Carbone I, Kohn LM (1999) A method for designing primer sets for speciation studies in filamentous ascomycetes. *Mycologia* 91(3): 553–556. <http://doi.org/10.2307/3761358>
- Dai DQ, Bhat DJ, Liu JK, Chukeatirote E, Zhao RL, Hyde KD (2012) *Bambusicola*, a new genus from bamboo with asexual and sexual morphs. *Cryptogamie Mycologie* 33(3): 363–379. <https://doi.org/10.7872/crym.v33.iss3.2012.363>

- Dai DQ, Phookamsak R, Wijayawardene NN, Li WJ, Bhat DJ, Xu JC, Taylor JE, Hyde KD, Chuukeatirote E (2017) Bambusicolous fungi. *Fungal Diversity* 82(1): 1–105. <https://doi.org/10.1007/s13225-016-0367-8>
- Huelsenbeck JP, Ronquist F (2001) MRBAYES: Bayesian inference of phylogenetic trees. *Bioinformatics* 17: 754–755. <https://doi.org/10.1093/bioinformatics/17.8.754>
- Hyde KD (1989) Ecology of tropical marine fungi. *Hydrobiologia* 178: 199–208. <https://doi.org/10.1007/BF00006027>
- Jaklitsch WM, Olariaga I, Voglmayr H (2016) *Teichospora* and the Teichosporaceae. *Mycological Progress* 15(31): 1–20. <https://doi.org/10.1007/s11557-016-1171-2>
- Jayasiri SC, Hyde KD, Ariyawansa HA, Bhat J, Buyck B, Cai L, Dai YC, Abd-Elsalam KA, Ertz D, Hidayat I, Jeewon R (2015) The Faces of fungi database: fungal names linked with morphology, molecular and human attributes. *Fungal Diversity* 74(1): 3–18. <https://doi.org/10.1007/s13225-015-0351-8>
- Jeewon R, Hyde KD (2016) Establishing species boundaries and new taxa among fungi: recommendations to resolve taxonomic ambiguities. *Mycosphere* 7(11): 1669–1677. <https://doi.org/10.5943/mycosphere/7/11/4>
- Jones EBG (2000) Marine fungi: some factors influencing biodiversity. *Fungal Diversity* 4: 53–73.
- Jones EBG, Pilantanapak A, Chatmala I, Sakayaroj J, Phongpaichit S, Choeyklin R (2006) Thai marine fungal diversity. *Songklanakarin Journal of Science and Technology* 28: 687–708.
- Katoh K, Standley K (2013) MAFFT Multiple Sequence Alignment Software Version 7: Improvements in Performance and Usability. *Molecular Biology and Evolution* 30(4): 772–780. <http://dx.doi.org/10.1093/molbev/mst010>
- Knapp DG, Kovács GM, Zajta E, Groenewald JZ, Crous PW (2015) Dark septate endophytic pleosporalean genera from semiarid areas. *Persoonia* 35: 87–100. <https://doi.org/10.3767/003158515X687669>
- Larsson A (2014) AliView: a fast and lightweight alignment viewer and editor for large data sets. *Bioinformatics* 30(22): 3276–3278. <http://doi.org/10.1093/bioinformatics/btu531>
- Li GJ, Hyde KD, Zhao RL, Hongsanan S, Abdel-Aziz FA, Abdel-Wahab MA, Alvarado P, Alves-Silva G, Ammirati JF, Ariyawansa HA, Baghela A (2016) Fungal diversity notes 253–366: taxonomic and phylogenetic contributions to fungal taxa. *Fungal Diversity* 78(1): 1–237. <http://doi.org/10.1007/s13225-016-0366-9>
- Liu JK, Hyde KD, Jones EG, Ariyawansa HA, Bhat DJ, Boonmee S, Maharachchikumbura SS, McKenzie EH, Phookamsak R, Phukhamsakda C, Shenoy BD (2015) Fungal Diversity Notes 1–110: Taxonomic and phylogenetic contributions to fungal species. *Fungal Diversity* 72(1): 1–197. <http://doi.org/10.1007/s13225-015-0324-y>
- MacKinnon J, MacKinnon K, Child G, Thorsell J (1986) *Managing Protected Areas in the Tropics* IUCN, Gland, Switzerland and Cambridge, UK, 295.
- Mapook A, Hyde KD, Dai DQ, Li J, Jones EG, Bahkali AH, Boonmee S (2016) *Muyocoproneles*, ord nov, (Dothideomycetes, Ascomycota) and a reappraisal of *Muyocoproneles* species from northern Thailand. *Phytotaxa* 265: 225–237. <http://doi.org/10.11646/phytotaxa.265.3.3>
- Marod D, Kutintara U (2012) Biodiversity observation and monitoring in Thailand. *The Biodiversity Observation Network in the Asia-Pacific Region*. Springer, Japan, 53–63. https://doi.org/10.1007/978-4-431-54032-8_5

- Doilom M, Dissanayake AJ, Wanasinghe DN, Boonmee S, Liu JK, Bhat DJ, Taylor JE, Bahkali AH, McKenzie EH, Hyde KD (2017) Microfungi on *Tectona grandis* (teak) in Northern Thailand. *Fungal Diversity* 82(1): 107–182. <http://doi.org/10.1007/s13225-016-0368-7>
- Mycobank (2018) MycoBank. <http://www.Mycobank.org>. [Accessed in March 2018]
- Nylander JAA (2004) MrModeltest v2 Program distributed by the author. Evolutionary Biology Centre, Uppsala University.
- O'Meara BC, Ané C, Sanderson MJ, Wainwright PC (2006) Testing for different rates of continuous trait evolution using likelihood. *Evolution* 60: 922–933. <https://doi.org/10.1111/j.0014-3820.2006.tb01171.x>
- Phukhamsakda C, Ariyawansa HA, Phillips AJ, Wanasinghe DN, Bhat DJ, McKenzie EH, Singtripop C, Camporesi E, Hyde KD (2016) Additions to Sporormiaceae: Introducing two novel genera, *Sparticola* and *Forliomyces*, from *Spartium*. *Cryptogamie, Mycologie* 37(1): 75–97. <https://doi.org/10.7872/crym/v37.iss1.2016.75>
- Phukhamsakda C, Bhat DJ, Hongsanan S, Tibpromma S, Yang JB, Promputtha I (2017) *Magnicamarosporium diospyricola* sp. nov. (Sulcatisporaceae) from Thailand. *Mycosphere* 8(4): 512–520. <https://doi.org/10.5943/mycosphere/8/4/3>
- Phukhamsakda C, Hongsanan S, Ryberg M, Ariyawansa HA, Chomnunti P, Bahkali AH, Hyde KD (2016) The evolution of Massarineae with Longipedicellataceae fam. nov. *Mycosphere* 7(11): 1713–1731. <https://doi.org/10.5943/mycosphere/7/11/7>
- Quaedvlieg W, Verkley GJ, Shin HD, Barreto RW, Alfenas AC, Swart WJ, Groenewald JZ, Crous PW (2013) Sizing up *Septoria*. *Studies in Mycology* 75: 307–339. <https://doi.org/10.3114/sim0017>
- Rambaut A, Drummond A (2008) FigTree: Tree figure drawing tool, version 1.2.2 Institute of Evolutionary Biology, University of Edinburgh
- Rambaut A, Suchard MA, Xie D, Drummond AJ (2014) Tracer v1.6, Available from <http://beast.bio.ed.ac.uk/Tracer>
- Rostrup E (1902) Flora of Koh Chang Contributions to the knowledge of the vegetation of the gulf of Siam. *Fungi Botanisk Tidsskrift* 24: 355–363. <https://doi.org/10.5962/bhl.title.55188>
- Schoch CL, Crous PW, Groenewald JZ, Boehm EW, Burgess TI, De Gruyter J, De Hoog GS, Dixon LJ, Grube M, Gueidan C, Harada Y (2009) A class-wide phylogenetic assessment of Dothideomycetes. *Studies in Mycology* 64: 1–15. <https://doi.org/10.3114/sim.2009.64.01>
- Schumacher T (1982) Ascomycetes from Northern Thailand. *Nordic Journal of Botany* 2: 257–263. <https://doi.org/10.1111/j.1756-1051.1982.tb01187.x>
- Silvestro D, Michalak I (2011) raxmlGUI: a graphical front-end for RAxML. *Organisms Diversity & Evolution* 12(4): 335–337. <https://doi.org/10.1007/s13127-011-0056-0>
- Stamatakis A (2006) RAXML-VI-HPC: maximum likelihood-based phylogenetic analyses with thousands of taxa and mixed models. *Bioinformatics* 22: 2688–2690. <https://doi.org/10.1093/bioinformatics/btl446>
- Stamatakis A (2014) RAxML Version 8: A tool for Phylogenetic Analysis and Post-Analysis of Large Phylogenies. *Bioinformatics* 30: 1312–1313. <https://doi.org/10.1093/bioinformatics/btu033>
- Stamatakis A, Hoover P, Rougemont J (2008) A rapid bootstrap algorithm for the RAxML web servers. *Systematic biology* 57: 758–771. <https://doi.org/10.1080/10635150802429642>

- Suetrong S, Schoch CL, Spatafora JW, Kohlmeyer J, Volkmann-Kohlmeyer B, Sakayaroj J, Phongpaichit S, Tanaka K, Hirayama K, Jones EB (2009) Molecular systematics of the marine Dothideomycetes. *Studies in Mycology* 64: 155–173. <https://doi.org/10.3114/sim.2009.64.09>
- Swofford DL (2002) PAUP*: phylogenetic analysis using parsimony (* and other methods) Sunderland, MA. <https://doi.org/10.1002/0471650129.dob0522>
- Tamura K, Stecher G, Peterson D, Filipski A, Kumar S (2013) MEGA6: Molecular Evolutionary Genetics Analysis Version 6.0. *Molecular Biology and Evolution* 30: 2725–2729. <https://doi.org/10.1093/molbev/mst197>
- Tanaka K, Harada Y (2003) Pleosporales in Japan (1): the genus *Lophiostoma*. *Mycoscience* 44(2): 85–96. <https://doi.org/10.1007/s10267-002-0085-9>
- Tanaka K, Harada Y (2003) Pleosporales in Japan (3) The genus *Massarina*. *Mycoscience* 44(3): 173–185. <https://doi.org/10.1007/s10267-003-0102-7>
- Tanaka K, Hirayama K, Yonezawa H, Sato G, Toriyabe A, Kudo H, Hashimoto A, Matsumura M, Harada Y, Kurihara Y, Shirouzu T (2015) Revision of the Massarineae (Pleosporales, Dothideomycetes). *Studies in Mycology* 82: 75–136. <https://doi.org/10.1016/j.simyco.2015.10.002>
- Teng SC (1936) Additional fungi from China II. *Sinensia* 7: 490–527.
- Vilgalys R, Hester M (1990) Rapid genetic identification and mapping of enzymatically amplified ribosomal DNA from several *Cryptococcus* species. *Journal of bacteriology* 172(8): 4238–4246. <https://doi.org/10.1128/jb.172.8.4238-4246.1990>
- Wanasinghe DN, Hyde KD, Konta S, To-Anun C, Jones EG (2017) Saprobic Dothideomycetes in Thailand: *Neoaquastroma* gen. nov. (Parabambusicolaceae) introduced based on morphological and molecular data. *Phytotaxa* 302: 133–144. <http://doi.org/10.11646/phytotaxa.302.2.3>
- Wendt L, Sir EB, Kuhnert E, Heitkämper S, Lambert C, Hladki AI, Romero AI, Luangsa-ard JJ, Srikitikulchai P, Peršoh D, Stadler M (2018) Resurrection and emendation of the Hypoxylaceae, recognised from a multigene phylogeny of the Xylariales. *Mycological Progress* 17(1–2): 115–154. <http://doi.org/10.1007/s11557-017-1311-3>
- White TJ, Bruns T, Lee SJ, Taylor JW (1990) Amplification and direct sequencing of fungal ribosomal RNA genes for phylogenetics. *PCR protocols: a guide to methods and applications* 18(1): 315–322. <https://doi.org/10.1016/B978-0-12-372180-8.50042-1>
- Wijayawardene NN, Hyde KD, Lumbsch HT, Liu JK, Maharachchikumbura SS, Ekanayaka AH, Tian Q, Phookamsak R (2018) Outline of Ascomycota: 2017. *Fungal Diversity* 88(1): 167–263. <http://doi.org/10.1007/s13225-018-0394-8>
- Wijayawardene NN, Hyde KD, Rajeshkumar KC, Hawksworth DL, Madrid H, Kirk PM, Braun U, Singh RV, Crous PW, Kukwa M, Lücking R (2017) Notes for genera-Ascomycota. *Fungal Diversity* 86(1): 1–594. <http://doi.org/10.1007/s13225-017-0386-0>
- Zhang Y, Fournier J, Pointing SB, Hyde KD (2008) Are *Melanomma pulvis-pyrius* and *Trematosphaeria pertusa* congeneric?. *Fungal Diversity* 33: 47–60. <http://doi.org/10.13140/2.1.3875.1364>
- Zhang Y, Wang HK, Fournier J, Crous PW, Jeewon R, Pointing SB, Hyde KD (2009) Towards a phylogenetic clarification of *Lophiostoma*/*Massarina* and morphologically similar genera in the Pleosporales. *Fungal Diversity* 38: 225–251.
- Zhaxybayeva O, Gogarten JP (2002) Bootstrap, Bayesian probability and maximum likelihood mapping: exploring new tools for comparative genome analyses. *BMC genomics* 3(1): 1–4. <https://doi.org/10.1186/1471-2164-3-4>

New *Fusarium* species from the Kruger National Park, South Africa

Marcelo Sandoval-Denis^{1,2}, Wijnand J. Swart², Pedro W. Crous^{1,2}

1 *Westerdijk Fungal Biodiversity Institute, Uppsalalaan 8, 3584 CT, Utrecht, The Netherlands* **2** *Faculty of Natural and Agricultural Sciences, Department of Plant Sciences, University of the Free State, P.O. Box 339, Bloemfontein 9300, South Africa*

Corresponding author: *Marcelo Sandoval-Denis* (m.sandoval@westerdijkinstituut.nl)

Academic editor: *G. Mugambi* | Received 18 April 2018 | Accepted 17 May 2018 | Published 1 June 2018

Citation: Sandoval-Denis M, Swart WJ, Crous PW (2018) New *Fusarium* species from the Kruger National Park, South Africa. *MycKeys* 34: 63–92. <https://doi.org/10.3897/mycokeys.34.25974>

Abstract

Three new *Fusarium* species, *F. convolutans*, *F. fredkrugeri*, and *F. transvaalense* (Ascomycota, Hypocreales, Nectriaceae) are described from soils collected in a catena landscape on a research supersite in the Kruger National Park, South Africa. The new taxa, isolated from the rhizosphere of three African herbaceous plants, *Kyphocarpa angustifolia*, *Melbania acuminata*, and *Sida cordifolia*, are described and illustrated by means of morphological and multilocus molecular analyses based on sequences from five DNA loci (CAL, EF-1 α , RPB1, RPB2 and TUB). According to phylogenetic inference based on Maximum-likelihood and Bayesian approaches, the newly discovered species are distributed in the *Fusarium buharicum*, *F. fujikuroi*, and *F. sambucinum* species complexes.

Keywords

Natural parks, phylogeny, fungi, multigene, morphology, diversity

Introduction

Fungi are common colonisers of the plant rhizobiome and endosphere, where they play a key role in modulating the interactions between plant roots and soil (Zachow et al. 2009; Visioli et al. 2014). The direct and indirect interaction between fungal growth in the rhizosphere and its effect on plant growth and health is well docu-

mented (Havlicek and Mitchell 2014; Hargreaves et al. 2015; Lareen et al. 2016). Such effects include either a positive feedback by producing plant growth promoting factors, solubilising and stimulating nutrient uptake by plant roots or by inhibiting the growth of concomitant pathogenic organisms (Schippers et al. 1987; Mommer et al. 2016). Conversely, deleterious effects have also been observed, either related to the presence of pathogenic fungal species or caused by fungal-induced modifications of plant root functions, impeding root growth or negatively altering nutrient availability (Schippers et al. 1987; Mommer et al. 2016). Likewise, plants can select and harbour a particular fungal community on its roots via root exudates (Lareen et al. 2016; Sasse et al. 2018), while abiotic influences including water availability, climate and season, soil type, grazers and other animals, orchestrate the development of a unique fungal diversity (Philippot et al. 2013; Havlicek and Mitchell 2014; Hargreaves et al. 2015; Lareen et al. 2016).

The genus *Fusarium* Link (Hypocreales, Nectriaceae) includes a vast number of species, commonly recovered from a variety of substrates including soil, air, water and decaying plant materials; being also able to colonise living tissues of plants and animals, including humans; acting as endophytes, secondary invaders or becoming devastating plant pathogens (Nelson et al. 1994). In addition to their ability to colonise a multiplicity of habitats, *Fusarium* is a cosmopolitan genus, present in almost any ecosystem in the world, including human-made settings such as air and dust in the indoor environment or even in hospitals (Perlroth et al. 2007; Aydogdu and Asan 2008; Pinheiro et al. 2011).

Being common inhabitants of plant root ecosystems, fusaria and, particularly *Fusarium graminearum* Schwabe, *F. proliferatum* (Matsush.) Nirenberg ex Gerlach & Nirenberg, *F. verticillioides* (Sacc.) Nirenberg (Syn. *F. moniliforme* J. Sheld.), *F. oxysporum* Schltdl., as well as species recently segregated from *Fusarium*, including *Neocosmospora phaseoli* (Burkh.) L. Lombard & Crous (Syn. *Fusarium phaseoli* Burkh.) and *N. virguliforme* (O'Donnell & T. Aoki) L. Lombard & Crous (Syn. *F. virguliforme* O'Donnell & T. Aoki), have been regularly studied for their interactions with the rhizobiome, motivated mainly by the importance of these organisms as soil-borne plant pathogens and the need to develop effective control mechanisms (Larkin et al. 1993; Hassan Dar et al. 1997; Pal et al. 2001; Fravel et al. 2003; Idris et al. 2006; Díaz Arias et al. 2013). Similarly, abundant data is available regarding the ecology and distribution of plant-associated fusaria, particularly related to pathogenic species or commonly isolated endophytes (Leslie and Summerell 2006). Little attention has however been given to the occurrence of non-pathogenic fungal species, including *Fusarium* spp. in root microbial communities (Zakaria and Ning 2013; Jumpponen et al. 2017; LeBlanc et al. 2017), while comprehensive DNA sequence-based surveys have been directed mostly to the study of highly relevant and abundant rhizosphere fungal genera such as *Trichoderma* Pers., *Verticillium* Nees or mycorrhizal fungi (Zachow et al. 2009; Bent et al. 2011; Ruano-Rosa et al. 2016; Saravanakumar et al. 2016).

The Kruger National Park (KNP) in South Africa is one of the largest natural reserves in Africa, encompassing a number of non-manipulated landscapes, with almost no human alteration (Carruthers 2017). Recently, four research “supersites” have been identified and established in KNP, each of these supersites representing unique geological, ecological and climatic features of the park (Smit et al. 2013). A multidisciplinary study was conducted in KNP aimed to determine functioning and interaction between abiotic and biotic components, as well as soil properties, hydrology and other processes that determine the structure, biodiversity and heterogeneity of a catena or hill slope ecosystem on one of these “supersites”, located deep inside the KNP (data not published). In order to assess the microbial soil population and community dynamics, mainly focused on bacteria, several rhizosphere samples were obtained from diverse African plants on one of these exceptional protected savannah landscapes. From these collections, interesting fusaria were isolated from the root ecosystem of three native African herbaceous plants i.e. *Kyphocarpa angustifolia* (Moq.) Lopr. (Amaranthaceae), *Melhania acuminata* Mast. (Malvaceae) and *Sida cordifolia* Linn. (Malvaceae). According to their unique morphological traits and clear phylogenetic delimitations, these isolates are described here as three new *Fusarium* species.

Methods

Study site and sampling

During March 2015, rhizosphere soil from three herbaceous plants was collected in the Southern Granites “supersite” catena (Stevenson-Hamilton supersite) in the KNP, between 25°06'28.6S, 31°34'41.9E and 25°06'25.7S, 31°34'33.7E (Fig. 1). A catena consists of different soil types observed from a crest to a valley bottom with a wetland or drainage exhibiting different water retention capabilities due to the slope or aspect (topography) and the depth of underlying geological rocks (Brown et al. 2004, Van Zijl and Le Roux 2014). The main characteristics of the Stevenson-Hamilton supersite are described in detail by Smit et al. (2013). Briefly, in this site, a single catena landscape covers approximately 1 km from top to bottom and consists of a hill slope, a sodic site (or grazing lawn), a riparian and floodplain area and a dry drainage line. Three species of plants were selected for sampling occurring at the two extremes of the catena. Two of these species (*Kyphocarpa angustifolia* and *Sida cordifolia*) occurred at both top and bottom sites while *Melhania acuminata* only occurred at the top site. The soil (100 mm depth) at the top of the slope is Clovelly with a high percentage of sand (90%) and a low cation exchange capacity (CEC) (mean sodium concentration of 1062 mg/kg) and pH (mean 5.85). The soil at the bottom of the slope is of the Sterkspruit type, with higher clay content thus higher CEC (mean sodium concentration of 3802 mg/kg) and higher pH (mean



Figure 1. Map of the Kruger National Park (KNP) in South Africa. The arrows indicate the location of the four research “supersites” (adapted from Smit et al. 2013). Sampling site is indicated with a black star. The inset shows the location of the KNP within South Africa, indicated by a grey box.

6.4). Rhizosphere soil of 10 plants of the same species occurring at each top or bottom site was sampled using a core soil sampler. A total of 50 samples consisting of ca. 200 g of soil from the roots of each plant were taken, deposited in zip-lock plastic bags and kept on ice in a cool bag at approximately 5 °C until analysed in the laboratory.

Isolation of *Fusarium* strains

Soil samples were mixed thoroughly and sieved to remove large elements. Fine soil particles were uniformly spread and distributed over the surface of pentachloronitrobenzene agar (PCNB; also known as the Nash-Snyder medium, recipe in Leslie and Summerell 2006) supplemented with streptomycin (0.3 g/l) and neomycin sulphate (0.12 g/l) and malt-extract agar (MEA; recipes on Crous et al. 2009) on 9 mm Petri dishes and incubated at 24 °C for 10 d under a natural day/night photoperiod. Each soil sample was processed in duplicate. Fungal growth was evaluated daily and growing colonies were transferred to fresh Potato Dextrose Agar (PDA;

recipe in Crous et al. 2009). Colonies were evaluated for their macro- and microscopic characteristics and a total of 19 fungal cultures showing features typical of *Fusarium* were subjected to single spore isolation as described previously (Sandoval-Denis et al. 2018). Single spore isolates were finally transferred and maintained in Oatmeal Agar plates and slants (OA; recipe in Crous et al. 2009). Fungal strains isolated in this study were deposited in the collection of the Westerdijk Fungal Biodiversity Institute (CBS; Utrecht, the Netherlands), the working collection of Pedro W. Crous (CPC), held at CBS (Table 1); and voucher specimens were deposited in The South African National Collection of Fungi (NCF) (Mycology Unit, Biosystematics Division, Plant Protection Institute, Agricultural Research Council, Pretoria, South Africa).

Morphological characterisation

Fusarium isolates were characterised morphologically according to procedures described elsewhere (Aoki et al. 2013; Leslie and Summerell 2006, Sandoval-Denis et al. 2018). Colonial growth rates and production of diffusible pigments were evaluated on PDA, colony features were also recorded on corn-meal agar (CMA; recipe in Crous et al. 2009) and OA. Colour notations followed those of Rayner (1970). For the study of micro-morphological features, cultures were grown for 7–10 d at 24 °C, using a 12 h light/dark cycle with near UV and white fluorescent light. Aerial and sporodochial conidiophores and conidia and formation of chlamydospores were evaluated on Synthetic Nutrient-poor Agar (SNA; Nirenberg 1976) and on Carnation Leaf Agar (CLA; Fisher et al. 1982). Measurements and photomicrographs were recorded from a minimum of 30 elements for each structure, using sterile water as mounting medium and a Nikon Eclipse 80i microscope with Differential Interference Contrast (DIC) optics and a Nikon AZ100 dissecting microscope, both equipped with a Nikon DS-Ri2 high definition colour digital camera and the Nikon software NIS-elements D software v. 4.30.

DNA isolation, amplification and sequencing

Isolates were grown for 7 d on MEA at 24 °C using the photoperiod described above. Fresh mycelium was scraped from the colony surface and subjected to total DNA extraction using the Wizard® Genomic DNA purification Kit (Promega Corporation, Madison, WI, USA), according to the manufacturer's instructions. Fragments of five DNA loci were amplified using primers and PCR conditions described by O'Donnell et al. (2009) for calmodulin (*CAL*), O'Donnell et al. (2010) for the RNA polymerase largest subunit (*RPB1*) and second largest subunit (*RPB2*), O'Donnell et al. (1998) for the translation elongation factor 1-alpha (*EF-1a*) and Woudenberg et al. (2009) for

Table 1. Origin, strain and GenBank/ENA accession number of strains and DNA sequences included in this study.

Species name	Strain ^{†‡}	Country	Host	Sequence accession number [§]				
				CAL	EF- α	RPB1	RPB2	TUB
<i>Fusarium agapanthi</i>	NRRL 54463 [†]	Australia	<i>Agapanthus</i> sp.	KU900611	KU900630	KU900620	KU900625	KU900635
<i>Fusarium ananatum</i>	CBS 118516 [†]	South Africa	<i>Ananas comosus</i> fruit	LT996175	LT996091	LT996188	LT996137	LT996112
<i>Fusarium andryazi</i>	CBS 119857 [†] = NRRL 31727	South Africa	<i>Sorghum bicolor</i> soil debris	LT996176	LT996092	LT996189	LT996138	LT996113
<i>Fusarium anthophyllum</i>	CBS 737.97 = NRRL 13602	Germany	<i>Hippeastrum</i> sp.	LT996177	LT996093	LT996190	LT996139	LT996114
<i>Fusarium armeniacum</i>	NRRL 6227	USA	Fescue hay			JX171446	JX171560	
<i>Fusarium asiaticum</i>	CBS 110257 = NRRL 13818	Japan	Barley			JX171459	JX171573	
<i>Fusarium bactridoides</i>	NRRL 20476	USA	<i>Cronartium conigenum</i>	AF158343	AF160290	Not public	Not public	U34434
<i>Fusarium begoniae</i>	CBS 403.97 [†] = NRRL 25300	Germany	<i>Begonia elatior</i> hybrid	AF158346	AF160293	LT996191	LT996140	U61543
<i>Fusarium bubaricum</i>	CBS 178.35 = NRRL 25488	USSR	<i>Gossypium</i> rotting stem base		KX302912	KX302920	KX302928	
<i>Fusarium bulbicola</i>	CBS 796.70 = NRRL 13371	Iran	<i>Hibiscus cannabinus</i> stalk			JX171449	JX171563	
<i>Fusarium</i>	CBS 220.76 [†] = NRRL 13618	Germany	<i>Nerine bowdenii</i>	KF466327	KF466415	KF466394	KF466404	KF466437
<i>brachylobosum</i>	NRRL 13829	Japan	River sediments			JX171460	JX171574	
<i>Fusarium circinatum</i>	CBS 405.97 [†] = NRRL 25331	USA	<i>Pinus radiata</i>	KM231393	KM231943	JX171510	HM068354	KM232080
<i>Fusarium coicis</i>	NRRL 66233 [†]	Australia	<i>Coix gastreemii</i>	LT996178	KP083251	KP083269	KP083274	LT996115
<i>Fusarium concentricum</i>	CBS 450.97 [†] = NRRL 25181	Costa Rica	<i>Musa sapientum</i> fruit	AF158335	AF160282	LT996192	JF741086	U61548
<i>Fusarium continuum</i>	F201128	China	<i>Zanthoxylum bungeanum</i> stem		KM236720	KM520389	KM236780	
<i>Fusarium convolutans</i>	CBS 144207 [†] = CPC 33733	South Africa	<i>Kyphocarpa angustifolia</i> rhizosphere		LT996094	LT996193	LT996141	
	CBS 144208 = CPC 33732	South Africa	<i>Kyphocarpa angustifolia</i> rhizosphere		LT996095	LT996194	LT996142	
<i>Fusarium culmorum</i>	CBS 417.86 = NRRL 25475	Denmark	Moldy barley kernel			JX171515	JX171628	
<i>Fusarium denticulatum</i>	CBS 735.97 = NRRL 25302	USA	<i>Ipomoea batatas</i>	AF158322	AF160269	LT996195	LT996143	U61550
<i>Fusarium dlamini</i>	CBS 119860 [†] = NRRL 13164	South Africa	Soil debris in cornfield	AF158330	AF160277	KU171681	KU171701	U34430
<i>Fusarium fracticaudum</i>	CBS 137234 ^{††}	Colombia	<i>Pinus maximonoi</i> stem	LT996179	KJ541059	LT996196	LT996144	KJ541051
<i>Fusarium fractiflexum</i>	NRRL 28852 [†]	Japan	<i>Gyphidium</i> sp.	AF158341	AF160288	Not public	LT575064	AF160315
	NRRL 26152	Niger	Unknown		AF160306			AF160321
<i>Fusarium frederigeri</i>	CBS 144209 [†] = CPC 33747	South Africa	<i>Melhantha acuminata</i> rhizosphere	LT996181	LT996097	LT996199	LT996147	LT996117
	CBS 144210 = NRRL 26061	Madagascar	<i>Siriga hermonithica</i>	AF158356	AF160303	LT996197	LT996145	AF160319
	CBS 144495 = CPC 33746	South Africa	<i>Melhantha acuminata</i> rhizosphere	LT996180	LT996096	LT996198	LT996146	LT996116

Species name	Strain ^{††}	Country	Host	Sequence accession number [§]				
				CAL	EF-1 α	RPB1	RPB2	TUB
<i>Fusarium fujikuroi</i>	NRRL 13566	China	<i>Oryza sativa</i>	AF158332	AF160279	JX171456	JX171570	U34415
<i>Fusarium globosum</i>	CBS 428.97 ^T = NRRL 26131	South Africa	<i>Zea mays</i>	KF466329	KF466417	KF466396	KF466406	KF466439
<i>Fusarium goulgardii</i>	NRRL 66250 ^T = RBG 5411	Australia	<i>Xanthorrhoea glauca</i>			KP083270	KP083280	
<i>Fusarium graminearum</i>	CBS 123657 = NRRL 31084	USA	Corn			JX171531	JX171644	
<i>Fusarium konzani</i>	CBS 119849 ^T	USA	<i>Sorghastrum nutans</i>	LT996182	LT996098	LT996200	LT996148	LT996118
<i>Fusarium kyushuense</i>	NRRL 25349	Japan	<i>Triticum aestivum</i>				GQ915492	
<i>Fusarium lactis</i>	CBS 411.97 ^{NT} = NRRL 25200	USA	<i>Ficus carica</i>	AF158325	AF160272	LT996201	LT996149	U61551
<i>Fusarium langsethiae</i>	NRRL 54940	Norway	Oats			JX171550	JX171662	
<i>Fusarium lateritium</i>	NRRL 13622	USA	<i>Ulmus</i> sp.		AY707173	JX171457	JX171571	
<i>Fusarium longipes</i>	NRRL 13368	Australia	Soil			JX171448	JX171562	
<i>Fusarium mangiferae</i>	NRRL 25226	Israel	<i>Mangifera indica</i>	AF158334	AF160281	JX171509	HM068353	U61561
<i>Fusarium mexicanum</i>	NRRL 47473	Mexico	<i>Mangifera indica</i> inflorescence	GU737389	GU737416	Not public	Not public	GU737308
<i>Fusarium napiforme</i>	CBS 748.97 ^T = NRRL 13604	Namibia	<i>Pennisetum typhoides</i>	AF158319	AF160266	HM347136	EF470117	U34428
<i>Fusarium nygamai</i>	CBS 749.97 ^T = NRRL 13448	Australia	<i>Sorghum bicolor</i> necrotic root	AF158326	AF160273	LT996202	EF470114	U34426
<i>Fusarium oxysporum</i>	CBS 716.74 = NRRL 20433	Germany	<i>Vicia faba</i> vascular bundle	AF158366	AF008479	JX171469	JX171583	U34435
	CBS 744.97 = NRRL 22902	USA	<i>Pseudotsuga menziesii</i>	AF158365	AF160312	LT996203	LT575065	U34424
<i>Fusarium palustre</i>	NRRL 54056 ^T	USA	<i>Spartina alterniflora</i>			KT597718	KT597731	
<i>Fusarium parvisorum</i>	CBS 137236 ^T	Colombia	<i>Pinus patula</i> roots	LT996183	KJ541060		LT996150	KJ541055
<i>Fusarium phyllophilum</i>	CBS 216.76 ^T = NRRL 13617	Italy	<i>Druacaena deremensis</i> leaf	KF466333	KF466421	KF466399	KF466410	KF466443
<i>Fusarium poae</i>	NRRL 13714	Unknown	Unknown			JX171458	JX171572	
<i>Fusarium proliferatum</i>	CBS 217.76 = NRRL 22944	Germany	<i>Cattleya</i> pseudobulb, hybrid	AF158333	AF160280	JX171504	HM068352	U34416
<i>Fusarium pseudocircinatum</i>	CBS 449.97 ^T = NRRL 22946	Ghana	<i>Solanum</i> sp.	AF158324	AF160271	LT996204	LT996151	U34427
<i>Fusarium pseudograminearum</i>	CBS 109956 ^T = NRRL 28062	Australia	<i>Hordeum vulgare</i> crowns			JX171524	JX171637	
<i>Fusarium pseudonygamai</i>	CBS 417.97 ^T = NRRL 13592	Nigeria	<i>Pennisetum typhoides</i>	AF158316	AF160263	LT996205	LT996152	U34421

Species name	Strain ^{††}	Country	Host	Sequence accession number [§]				
				CAL	EF-1 α	RPBI	RPB2	TUB
<i>Fusarium ramigenum</i>	CBS 418.98 ^T = NRRL 25208	USA	<i>Ficus carica</i>	KF466335	KF466423	KF466401	KF466412	KF466445
<i>Fusarium sacchari</i>	CBS 223.76 = NRRL 13999	India	<i>Saccharum officinarum</i>	AF158331	AF160278	JX171466	JX171580	U34414
<i>Fusarium sambucinum</i>	NRRL 22187 = NRRL 20727	England	<i>Solanum</i> sp.			JX171493	JX171606	
<i>Fusarium sarcocrochrum</i>	CBS 745.79 = NRRL 20472	Switzerland	<i>Viscum album</i>			JX171472	JX171586	
<i>Fusarium sibiricum</i>	NRRL 53430 ^T	Russia	<i>Avena sativa</i>				HQ154472	
<i>Fusarium sororula</i>	CBS 137242 ^T	Colombia	<i>Pinus patula</i> stems	LT996184	KJ541067	LT996206	LT996153	KJ541057
	NRRL 66179	USA	<i>Hibiscus moscheutos</i>	KX302913	KX302921	KX302921	KX302929	
	NRRL 66180	USA	<i>Hibiscus moscheutos</i>	KX302914	KX302922	KX302922	KX302930	
	NRRL 66181	USA	<i>Hibiscus moscheutos</i>	KX302915	KX302923	KX302923	KX302931	
	NRRL 66182	USA	<i>Hibiscus moscheutos</i>	KX302916	KX302924	KX302924	KX302932	
	NRRL 66183	USA	<i>Hibiscus moscheutos</i>	KX302917	KX302925	KX302925	KX302933	
	NRRL 66184	USA	<i>Hibiscus moscheutos</i>	KX302918	KX302926	KX302926	KX302934	
	CBS 201.63 = NRRL 36351	Portugal	<i>Arachis hypogaea</i> stored nut				GQ915484	
<i>Fusarium sporotrichioides</i>	NRRL 3299	USA	Corn			JX171444	HQ154454	
<i>Fusarium sterilihyposum</i>	NRRL 25623	South Africa	Mango	AF158353	AF160300	Not public	Not public	AF160316
<i>Fusarium stilboides</i>	NRRL 20429	Nyasaland	Coffee bark	AF158342	AF160289	JX171468	JX171582	
<i>Fusarium subglutinans</i>	CBS 747.97 = NRRL 22016	USA	Corn			JX171486	JX171599	U34417
	CBS 190.34 = NRRL 20897	Unknown	Unknown			KX302927	KX302935	
	CBS 189.34 ^T = NRRL 13384	Costa Rica	Soil of banana plantation			JX171451	JX171565	
<i>Fusarium sublanatum</i>	CBS 219.76 = NRRL 13613	Germany	<i>Succisa pratensis</i> flower	AF158344	AF160291	LT996207	LT996154	U34419
<i>Fusarium succisae</i>	CBS 454.97 ^T = NRRL 25451	Sudan	<i>Striga hermonthica</i>	LT996185	KU711697	LT996208	LT996155	KU603909
<i>Fusarium sudanense</i>	NRRL 25622 = NRRL 26616	South Africa	<i>Zea mays</i>	AF158354	AF160301	Not public	Not public	AF160317
<i>Fusarium temperatum</i>	CBS 483.94 ^T	Australia	Soil	KU603951	KU711698	LT996209	LT996156	KU603908
<i>Fusarium terricola</i>	CBS 733.97 = NRRL 22045	South Africa	<i>Sorghum bicolor</i>	LT996186	AF160270	JX171487	JX171600	U34418
<i>Fusarium thapsinum</i>	NRRL 66243 ^T	Australia	<i>Sorghum interjectum</i>	LT996187	KP083263	KP083267	KP083275	LT996119
<i>Fusarium fjaetaba</i>	NRRL 54149	USA	<i>Torreya</i> sp.		HM068337	JX171548	HM068359	

Species name	Strain ^{†‡}	Country	Host	Sequence accession number [§]					
				CAL	EF-1 α	RPB1	RPB2	TUB	
<i>Fusarium transvaalense</i>	CBS 144211 [†] = CPC 30923	South Africa	<i>Sida cordifolia</i> rhizosphere		LT996099	LT996210	LT996157	LT996120	
	CBS 144212 = CPC 30929	South Africa	<i>Melhania acuminata</i> rhizosphere		LT996100	LT996211	LT996158	LT996121	
	CBS 144213 = CPC 33751	South Africa	<i>Melhania acuminata</i> rhizosphere				LT996159	LT996122	
	CBS 144214 = CPC 30946	South Africa	<i>Sida cordifolia</i> rhizosphere		LT996101	LT996212	LT996160	LT996123	
	CBS 144215 = CPC 33723	South Africa	<i>Sida cordifolia</i> rhizosphere		LT996102		LT996161	LT996124	
	CBS 144216 = CPC 30918	South Africa	<i>Sida cordifolia</i> rhizosphere		LT996103	LT996213	LT996162	LT996125	
	CBS 144217 = CPC 30919	South Africa	<i>Sida cordifolia</i> rhizosphere		LT996104	LT996214	LT996163	LT996126	
	CBS 144218 = CPC 30922	South Africa	<i>Sida cordifolia</i> rhizosphere		LT996105	LT996215	LT996164	LT996127	
	CBS 144219 = CPC 30926	South Africa	<i>Sida cordifolia</i> rhizosphere		LT996106	LT996216	LT996165	LT996128	
	CBS 144220 = CPC 30927	South Africa	<i>Sida cordifolia</i> rhizosphere		LT996107	LT996217	LT996166	LT996129	
	CBS 144221 = CPC 33740	South Africa	<i>Kyphocarpa angustifolia</i> rhizosphere				LT996167	LT996130	
	CBS 144222 = CPC 30939	South Africa	<i>Kyphocarpa angustifolia</i> rhizosphere		LT996108	LT996218	LT996168	LT996131	
	CBS 144223 = CPC 30941	South Africa	<i>Kyphocarpa angustifolia</i> rhizosphere		LT996109		LT996169	LT996132	
	CBS 144224 = CPC 30928	South Africa	<i>Melhania acuminata</i> rhizosphere		LT996110	LT996219	LT996170	LT996133	
CBS 144496 = CPC 33750	South Africa	<i>Melhania acuminata</i> rhizosphere				LT996171	LT996134		
<i>Fusarium tuipense</i>	NRRL 31008	Australia	Soil			JX171529	JX171642		
	NRRL 53984	Brazil	<i>Mangifera indica</i>		GU737377	GU737404	Not public	GU737296	
	CBS 178.32 = NRRL 22949	Germany	<i>Lactarius pubescens</i>		AF158328	AF160275	LT996220	U34433	
	CBS 458.93 [†]	Austria	Winter wheat halm base					KM232382	
	CBS 734.97 = NRRL 22172	Germany	<i>Zea mays</i>		AF158315	AF160262	LT996221	EF470122	
	F201114	China	<i>Zanthoxylum bungeanum</i>			KM236706	KM520380	KM236766	
	CBS 258.52 = NRRL 25486	Ivory Coast	<i>Coffea</i> sp. trunk		AY707136	JX171517	HM068355	AY707118	
	† CBS; Westerdijk Fungal Biodiversity Institute. CPC; Collection of Pedro W. Crous, held at CBS. F; College of Forestry, Northwest A&F University, Taicheng Road, Yangling, Shaanxi China. NRRL; Agricultural Research Service, Peoria, IL, USA.								
	††; ex-isotype culture. ††; ex-paratype culture. †; ex-type culture. NT; ex-neotype culture.								
	§ CAL; Calmodulin. EF-1 α ; Translation elongation factor 1-alpha. RPB1; RNA polymerase largest subunit. RPB2; RNA polymerase second largest subunit. TUB; Tubulin. New sequences are shown in bold . Sequences marked as "Not public" were obtained from Kerry O'Donnell's alignment datasets.								

† CBS; Westerdijk Fungal Biodiversity Institute. CPC; Collection of Pedro W. Crous, held at CBS. F; College of Forestry, Northwest A&F University, Taicheng Road, Yangling, Shaanxi China. NRRL; Agricultural Research Service, Peoria, IL, USA.

††; ex-isotype culture. ††; ex-paratype culture. †; ex-type culture. NT; ex-neotype culture.

§ CAL; Calmodulin. EF-1 α ; Translation elongation factor 1-alpha. RPB1; RNA polymerase largest subunit. RPB2; RNA polymerase second largest subunit. TUB; Tubulin. New sequences are shown in **bold**. Sequences marked as "Not public" were obtained from Kerry O'Donnell's alignment datasets.

beta-tubulin (*TUB*). Sequencing was made in both strand directions using the same primer pairs as for PCR amplification on an Applied Biosystems, Hitachi 3730xl DNA analyser (Applied Biosystems Inc., Foster City, California, USA). Consensus sequences were assembled using Seqman Pro v. 10.0.1 (DNASTAR, Madison, WI, USA). All DNA sequences generated in this study were lodged in GenBank and the European Nucleotide Archive (ENA) (Table 1).

Molecular identification and phylogenetic analyses

A first analysis was based on pairwise alignments and *blastn* searches on the *Fusarium* MLST (<http://www.westerdijkinstituut.nl/fusarium/>) and NCBI (<https://blast.ncbi.nlm.nih.gov/Blast.cgi>) databases, respectively, using *EF-1a* and *RPB2* sequences in order to resolve the position of the KNP isolates amongst the different species complexes recognised in *Fusarium* (O'Donnell et al. 2013). Sequences from individual loci were aligned using MAFFT (Katoh and Standley 2013), on the web server of the European Bioinformatics Institute (EMBL–EBI; <http://www.ebi.ac.uk/Tools/msa/mafft/>) (Li et al. 2015).

Phylogenetic analyses were based on Maximum-likelihood (ML) and Bayesian (B) analyses, both algorithms run on the CIPRES Science Gateway portal (Miller et al. 2012). Evolutionary models were calculated using MrModelTest v. 2.3 using the Akaike information criterion (Nylander 2004; Posada and Crandall 1998). For ML, RAxML-HPC2 v. 8.2.10 on XSEDE was used (Stamatakis 2014), clade stability was tested with a bootstrap analysis (BS) using the rapid bootstrapping algorithm with default parameters. The B analyses were run using MrBayes v. 3.2.6 on XSEDE (Ronquist and Huelsenbeck 2003) using four incrementally heated MCMC chains for 5M generations, with the stop-rule option on and sampling every 1000 trees. After convergence of the runs (average standard deviation of split frequencies below 0.01) the first 25% of samples were discarded as the burn-in fraction and 50% consensus trees and posterior probabilities (PP) were calculated from the remaining trees.

Phylogenies were first made individually for each locus dataset and visually compared for topological incongruence amongst statistically supported nodes (ML-BS \geq 70% and B-PP \geq 0.95) (Mason-Gamer and Kellogg 1996, Wiens 1998), before being concatenated for multi-locus analyses using different locus combinations according to strains and DNA sequences currently available in public databases, in addition to previously published phylogenies (O'Donnell et al. 2000, 2013; Herron et al. 2015; Lupien et al. 2017; Moussa et al. 2017, Sandoval-Denis et al. 2018). A further 232 sequences representing 72 taxa were retrieved from GenBank and included in the phylogenetic analyses, while an additional 58 DNA sequences were obtained from 24 fungal strains requested from the CBS and NRRL (Agricultural Research Service, Peoria, IL, USA) culture collections (Table 1). All alignments and trees generated in this study were uploaded to TreeBASE (<https://treebase.org>).

Results

Phylogenetic analyses

Pairwise DNA alignments and BLAST searches using *EF-1a* and *RPB2* sequences showed that the 19 isolates from KNP belonged to three different species complexes of the genus *Fusarium* i.e. the *F. buharicum* Jacz. ex Babajan & Teterevn.-Babajan species complex (FBSC; two isolates), the *F. fujikuroi* Nirenberg species complex (FFSC; two isolates) and the *F. sambucinum* Fuckel species complex (FSAMSC; 15 isolates). According to these results, sequences of related taxa and lineages were retrieved from GenBank and incorporated into individual phylogenetic analyses for each species complex.

Multi-locus analyses were carried out in order to further delimit the KNP *Fusarium* isolates amongst the known diversity in their respective species complexes. With the exception of the FFSC, the topologies observed from ML and B analyses of single and multi-locus datasets were highly congruent, with only minor differences affecting unsupported nodes on the trees (all trees available in TreeBASE). The characteristics of the different alignments and tree statistics for all the species complexes are shown in Table 2.

The analysis of the FBSC included sequences of *EF-1a*, *RPB1* and *RPB2* loci from 18 isolates representing 10 taxa, including members of the *Fusarium torreyae* T. Aoki, J.A. Sm., L.L. Mount, Geiser & O'Donnell species complex (FTYSC) and *Fusarium lateritium* Nees species complex (FLSC) as outgroup (Fig. 2). The four ingroup taxa resolved with high statistical support. Two KNP isolates from *K. angustifolia* obtained from the bottom site of the catena (CBS 144207 and 144208) clustered in a sister relationship with the clade representing *Fusarium subglunatum* Reinking, but were genetically clearly delimited.

The phylogeny of the FFSC included sequences of *CAL*, *EF-1a*, *RPB1*, *RPB2* and *TUB* loci from 48 strains and 44 taxa, including two outgroups (*F. oxysporum* CBS 716.74 and 744.97) (Fig. 3). The phylogeny showed a clear delimitation between the biogeographic clades recognised in this species complex (African, American and Asian clades *sensu* O'Donnell et al. 1998). Both American and Asian clades were shown as monophyletic with high ML-BS and B-PP support; in contrast, the African clade was resolved as polyphyletic, comprising two distinct and highly supported lineages. A terminal, speciose clade (African A) encompassing 17 taxa and a basal clade (African B), close to the American clade which included the ex-type of *Fusarium dlamini* Marasas, P.E. Nelson & Toussoun (CBS 119860) and a sister terminal clade (ML-BS=100, B-PP=1) comprising two KNP isolates from *M. acuminata* (CBS 144209 and 144495) and two unidentified African *Fusarium* isolates (CBS 144210 and NRRL 26152). From the loci used here, only *TUB* resolved both African clades as sister groups; however, its monophyly was not supported by clade stability measurements (data not shown). Conversely, individual *CAL*, *EF-1a* and *RPB2* phylog-

Table 2. Characteristics of the different datasets and statistics of phylogenetic analyses used in this study.

Analysis [†]	Locus [‡]	Number of Sites [§]				Evolu-tionary model	Number of trees sampled in B	Maximum-likelihood statistics	
		Total	Con-served	Phyloge-netically informative	B unique patterns			Best tree optimised likelihood	Tree length
<i>Fusarium buharicum</i> SC	<i>EF-1a</i>	495	300	119	198	GTR+G	414	-11313.23702	0.598675
	<i>RPB1</i>	930	682	203	211	SYM+G			
	<i>RPB2</i>	1663	1251	330	310	GTR+I+G			
<i>Fusarium fujikuroi</i> SC	<i>CAL</i>	545	423	67	167	SYM+G	282	-20603.30043	0.567054
	<i>EF-1a</i>	677	428	127	295	GTR+I+G			
	<i>RPB1</i>	1534	1219	185	137	SYM+I+G			
	<i>RPB2</i>	1551	1211	227	315	GTR+I+G			
	<i>TUB</i>	488	351	66	336	SYM+G			
<i>Fusarium sambucinum</i> SC	<i>RPB1</i>	854	594	201	213	SYM+I+G	241	-9871.793718	0.740271
	<i>RPB2</i>	1580	1128	346	396	GTR+G			

[†] SC: Species complex.

[‡] *CAL*: Calmodulin. *EF-1a*: Translation elongation factor 1-alpha. *RPB1*: RNA polymerase largest sub-unit. *RPB2*: RNA polymerase second largest subunit. *TUB*: Tubulin.

[§] B: Bayesian inference.

^{||} G: Gamma distributed rate variation among sites. GTR: Generalised time-reversible. I: Proportion of invariable sites. SYM: Symmetrical model.

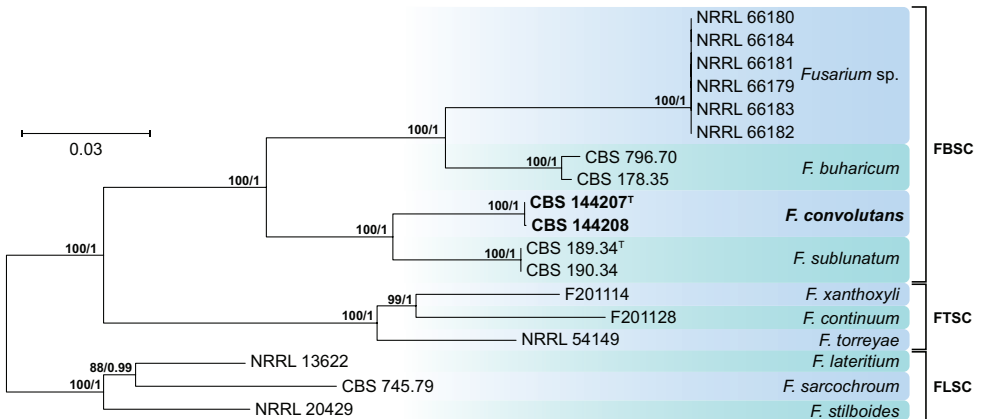


Figure 2. Maximum-likelihood (ML) phylogram obtained from combined *EF-1a*, *RPB1* and *RPB2* sequences of 18 strains belonging to the *Fusarium buharicum* (FBSC), *Fusarium tricinctum* (FTSC) and *Fusarium lateritium* (FLSC) species complexes. Numbers on the nodes are ML bootstrap values above 70% and Bayesian posterior probability values above 0.95. Branch lengths are proportional to distance. Ex-type strains are indicated with ^T. Strains corresponding to new species described here are shown in **bold**.

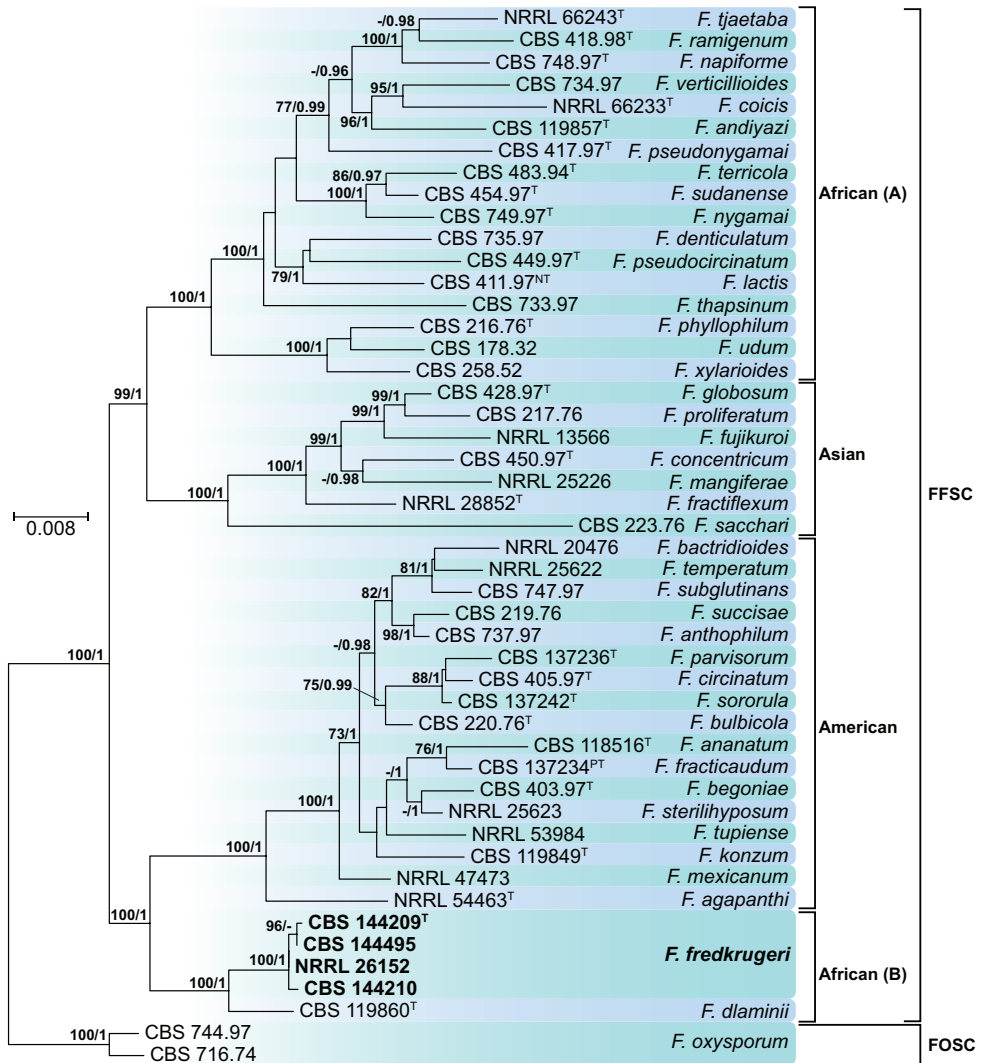


Figure 3. Maximum-likelihood (ML) phylogram obtained from combined *CAL*, *EF-1a*, *RPB1*, *RPB2* and *TUB* sequences of 48 strains belonging to the *Fusarium fujikuroi* (FFSC) and *Fusarium oxysporum* (FOOSC) species complexes. Numbers on the nodes are ML bootstrap values above 70% and Bayesian posterior probability values above 0.95. Branch lengths are proportional to distance. Ex-type, ex-neotype and ex-paratype strains are indicated with ^T, ^{NT} and ^{PT}, respectively. Strains corresponding to new species described here are shown in **bold**.

enies resolved African B as basal to the ingroup, while *RPB1* allocated this clade as basal to the American clade. Nonetheless, all the individual phylogenies, in addition to the combined dataset, clearly demonstrated genealogical uniqueness of the terminal clade encompassing KNP isolates.

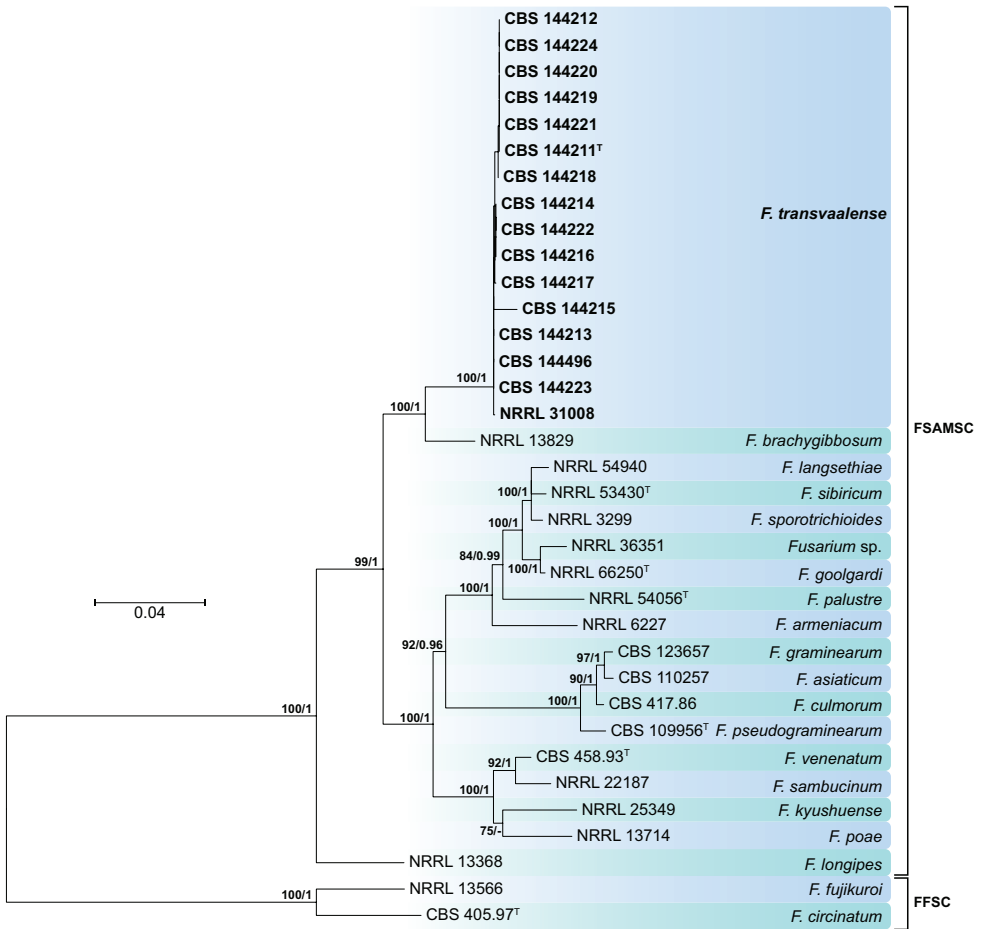


Figure 4. Maximum-likelihood (ML) phylogram obtained from combined *RPB1* and *RPB2* sequences of 35 strains belonging to the *Fusarium sambucinum* (FSAMSC) and *Fusarium fujikuroi* (FFSC) species complexes. Numbers on the nodes are ML bootstrap values above 70% and Bayesian posterior probability values above 0.95. Branch lengths are proportional to distance. Ex-type strains are indicated with ^T. Strains corresponding to new species described here are shown in **bold**.

The FSAMSC was studied using combined *RPB1* and *RPB2* sequences. The phylogeny included 35 isolates from 20 taxa, including the two outgroups *Fusarium circinatum* Nirenberg & O'Donnell (CBS 405.97) and *Fusarium fujikuroi* Nirenberg (NRRL 13566) (Fig. 4). Fifteen KPN *Fusarium* isolates from the three sampled plant species (three isolates from *K. angustifolia*, four isolates from *M. acuminata* and eight isolates from *S. cordifolia*), all obtained from the top site of the catena, clustered with an unidentified *Fusarium* isolate (NRRL 31008) in a distinct clade (ML-BS=100, B-PP=1), close to *Fusarium brachygibbosum* Padwick (strain NRRL 13829).

The clades including KNP isolates and corresponding to previously undisclosed lineages of *Fusarium* are described in the taxonomy section as the three novel species, *F. convolutans*, *F. fredkrugeri* and *F. transvaalense*.

Taxonomy

Fusarium convolutans Sandoval-Denis, Crous & W.J. Swart, sp. nov.

Mycobank: MB825102

Fig. 5

Diagnosis. Different from *F. circinatum*, *F. pseudocircinatum* O'Donnell & Nirenberg and *F. sterilibyphosum* Britz, Marasas & M.J. Wingf. by the absence of aerial conidia (microconidia) and the presence of chlamydospores. Different from *F. buharicum* Jacz. ex Babajan & Teterevn.-Babajan and *F. sublunatum* by its shorter, less septate and less curved conidia and by the presence of sterile hyphal coils.

Type. South Africa, Kruger National Park, Skukuza, Granite Supersite, 25°06'33.9"S, 31°34'40.9E, from rhizosphere soil of *Kyphocarpa angustifolia*, 23 Mar 2015, W.J. Swart, holotype CBS H-23495, dried culture on OA, ex-holotype strain CBS 144207 = CPC 33733.

Description. Colonies on PDA growing in the dark with an average radial growth rate of 2.1–4.8 mm/d, 4.4–5.8 mm/d and 4.6–6.3 mm/d at 24, 27 and 30 °C, respectively; reaching 11–28 mm diam. in 7 d at 24 °C and a maximum of 23–37 mm diam. in 7 d at 30 °C. Minimum temperature for growth 12 °C, maximum 36 °C, optimal 27–33 °C. Colony surface white to cream coloured, flat and highly irregular in shape, velvety to felty, with scant and short aerial mycelium; colony margins highly irregular to rhizoid, with abundant white to grey submerged mycelium. Reverse white, straw to yellow diffusible pigment produced between 21–33 °C, scarcely produced and turning luteous to orange at 36 °C. Colonies on CMA and OA incubated in the dark reaching 40–48 mm diam. in 7 d at 24 °C. Colony surface white to cream coloured, flat or slightly elevated at the centre, velvety to dusty; aerial mycelium abundant, short and dense, concentrated on the colony centre; margins membranous and regular, buff to honey coloured, without aerial mycelium. Reverse ochreous without diffusible pigments. Sporulation scant from conidiophores formed on the aerial mycelium, sporodochia not formed. *Conidiophores* on the aerial mycelium straight or flexuous, smooth- and thin-walled, simple, mostly reduced to conidiogenous cells borne laterally on hyphae or up to 50 µm tall, bearing terminal single or paired monophialides; *phialides* subulate to subcylindrical, smooth- and thin-walled, 15.5–22 µm long, (3.5–)4–5 µm at the widest point, with inconspicuous periclinal thickening and a short-flared collarette; *conidia* clustering in discrete false heads at the tip of monophialides, lunate to falcate, curved or somewhat straight, tapering gently toward the basal part, robust; apical cell often equal in length or slightly shorter than the adjacent cell, blunt

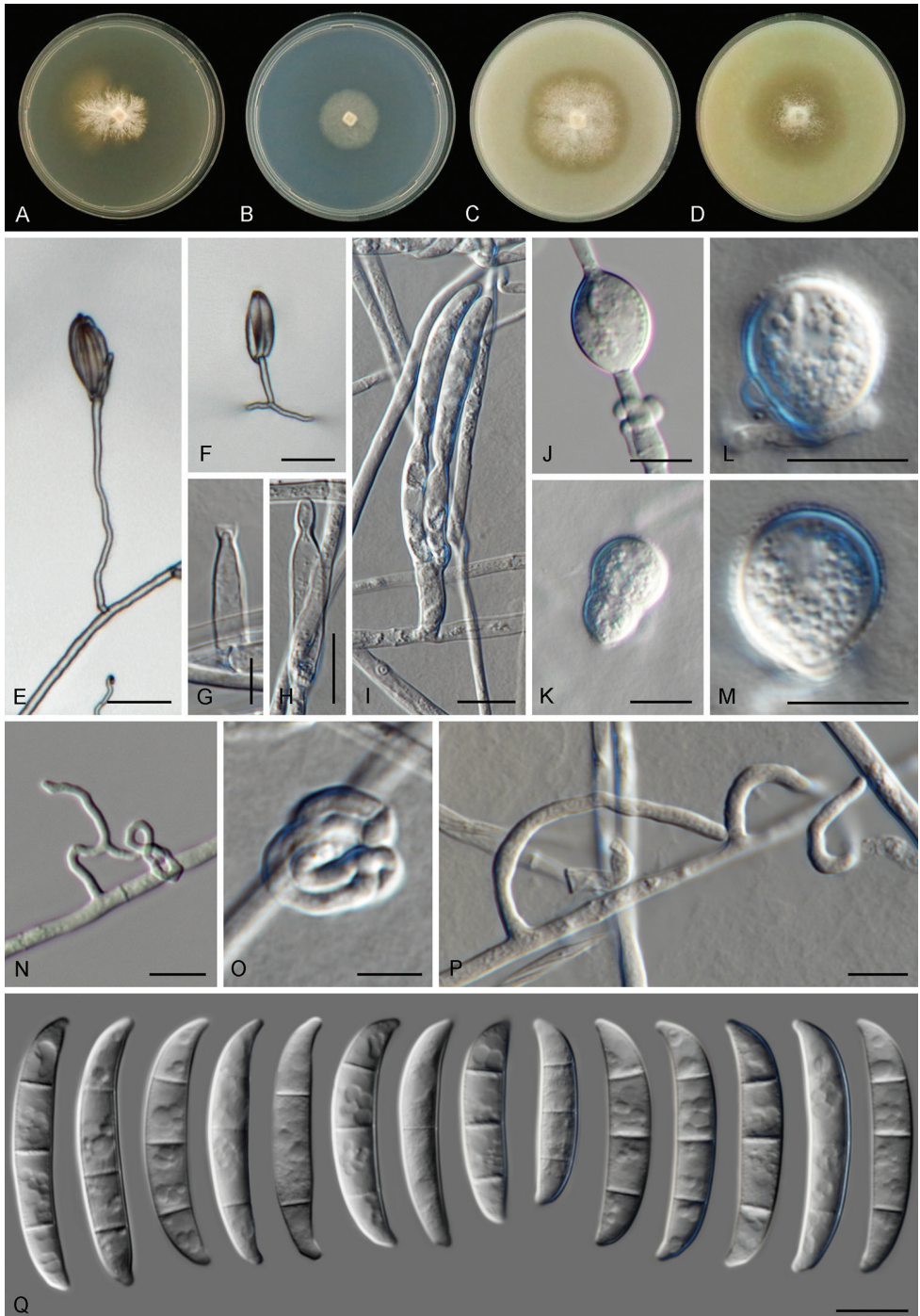


Figure 5. *Fusarium convolutans* sp. nov. **A–D** Colonies on PDA, SNA, OA and CMA, respectively, after 7 d at 24 °C in the dark **E–I** Conidiophores, phialides and conidia **J–M** Chlamydospores **N–P** Sterile hyphal projections **Q** Conidia. Scale bars: 20 µm (**E, F**); 5 µm (**G–I**); 10 µm (**J–Q**).

to conical; basal cell papillate to distinctly notched, (1–2–)3-septate, hyaline, thin- and smooth-walled. One-septate conidia: $24 \times 4.5 \mu\text{m}$; two-septate conidia: $24.5 \times 6 \mu\text{m}$; three-septate conidia: $(25.5\text{--})29\text{--}36.5\text{--}(38.5) \times (4\text{--})5\text{--}6.5\text{--}(7.5) \mu\text{m}$. *Chlamydospores* abundantly formed, globose to subglobose, smooth- and thick-walled, $(9.5\text{--})11\text{--}13.5\text{--}(14) \mu\text{m}$ diam.; terminal or intercalary in the hyphae or conidia, often borne laterally at the tip of elongated, cylindrical, stalk-like projections, solitary or in small clusters. Sterile, coiled, sometimes branched hyphal projections abundantly formed laterally from the substrate and aerial mycelium.

Distribution. South Africa.

Etymology. From Latin, “convolutans”, participle of *convolutare*, coiling, in reference to the abundant sterile, coiled lateral hyphal projections.

Additional isolate examined. South Africa, Kruger National Park, Skukuza, Granite Supersite, $25^{\circ}06'33.9''\text{S}$, $31^{\circ}34'40.9\text{E}$, from rhizosphere soil of *Kyphocarpa angustifolia*, 23 Mar 2015, W.J. Swart, CBS 144208 = CPC 33732.

Notes. The main morphological feature of *F. convolutans*, namely the production of sterile, coiled hyphal projections, grossly resembles other *Fusarium* species producing similar structures i.e. *F. circinatum*, *F. pseudocircinatum* and *F. sterilihyphosum*. The three latter species, however, are genetically unrelated to *F. convolutans*, being allocated in the FFSC; and are also easily differentiable by the characteristics of the aerial conidia (typical *Fusarium* microconidia are absent in the new species) and the lack of chlamydospores (present in the new species) (Leslie and Summerell 2006). *Fusarium convolutans* can be easily differentiated morphologically from their phylogenetically closely related species, *F. buharicum* and *F. sublunatum*. It has relative simple conidiophores and shorter, less septate and markedly less curved conidia (up to $38.5 \mu\text{m}$ long and 1–3-septate vs. up to 87 and $81 \mu\text{m}$ long, 0–8-septate in *F. buharicum* and *F. sublunatum*, respectively) (Gerlach and Nirenberg 1982). *Fusarium buharicum* and *F. sublunatum* also lack sterile hyphal coils.

***Fusarium fredkrugeri* Sandoval-Denis, Crous & W.J. Swart, sp. nov.**

Mycobank: MB825103

Fig. 6

Diagnosis. Differs from *Fusarium dlamini* Marasas, P.E. Nelson & Toussoun by producing only one type of aerial conidia, shorter sporodochial conidia and the absence of chlamydospores.

Type. South Africa, Kruger National Park, Skukuza, Granite Supersite, $25^{\circ}06'48.6''\text{S}$, $31^{\circ}34'36.5''\text{E}$, from rhizosphere soil of *Melbania acuminata*, 23 Mar 2015, W.J. Swart, holotype CBS H-23496, dried culture on OA, culture ex-holotype CBS 144209 = CPC 33747.

Description. Colonies on PDA growing in the dark with an average radial growth rate of 4.7–5.8 mm/d and reaching 22–35 mm diam. in 7 d at 24°C , filling an entire 9 cm Petri dish in 7 d at 27 and 30°C . Minimum temperature for growth 12°C , maxi-

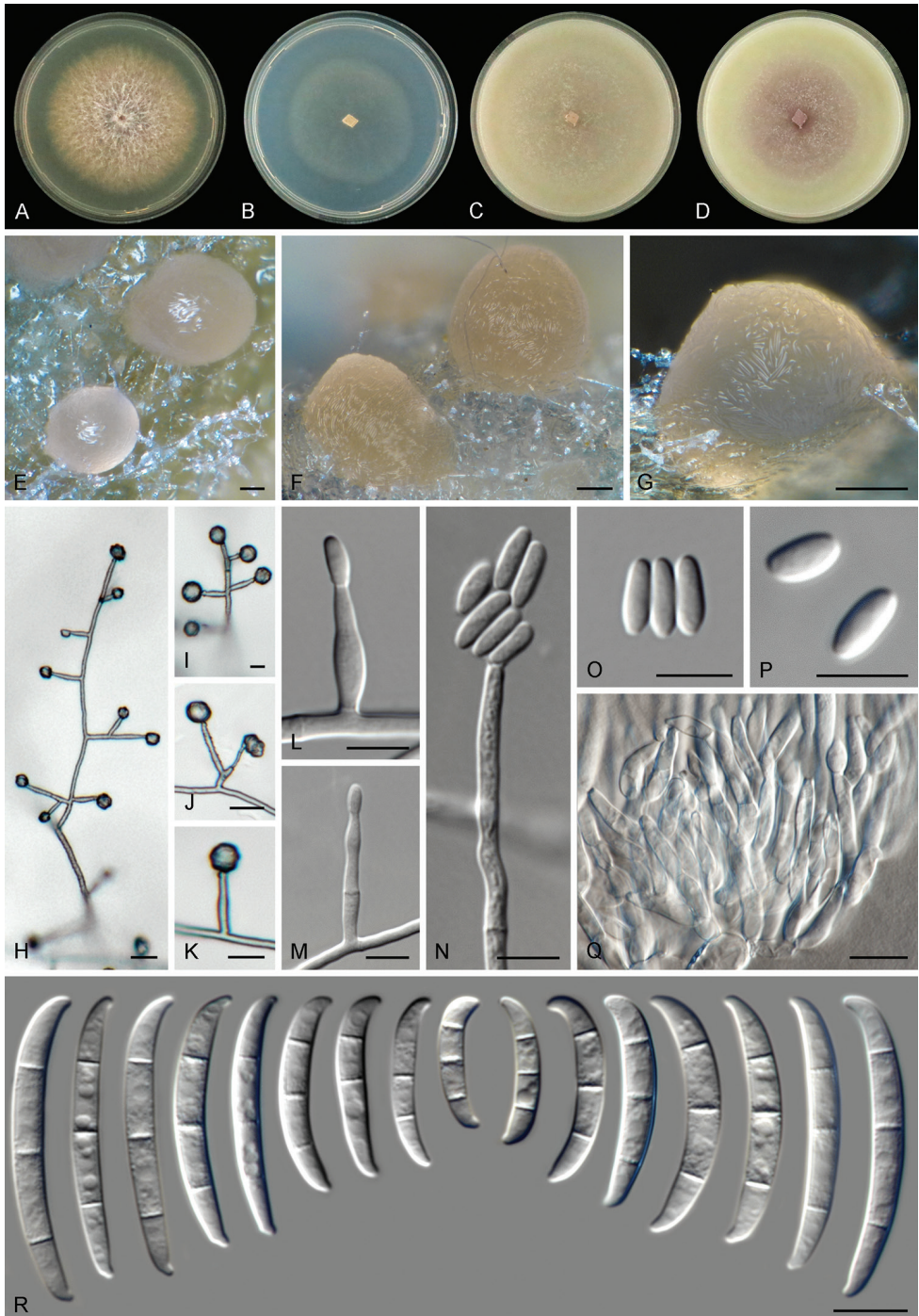


Figure 6. *Fusarium fredkrugeri* sp. nov. **A–D** Colonies on PDA, SNA, OA and CMA, respectively, after 7 d at 24 °C in the dark **E–G** Sporodochia formed on the surface of carnation leaves **H–N** Aerial conidiophores, phialides and conidia **O, P** Aerial conidia **Q** Sporodochial conidiophores and phialides **R** Sporodochial conidia. Scale bars: 100 µm (**E–G**); 10 µm (**H–R**).

mum 36 °C, optimal 27–30 °C. Colony surface at first white to cream coloured, later turning bay to chestnut with pale luteous to luteous periphery; flat, felty to cottony with abundant erect- aerial mycelium forming white patches; colony margins regular and filiform with abundant submerged mycelium. Reverse pale luteous, a blood sepia to chestnut coloured diffusible pigment is scarcely produced at 24 °C, pigment production is markedly enhanced at 27–30 °C, becoming greyish-sepia at 33 °C. Colonies on CMA and OA incubated at 24 °C in the dark reaching 65–67 mm diam. or occupying an entire 9 cm Petri dish in 7 d, respectively. Colony surface pale bay coloured, flat, felty to velvety, aerial mycelium scant, forming white to cream patches; margins regular. Reverse pale bay to pale vinaceous. Sporulation abundant from conidiophores formed on the substrate and aerial mycelium and from sporodochia. *Conidiophores* on the aerial mycelium straight or flexuous, erect or prostrate, septate, smooth- and thin-walled, often appearing rough by accumulation of extracellular material, commonly simple or reduced to conidiogenous cells borne laterally on hyphae or up to 200 µm tall and irregularly branched at various levels, branches bearing lateral and terminal monophialides borne mostly single or in pairs; *phialides* subulate, ampulliform, lageniform to subcylindrical, smooth- and thin-walled, (8.5–)9.5–17.5(–24.5) µm long, 2–3(–3.5) µm at the widest point, without periclinal thickening, collarets inconspicuous; *conidia* formed on aerial conidiophores, hyaline, obovoid, ellipsoidal to slightly reniform or allantoid, smooth- and thin-walled, 0-septate, (4.5–)5–8.5(–12.5) × (1.5–)2–3.5(–6) µm, clustering in discrete false heads at the tip of monophialides. *Sporodochia* pale orange to pink coloured, often somewhat translucent, formed abundantly on the surface of carnation leaves and on the agar surface. *Conidiophores* in sporodochia 26–46 µm tall, densely aggregated, irregularly and verticillately branched up to three times, with terminal branches bearing 2–3 monophialides; *sporodochial phialides* doliiform to subcylindrical, (9–)11.5–15.5(–18.5) × (2.5–)3–4(–4.5) µm, smooth- and thin-walled, with periclinal thickening and an inconspicuous apical collarette. *Sporodochial conidia* falcate, tapering toward the basal part, robust, moderately curved and slender; apical cell more or less equally sized than the adjacent cell, blunt to slightly papillate; basal cell papillate to distinctly notched, (1–)3–4-septate, hyaline, thin- and smooth-walled. One-septate conidia: 13–17(–18) × (2.5–)3–4 µm; two-septate conidia: 15 × 4.5 µm; three-septate conidia: (16–)28.5–39(–45) × (3–)4–5(–5.5) µm; four-septate conidia: 39.5–40(–41) × 4.5–5 µm; overall (13–)27.5–39.5(–45) × (3–)3.5–5.5 µm. Chlamydospores absent.

Distribution. Madagascar, Niger and South Africa.

Etymology. In honour and memory of Dr. Frederick J. Kruger, pioneer of forest hydrology, fynbos ecology and invasive species and fundamental for the collections included in this study.

Additional isolates examined. Madagascar, from *Striga hermonthica*, unknown date, A.A. Abbasher, CBS 144210 = NRRL 26061 = BBA 70127. South Africa, Kruger National Park, Skukuza, Granite Supersite, 25°06'48.6"S, 31°34'36.5"E, from rhizosphere soil of *Melbania acuminata*, 23 Mar 2015, W.J. Swart, CBS 144495 = CPC 33746.

Notes. This species is genetically closely related to *F. dlaminii*, both species having similar colonial morphology, optimal growth conditions and biogeography. Moreo-

ver, both species exhibit relatively short aerial phialides producing conidia in heads, somewhat resembling those produced by *F. oxysporum* rather than most members of the FFSC (Leslie and Summerell 2006; Marasas et al. 1985). However, besides exhibiting much faster growth rates, *F. fredkrugeri* presents clearly distinctive morphological features such as the production of only one type of aerial conidia (vs. two types in *F. dlamini*: allantoid to fusiform and 0-septate; and napiform 0–1-septate); orange to pink sporodochia, produced on carnation leaves but also abundantly on the agar surface (vs. orange sporodochia, produced only on the surface of carnation leaves in *F. dlamini*) (Leslie and Summerell 2006). Additionally, *F. fredkrugeri* produces shorter and less septate sporodochial conidia ((1–)3–4-septate and up to 45 µm long in the latter species vs. mostly 5-septate and up to 54 µm long in *F. dlamini*) while chlamydospores are not produced. The latter feature, coupled with the somewhat more complex conidiophores also clearly differentiates *F. fredkrugeri* from *F. oxysporum*.

***Fusarium transvaalense* Sandoval-Denis, Crous & W.J. Swart, sp. nov.**

Mycobank: MB825104

Fig. 7

Diagnosis. Different from most species in FSAMSC by its slender sporodochial conidia with tapered and somewhat rounded apex; its smooth- to tuberculate, often pigmented chlamydospores and the formation of large mycelial tufts on OA.

Type. South Africa, Kruger National Park, Skukuza, Granite Supersite, 25°06'45.5"S, 31°34'35.0"E, from rhizosphere soil of *Sida cordifolia*, 23 Mar 2015, W.J. Swart, holotype CBS H-23497, dried culture on SNA, culture ex-holotype CBS 144211 = CPC 30923.

Description. Colonies on PDA growing in the dark with an average radial growth rate of 8.5–9.3 mm/d, reaching 34–37 mm diam. in 7 d at 24 °C, filling an entire 9 cm Petri dish in 7 d at 27–33 °C. Minimum temperature for growth 12 °C, maximum 36 °C, optimal 27–30 °C. Colony surface at first white, turning coral to dark vinaceous with white periphery and abundant yellow hyphae at the centre; flat, velvety to woolly, with abundant aerial mycelium and erect hyphal strings reaching several mm tall; colony margins regular and filiform. Reverse with yellow, coral or dark vinaceous patches, coral diffusible pigments strongly produced between 15–30 °C, turning scarlet to orange at 33–36 °C. Colonies on CMA and OA incubated at 24 °C in the dark occupying an entire 9 cm Petri dish in 7 d. Colony surface coral, rust to chestnut coloured in irregular patches, flat, felty to woolly, aerial mycelium scarce on CMA, mostly as radially dispersed white patches, on OA aerial mycelium abundant, especially on the periphery of the colony, forming dense, pustule-like, white mycelial tufts, formed by abundant intermingled hyphae and chlamydospores, 1–1.5 cm tall, with flesh to coral coloured stipes; margins on CMA and OA regular. Reverse pale luteous with red to coral periphery. Sporulation abundant from conidiophores formed on the aerial mycelium, at the agar level and from sporodochia. *Conidiophores* on the aerial mycelium straight or flexuous, septate, smooth- and thin-walled, up to 150 µm tall, sometimes

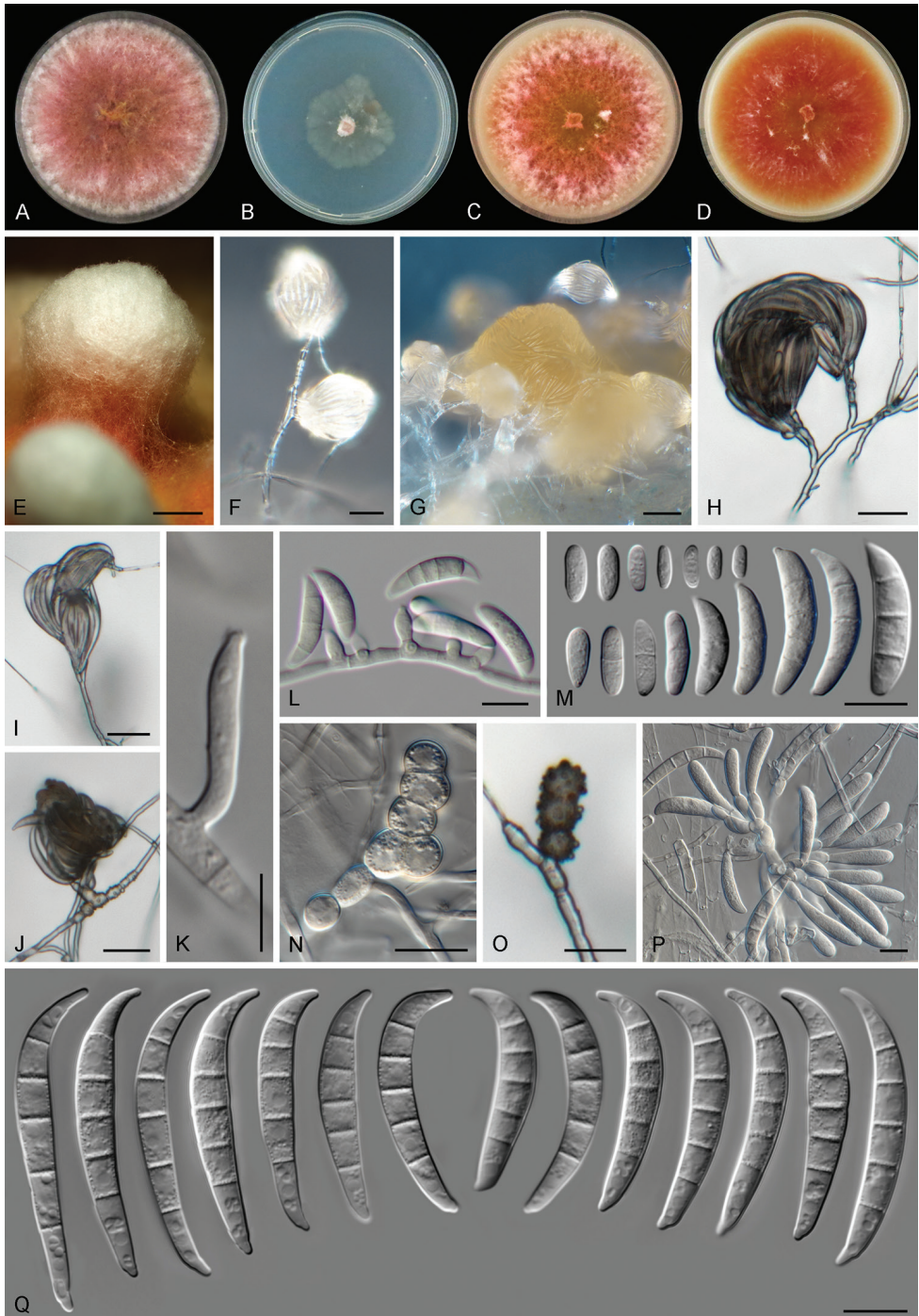


Figure 7. *Fusarium transvaalense* sp. nov. **A–D** Colonies on PDA, SNA, OA and CMA, respectively, after 7 d at 24 °C in the dark **E** Pustule-like growth on OA **F, G** Sporodochia formed on the surface of carnation leaves **H–L** Aerial conidiophores phialides and conidia **M** Aerial conidia **N, O** Chlamydospores **P** Sporodochial conidiophores and phialides **Q** Sporodochial conidia. Scale bars: 2 mm (**E**); 20 μm (**F–J**); 5 μm (**K**); 10 μm (**L–Q**).

emerging from irregular, swollen, pigmented and rough-walled cells on the hyphae; simple or sparingly and irregularly branched, branches bearing terminal, rarely lateral monophialides or reduced to conidiogenous cells borne laterally on hyphae; *phialides* on the aerial conidiophores short ampulliform, subulate to subcylindrical, smooth- and thin-walled, (7–)9–14(–15) μm long, (3–)4–5 μm at the widest point, without periclinal thickening and with a minute, inconspicuous collarette; *conidia* formed on aerial conidiophores of two types: a) hyaline, obovoid, ellipsoidal to clavate, smooth- and thin-walled, 0–1-septate, 2–14 \times 2–4 μm ; b) lunate to short falcate with a pointed apex and a somewhat flattened base, smooth- and thin-walled, 3–5-septate. Three-septate conidia: (16–)18–27(–29) \times 5–6 μm ; four-septate conidia: 21–24(–25) \times 5–6 μm ; five-septate conidia: (25–)27–33 \times 5–6 μm . *Sporodochia* cream to orange coloured, formed abundantly on the surface of carnation leaves and rarely on the agar surface, at first very small and sparse later becoming aggregated. *Conidiophores* in sporodochia 22–31 μm tall, irregularly branched, bearing clusters of 3–6 monophialides; *sporodochial phialides* doliiiform to ampulliform, (5–)9–14(–18) \times (3–)4–5 μm , smooth- and thin-walled, with periclinal thickening and a short apical collarette. *Sporodochial conidia* falcate, wedge-shaped, tapering towards both ends, markedly curved and robust; apical cell longer than the adjacent cell, pointed; basal cell distinctly notched, sometimes somewhat extended (1–)3–5(–6)-septate, hyaline, smooth- and thick-walled. One-septate conidia: 19 \times 4 μm ; three-septate conidia: 20–27(–28) \times 5–7 μm ; four-septate conidia: (29–)30–32 \times 5–7 μm ; five-septate conidia: (26–)29–41(–53) \times 4–5(–6) μm ; six-septate conidia: 36 \times 7 μm ; overall (19–)25.9–40(–53) \times (3.5–)4–6(–7) μm . *Chlamydosporae* abundant, hyaline or pigmented, smooth- to rough-walled or tuberculate, 7–8 μm diam., terminal or intercalary, solitary, in chains or in clusters.

Distribution. Australia and South Africa

Etymology. After Transvaal, the name of a former colony and Republic located between the Limpopo and Vaal rivers, currently a province of South Africa and where this species was found. From Latin *trans* meaning “on the other side of” and Vaal a South African river.

Additional isolates examined. South Africa, Kruger National Park, Skukuza, Granite Supersite, 25°06'48.6"S, 31°34'36.5"E, from rhizosphere soil of *Melbania acuminata*, 23 Mar 2015, W.J. Swart, CBS 144224 = CPC 30928, CBS 144212 = CPC 30929; 25°06'45.6"S, 31°34'37.7"E, CBS 144496 = CPC 33750, CBS 144213 = CPC 33751; 25°06'48.8"S, 31°34'36.6"E, from rhizosphere soil of *Sida cordifolia*, 23 Mar 2015, W.J. Swart, CBS 144214 = CPC 30946; 25°06'45.7"S, 31°34'35.1"E, CBS 144215 = CPC 33723; 25°06'45.5"S, 31°34'35.0"E, CBS 144216 = CPC 30918, CBS 144217 = CPC 30919, CBS 144218 = CPC 30922, , CBS 144219 = CPC 30926, CBS 144220 = CPC 30927); 25°06'51.4"S, 31°34'37.5"E, from rhizosphere soil of *Kyphocarpa angustifolia*, 23 Mar 2015, W.J. Swart, CBS 144221 = CPC 33740; 25°06'51.8"S, 31°34'38.1"E, CBS 144222 = CPC 30939, CBS 144223 = CPC 30941.

Notes. *Fusarium transvaalense* exhibits a sporodochial conidial morphology typical of members of FSAMSC with marked dorsiventral curvature and tapered ends. Several species in FSAMSC form comparable conidia in culture i.e. *F. crookwellense*

L.W. Burgess, P.E. Nelson & Toussoun, *F. sambucinum*, *F. sporotrichioides* Sherb., *F. venenatum* Nirenberg and *F. culmorum* (Wm.G. Sm.) Sacc. However, with the exception of *F. sporotrichioides*, the conidia of most species above-mentioned, differ by being more robust and often more pointed apically. *Fusarium transvaalense* differs from *F. sporotrichioides* by the absence of pyriform aerial conidia.

Two strains NRRL 13829 and NRRL 31008, previously identified as *F. brachygibbosum* Padwick showed different degrees of genetic similitude with the new species. While NRRL 31008 clustered within *F. transvaalense*, NRRL 13829 formed a clearly delimited sister lineage. Morphologically, *F. transvaalense* exhibits significant differences allowing its separation from *F. brachygibbosum*. Both species produce sporodochial conidia with similar septation and sizes; however, *F. brachygibbosum* commonly exhibits a bulge in the middle portion of the conidia (Padwick 1945), a feature not present in *F. transvaalense*. In addition, the latter species produces comparatively larger sporodochial conidia, when elements with the same degree of septation are compared; its chlamydospores are smaller, smooth-walled to markedly tuberculate and pigmented (7–8 µm vs. 10.7–15.3 µm, smooth-walled and hyaline in *F. brachygibbosum*) and has a distinctive colonial growth on OA, forming large, pustule-like hyphal tufts, a feature not reported for *F. brachygibbosum* (Padwick 1945).

Discussion

In this study, three new *Fusarium* spp. were introduced, isolated from rhizosphere soils of three native African shrubs in a protected savannah ecosystem deep inside the Kruger National Park, South Africa.

Some remarkable differences were noted regarding the distribution of the novel fungal species and their respective hosts on this particular site. For instance, *F. transvaalense*, which exhibited the greatest relative abundance, was found in high quantities from the rhizospheres of the three hosts sampled, showing a considerable genetic diversity. Interestingly, this species was only on the top of the catena, even when two of its hosts, *K. angustifolia* and *S. cordifolia*, were found and sampled either at the top and bottom sites. Similarly, *F. fredkrugeri* was recovered only from soils under *M. acuminata*, a host species which occurred only at the top location. In contrast, *F. convolutans* was found in the rhizosphere of *K. angustifolia*, occurring only at the bottom of the catena, while none of the three fungal species was found associated with *S. cordifolia* at the bottom of the site. Nevertheless, not being an objective of this work, it was not possible to categorically assign these new species to specific hosts or locations. Likely, these fungi could be in low abundance and thus not detectable using the current methods. However, plant species composition varies considerably through a catena ecosystem, in relation to the different soil characteristics, pH gradient and water availability, which also greatly influence microbial and animal biodiversity (Lareen et al. 2016; Mohammadi et al. 2017). However, the full patterns of variation between locations on this particular catena still need to be systematically assessed and compared. As evidenced

here, certain differences do exist between the soils at the upper and bottom locations of the Stevenson-Hamilton supersite, which might explain the fungal diversity variation observed here. The cation exchange capacity (CEC; capacity of a soil to hold exchangeable cations) varies considerably between sampling sites, basically depending on the proportion of sand versus clay content of each soil type (Ketterings et al. 2007; Van Zijl and Le Roux 2014). It is known that CEC greatly impacts the soil's ability to retain essential nutrients and prevents soil acidification (Ketterings et al. 2007). Nutrient content also increased from the top to the bottom of the slope which is consistent with the increase in CEC. Nutrient poor soils are also a driver of biological diversity and most likely influenced fungal diversity in these particular locations (Havlicek and Mitchell 2014, Mapelli et al. 2017).

The three *Fusarium* species, described here, were not associated with any visible symptomatology on their hosts. However, they cannot be ruled out as pathogens since they were not assessed for pathogenicity against the sampled plants nor any other putative host species at the same locations. Likewise, it is unknown if these fungi exert any beneficial or deleterious effect on their ecosystems. These are important unsolved questions that need further evaluation. However, as shown by phylogenetic analyses, each of the three new species was in close genetic proximity with well-known plant pathogenic *Fusarium* spp. on their respective species complexes, which could suggest a potential pathogenic role. *Fusarium convolutans* clustered within the FBSC, together with three known plant pathogenic *Fusarium* spp. i.e. *F. buharicum*, a pathogen of *Hibiscus cannabinus* L. and *Gossypium* L.; *F. sublunatum*, known to affect banana and *Theobroma cacao* L. in Central America (Gerlach and Nirenberg 1982, Leslie and Summerell 2006) and a newly discovered although unnamed phylogenetic species causing wilt, crown and root rot of *Hibiscus moscheutos* L. (Lupien et al. 2017). *Fusarium transvaalense* belonged to the FSAMSC, a genetically diverse group common in temperate and subtropical zones (Leslie and Summerell 2006). *Fusarium sambucinum*, the conserved type species of the genus (Gams et al. 1997) being an aggressive plant pathogen and one of the most important agents of potato dry rot (Peters et al. 2008); while the latter species and several others in the complex have been reported causing disease on diverse crops, including many cereals and fruits (Leslie and Summerell 2006).

Fusarium fredkrugeri is here recognised and formally proposed as a new species. Although the clade representing this taxon had already been identified as a distinct unnamed phylogenetic species by O'Donnell et al. (2000), it had not been given a formal description pending the collection of additional isolates. Two other African isolates previously determined to belong to this clade i.e. CBS 144210 from *Striga hermonthica* (Del.) Benth. in Madagascar and NRRL 26152 from an unknown substrate in Niger, were incorporated into the analyses, although the latter strain is not viable anymore (NRRL, pers. comm.), thus not available for morphological assessment. Strain CBS 144210, however, is known as a pathogen of the 'purple witchweed', a parasite plant common to sub-Saharan Africa and known to devastate *Sorghum bicolor* (L.) Moench and *Oryza sativa* L. plantations (O'Donnell et al. 2000; Yoshida et al. 2010). As previously demonstrated by O'Donnell et al. (2000), our phylogenetic results showed that

the clade comprising *F. fredkrugeri* and its sister species *F. dlamini* does not cluster within the main African core of species in the FFSC. Thus, despite the African origin of our isolates, the predicted biogeographic patterns did not match the observed phylogeny. It has been hypothesised that this should not be the result of genetic markers tracing different phylogenies, but the consequence of losing the phylogenetic signal due to saturated sites and introns (O'Donnell et al. 2000). However, the inclusion in our analysis of additional, highly informative and slowly evolving loci such as *RPB1* and *RPB2* yielded similar results, which points out the need to re-evaluate the phylogeographic arrangement of this important species complex including the vast new data generated during the last 20 years that challenges the established assumptions (Kvas et al. 2009; Walsh et al. 2010; O'Donnell et al. 2013; Laurence et al. 2015). Nevertheless, although rather unlikely, alternative factors such as anthropogenic dispersion of *F. fredkrugeri*, its host or additional invasive alternative hosts, cannot be rejected as an explanation for the discordance between biogeography and phylogenetic results. However, these scenarios are difficult to imagine given the characteristics of the sampled site, not being an agroecosystem but a protected, isolated zone, with minimal human intervention (Smit et al. 2013).

This study is a new example of how easily new *Fusarium* spp. can be found when mycological studies are directed to neglected natural ecosystems of minimal anthropogenic disturbance (Phan et al. 2004; Leslie and Summerell 2011; Summerell et al. 2011; Burgess 2014, Laurence et al. 2015). Although irrelevant for some researchers, finding and properly describing new species, regardless of whether they have little or no pathogenic or mycotoxigenic potential, is of utmost importance to improve our understanding on the diversity, biogeographic and phylogeographic patterns of such a complex and heterogeneous genus as *Fusarium*. In addition, this study remarks on the significance and need to further stimulate the exploration of conserved, non-manipulated natural environments (supersites) and their potential impact on biodiversity research on the fungal kingdom.

Acknowledgments

Todd J. Ward and James Swezey (Agricultural Research Service, Peoria, IL, USA) are thanked for providing strains. We kindly thank Kerry O'Donnell (Mycotoxin Prevention and Applied Microbiology Research Unit, Agricultural Research Service, US Department of Agriculture, Peoria, IL, USA) for providing DNA sequence datasets. Mercia Coetzee (Central University of Technology, Bloemfontein, South Africa) is thanked for her technical support in the field. Alejandra Giraldo (Westerdijk Fungal Biodiversity Institute, Utrecht, The Netherlands) is thanked for her assistance with fungal isolation. Eddie Riddell and Navashni Govender (SANParks) are acknowledged for their research support in the Kruger National Park. We also thank Konstanze Bensch (Mycobank curator) and Uwe Braun (Geobotanik und Botanischer Garten, Martin-Luther-Universität Halle-Wittenberg, Halle, Germany) for their help regarding Latin names.

References

- Aoki T, Smith JA, Mount LL, Geiser DM, O'Donnell K (2013) *Fusarium torreyae* sp. nov., a pathogen causing canker disease of Florida torreya (*Torreya taxifolia*), a critically endangered conifer restricted to northern Florida and southwestern Georgia. *Mycologia* 105: 312–319. <https://doi.org/10.3852/12-262>
- Aydogdu H, Asan A (2008) Airborne fungi in child day care centers in Edirne City, Turkey. *Environmental Monitoring and Assessment* 147: 423–444. <https://doi.org/10.1007/s10661-007-0130-4>
- Bent E, Kiekel P, Brenton R, Taylor DL (2011) Root-associated ectomycorrhizal fungi shared by various boreal forest seedlings naturally regenerating after a fire in interior Alaska and correlation of different fungi with host growth responses. *Applied and Environmental Microbiology* 77: 3351–3359. <https://doi.org/10.1128/AEM.02575-10>
- Brown DJ, Clayton MK, McSweeney K (2004) Potential terrain controls on soil color, texture contrast and grain-size deposition for the original catena landscape in Uganda. *Geoderma* 122: 51–72. <http://doi.org/10.1016/j.geoderma.2003.12.004>
- Burgess LW (2014) 2011 McAlpine Memorial Lecture – A love affair with *Fusarium*. *Australasian Plant Pathology* 43: 359–368. <https://doi.org/10.1007/s13313-013-0261-8>
- Carruthers J (2017) *National Park Science: A Century of Research in South Africa (Ecology, Biodiversity and Conservation)*. Cambridge University Press, 554 pp. <https://doi.org/10.1017/9781108123471>
- Crous PW, Verkley GJM, Groenewald JZ, Samson RA (2009) *Fungal Biodiversity*. CBS Laboratory Manual Series (CBS-KNAW Fungal Biodiversity Centre, Utrecht) 1: 1–270.
- Díaz Arias MM, Leandro LF, Munkvold GP (2013) Aggressiveness of *Fusarium* species and impact of root infection on growth and yield of soybeans. *Phytopathology* 103: 822–832. <https://doi.org/10.1094/PHYTO-08-12-0207-R>
- Fisher NL, Burgess LW, Toussoun TA, Nelson PE (1982) Carnation leaves as a substrate and for preserving cultures of *Fusarium* species. *Phytopathology* 72: 151–153. <https://doi.org/10.1094/Phyto-72-151>
- Fravel D, Olivain C, Alabouvette C (2003) *Fusarium oxysporum* and its biocontrol. *New Phytologist* 157: 493–502. <https://doi.org/10.1046/j.1469-8137.2003.00700.x>
- Gams W, Nirenberg HI, Seifert KA, Brayford D, Thrane U (1997) (1275) Proposal to conserve the name *Fusarium sambucinum* (Hyphomycetes). *Taxon* 46: 111–113. <https://doi.org/10.2307/1224298>
- Gerlach W, Nirenberg HI (1982) The genus *Fusarium* – a pictorial atlas. *Mitteilungen der Biologischen Bundesanstalt für Land- und Forstwirtschaft Berlin-Dahlem* 209: 1–406.
- Hargreaves SK, Williams RJ, Hofmöckel KS (2015) Environmental filtering of microbial communities in agricultural soil shifts with crop growth. *PLoS One* 30: e0134345. <https://doi.org/10.1371/journal.pone.0134345>
- Hassan Dar GH, Zargar MY, Beigh GM (1997) Biocontrol of *Fusarium* root rot in the common bean (*Phaseolus vulgaris* L.) by using symbiotic *Glomus mosseae* and *Rhizobium leguminosarum*. *Microbial Ecology* 34: 74–80. <https://doi.org/10.1007/s002489900036>

- Havlicek E, Mitchell EAD (2014) Soils supporting biodiversity. In: Dighton J, Krumins JA (Eds) *Interactions in Soil: Promoting Plant Growth, Biodiversity, Community and Ecosystems*. Springer, Dordrecht, 27–28. https://doi.org/10.1007/978-94-017-8890-8_2
- Herron DA, Wingfield MJ, Wingfield BD, Rodas CA, Marinowitz S, Steenkamp ET (2015) Novel taxa in the *Fusarium fujikuroi* species complex from *Pinus* spp. *Studies in Mycology* 80: 131–150. <https://doi.org/10.1016/j.simyco.2014.12.001>
- Idris HA, Labuschagne N, Korsten L (2007) Screening rhizobacteria for biological control of *Fusarium* root and crown rot of sorghum in Ethiopia. *Biological Control* 40: 97–106. <https://doi.org/10.1016/j.biocontrol.2006.07.017>
- Jumpponen A, Herrera J, Porras-Alfaro A, Rudgers J (2017) Biogeography of root-associated fungal endophytes. In: Tedersoo L (Ed.) *Biogeography of Mycorrhizal Symbiosis*. *Ecological Studies* 230 (Springer), 195–222. <https://doi.org/10.1007/978-3-319-56363-3>
- Katoh K, Standley DM (2013) MAFFT multiple sequence alignment software version 7: improvements in performance and usability. *Molecular Biology and Evolution* 30: 772–780. <https://doi.org/10.1093/molbev/mst010>
- Ketterings Q, Reid S, Rao R (2007) Cation Exchange Capacity (CEC), Agronomy Fact Sheet Series (22). Cornell University Cooperative Extension.
- Kvas M, Marasas WFO, Wingfield BD, Wingfield MJ, Steenkamp ET (2009) Diversity and evolution of *Fusarium* species in the *Gibberella fujikuroi* complex. *Fungal Diversity* 34: 1–21.
- Lareen A, Burton F, Schäfer P (2016) Plant root-microbe communication in shaping root microbiomes. *Plant Molecular Biology* 90: 575–587. <https://doi.org/10.1007/s11103-015-0417-8>
- Larkin RP, Hopkins DL, Martin FN (1993) Effect of successive watermelon plantings on *Fusarium oxysporum* and other microorganisms in soils suppressive and conducive to Fusarium wilt of watermelon. *Phytopathology* 83: 1097–1105. <https://doi.org/10.1094/Phyto-83-1097>.
- Laurence MH, Walsh JL, Shuttleworth LA, Robinson DM, Johansen RM, Petrovic T, Vu TTH, Burgess LW, Summerell BA, Liew ECY (2015) Six novel species of *Fusarium* from natural ecosystems in Australia. *Fungal Diversity* 77: 349–366. <https://doi.org/10.1007/s13225-015-0337-6>
- LeBlanc N, Essarioui A, Kinkel L, Kistler HC (2017) Phylogeny, plant species, and plant diversity influence carbon use phenotypes among *Fusarium* populations in the rhizosphere microbiome. *Phytobiomes* 1: 150–157. <https://doi.org/10.1094/PBIOMES-06-17-0028-R>
- Leslie JF, Summerell BA (2006) *The Fusarium laboratory manual*. Blackwell Publishing, Ames. 1–388. <https://doi.org/10.1002/9780470278376>
- Leslie JF, Summerell BA (2011) In search of new *Fusarium* species. *Plant Breeding and Seed Science* 63: 94–101. <https://doi.org/10.2478/v10129-011-0020-3>
- Li W, Cowley A, Uludag M, Gur T, McWilliam H, Squizzato S, Park YM, Buso N, Lopez R (2015) The EMBL-EBI bioinformatics web and programmatic tools framework. *Nucleic Acids Research* 43: W580–584. <https://doi.org/10.1093/nar/gkv279>
- Lupien SL, Dugan FM, Ward KM, O'Donnell K (2017) Wilt, crown, and root rot of common rose mallow (*Hibiscus moscheutos*) caused by a novel *Fusarium* sp. *Plant Disease* 101: 354–358. <https://doi.org/10.1094/PDIS-05-16-0717-RE>

- Mapelli F, Marasco R, Fusi M, Scaglia B, Tsiamis G, Rolli E, Fodelianakis S, Bourtzis K, Ventura S, Tambone F, Adani F, Borin S, Daffonchio D (2017) The stage of soil development modulates rhizosphere effect along a High Arctic desert chronosequence. *The ISME Journal*: 1–11. <https://doi.org/10.1038/s41396-017-0026-4>
- Marasas WFO, Nelson PE, Toussoun TA (1985) *Fusarium dlamini*, a new species from Southern Africa. *Mycologia* 77: 971–975. <https://doi.org/10.2307/3793311>
- Mason-Gamer R, Kellogg E (1996) Testing for phylogenetic conflict among molecular data sets in the tribe Triticeae (Gramineae). *Systematic Biology* 45: 524–545. <https://doi.org/10.1093/sysbio/45.4.524>
- Miller MA, Pfeiffer W, Schwartz T (2012) The CIPRES science gateway: enabling high-impact science for phylogenetics researchers with limited resources. In: Proceedings of the 1st Conference of the Extreme Science and Engineering Discovery Environment: Bridging from the extreme to the campus and beyond, Association for Computing Machinery, Chicago, USA, 1–8. <https://doi.org/10.1145/2335755.2335836>
- Mohammadi MF, Jalali SW, Kooch Y, Theodose TA (2017) Tree species composition, biodiversity and regeneration in response to catena shape and position in a mountain forest. *Scandinavian Journal of Forest Research* 32: 80–90. <https://doi.org/10.1080/02827581.2016.1193624>
- Mommer L, Kirkegaard J, van Ruijven J (2016) Root-root interactions: towards a rhizosphere framework. *Trends in Plant Science* 21: 209–217. <https://doi.org/10.1016/j.tplants.2016.01.009>
- Moussa TAA, Al-Zahrani HS, Kadasa NMS, Ahmed SA, de Hoog GS, Al-Hatmi AMS (2017) Two new species of the *Fusarium fujikuroi* species complex isolated from the natural environment. *Antonie Van Leeuwenhoek* 110: 819–832. <https://doi.org/10.1007/s10482-017-0855-1>
- Nelson PE, Dignani MC, Anaissie EJ (1994) Taxonomy, biology, and clinical aspects of *Fusarium* species. *Clinical Microbiology Reviews* 7: 479–504. <https://doi.org/10.1128/CMR.7.4.479>
- Nirenberg HI (1976) Untersuchungen über die morphologische und biologische Differenzierung in der *Fusarium*-Sektion Liseola. *Mitteilungen der Biologischen Bundesanstalt für Land- und Forstwirtschaft Berlin-Dahlem* 169: 1–117. <https://doi.org/10.1002/jpln.19771400220>
- Nylander JAA (2004) MrModeltest v2. Program distributed by the author. Evolutionary Biology Centre, Uppsala University.
- O'Donnell K, Kistler HC, Cigelnik E, Ploetz RC (1998) Multiple evolutionary origins of the fungus causing Panama disease of banana: concordant evidence from nuclear and mitochondrial gene genealogies. *Proceedings of the National Academy of Sciences of the United States of America* 95: 2044–2049. <https://doi.org/10.1073/pnas.95.5.2044>
- O'Donnell K, Nirenberg HI, Aoki T, Cigelnik E (2000) A multigene phylogeny of the *Gibberella fujikuroi* species complex: detection of additional phylogenetically distinct species. *Mycoscience* 41: 61–78. <https://doi.org/10.1007/BF02464387>
- O'Donnell K, Rooney AP, Proctor RH, Brown DW, McCormick SP, Ward TJ, Frandsen RJ, Lysøe E, Rehner SA, Aoki T, Robert VA, Crous PW, Groenewald JZ, Kang S, Geiser DM

- (2013) Phylogenetic analyses of RPB1 and RPB2 support a middle Cretaceous origin for a clade comprising all agriculturally and medically important fusaria. *Fungal Genetics and Biology* 52: 20–31. <https://doi.org/10.1016/j.fgb.2012.12.004>
- O'Donnell K, Sutton DA, Rinaldi MG, Gueidan C, Crous PW, Geiser DM (2009) Novel multilocus sequence typing scheme reveals high genetic diversity of human pathogenic members of the *Fusarium incarnatum* – *F. equiseti* and *F. chlamydosporum* species complexes within the United States. *Journal of Clinical Microbiology* 47: 3851–3861. <https://doi.org/10.1128/JCM.01616-09>
- O'Donnell K, Sutton DA, Rinaldi MG, Sarver BA, Balajee SA, Schroers HJ, Summerbell RC, Robert VA, Crous PW, Zhang N, Aoki T, Jung K, Park J, Lee YH, Kang S, Park B, Geiser DM (2010) Internet-accessible DNA sequence database for identifying fusaria from human and animal infections. *Journal of Clinical Microbiology* 48: 3708–3718. <https://doi.org/10.1128/JCM.00989-10>
- Padwick GW (1945) Notes on Indian fungi III. *Mycological Papers* 12: 1–15.
- Pal KK, Tilak KVBR, Saxena AK, Dey R, Singh CS (2001) Suppression of maize root diseases caused by *Macrophomina phaseolina*, *Fusarium moniliforme* and *Fusarium graminearum* by plant growth promoting rhizobacteria. *Microbiological Research* 156: 209–223. <https://doi.org/10.1078/0944-5013-00103>
- Perlot J, Choi B, Spellberg B (2007) Nosocomial fungal infections: epidemiology, diagnosis, and treatment. *Medical Mycology* 4: 321–346. <https://doi.org/10.1080/13693780701218689>
- Peters JC, Lees AK, Cullen DW, Sullivan L, Strouda GP, Cunnington AC (2008) Characterization of *Fusarium* spp. responsible for causing dry rot of potato in Great Britain. *Plant Pathology* 57: 262–271. <https://doi.org/10.1111/j.1365-3059.2007.01777.x>
- Phan HT, Burgess LW, Summerell BA, Bullock S, Liew EY, Smith-White JL, Clarkson JR (2004) *Gibberella gaditjirrii* (*Fusarium gaditjirrii*) sp. nov., a new species from tropical grasses in Australia. *Studies in Mycology* 50: 261–272.
- Philippot L, Raaijmakers JM, Lemanceau P, Van Der Putten WH (2013) Going back to the roots: the microbial ecology of the rhizosphere. *Nature Reviews Microbiology* 11: 789–799. <https://doi.org/10.1038/nrmicro3109>
- Pinheiro AC, Macedo MF, Jurado V, Saiz-Jimenez C, Viegas C, Brandão J, Rosado L (2011) Mould and yeast identification in archival settings: preliminary results on the use of traditional methods and molecular biology options in Portuguese archives. *International Biodegradation & Biodegradation* 65: 619–627. <https://doi.org/10.1016/j.ibiod.2011.02.008>
- Posada D, Crandall KA (1998) MODELTEST: testing the model of DNA substitution. *Bioinformatics* 14: 817–818. <https://doi.org/10.1093/bioinformatics/14.9.817>
- Rayner RW (1970) *A Mycological Colour Chart*. CMI and British Mycological Society, Kew, Surrey, 34 pp.
- Ronquist F, Huelsenbeck JP (2003) MrBayes 3: Bayesian phylogenetic inference under mixed models. *Bioinformatics* 19: 1572–1574. <https://doi.org/10.1093/bioinformatics/btg180>
- Ruano-Rosa D, Prieto P, Rincón AM, Gómez-Rodríguez MV, Valderrama R, Barroso JB, Mercado-Blanco J (2016) Fate of *Trichoderma harzianum* in the olive rhizosphere: time course of the root colonization process and interaction with the fungal pathogen *Verticillium dahliae*. *BioControl* 61: 269–282. <https://doi.org/10.1007/s10526-015-9706-z>

- Sandoval-Denis M, Guarnaccia V, Polizzi G, Crous PW (2018) Symptomatic *Citrus* trees reveal a new pathogenic lineage in *Fusarium* and two new *Neocosmospora* species. *Persoonia* 40: 1–25. <https://doi.org/10.3767/persoonia.2018.40.01>
- Saravanakumar K, Fan L, Fu K, Yu C, Wang M, Xia H, Sun J, Li Y, Chen J (2016) Cellulase from *Trichoderma harzianum* interacts with roots and triggers induced systemic resistance to foliar disease in maize. *Scientific Reports* 6: 35543. <https://doi.org/10.1038/srep35543>
- Sasse J, Martinoia E, Northen T (2018) Feed your friends: do plant exudates shape the root microbiome? *Trends in Plant Science*. 23: 25–41. <https://doi.org/10.1016/j.tplants.2017.09.003>
- Schippers B, Bakker AW, Bakker PAHM (1987) Interactions of deleterious and beneficial rhizosphere microorganisms and the effect of cropping practices. *Annual Review of Phytopathology* 25: 339–358. <https://doi.org/10.1146/annurev.py.25.090187.002011>
- Smit IPJ, Riddell ES, Cullum C, Petersen R (2013) Kruger National Park research supersites: establishing long-term research sites for cross-disciplinary, multiscaled learning. *Koedoe – African Protected Area Conservation and Science* 55: Art. 1107 <https://doi.org/10.4102/koedoe.v55i1.1107>
- Stamatakis A (2014) RAxML version 8: a tool for phylogenetic analysis and post-analysis of large phylogenies. *Bioinformatics* 30: 1312–1313. <https://doi.org/10.1093/bioinformatics/btu033>
- Summerell B, Leslie J, Liew E, Laurence M, Bullock S, Petrovic T, Bentley AR, Howard CG, Peterson SA, Walsh JL, Burgess LW (2011) *Fusarium* species associated with plants in Australia. *Fungal Diversity* 46: 1–27. <https://doi.org/10.1007/s13225-010-0075-8>
- Van Zijl G, Le Roux P (2014) Creating a conceptual hydrological soil response map for the Stevenson Hamilton Research Supersite, Kruger National Park, South Africa. *Water SA* 40: 331–336. <http://doi.org/10.4314/wsa.v40i2.15>
- Visioli G, D’Egidio S, Sanangelantoni AM (2014) The bacterial rhizobiome of hyperaccumulators: future perspectives based on omics analysis and advanced microscopy. *Frontiers in Plant Science* 5: 752. <https://doi.org/10.3389/fpls.2014.00752>
- Walsh J, Laurence M, Liew E, Sangalang A, Burgess L, Summerell B, Petrovic T (2010) *Fusarium*: two endophytic novel species from tropical grasses of northern Australia. *Fungal Diversity* 44:149–159. <https://doi.org/10.1007/s13225-010-0035-3>
- Wiens JJ (1998) Testing phylogenetic methods with tree congruence: phylogenetic analysis of polymorphic morphological characters in phrynosomatid lizards. *Systematic Biology* 47: 427–444. <https://doi.org/10.1080/106351598260806>
- Woudenberg JHC, Aveskamp MM, De Gruyter J, Spiers AG, Crous PW (2009) Multiple *Didymella* teleomorphs are linked to the *Phoma clematidina* morphotype. *Persoonia* 22: 56–62. <https://doi.org/10.3767/003158509X427808>
- Yoshida S, Maruyama S, Nozaki H, Shirasu K (2010) Horizontal gene transfer by the parasitic plant *Striga hermonthica*. *Science* 328: 1128. <https://doi.org/10.1126/science.1187145>
- Zachow C, Berg C, Müller H, Meincke R, Komon-Zelazowska M, Druzhinina IZ, Kubicek CP, Berg G (2009) Fungal diversity in the rhizosphere of endemic plant species of Tenerife (Canary Islands): relationship to vegetation zones and environmental factors. *The ISME Journal* 3: 79–92. <https://doi.org/10.1038/ismej.2008.87>
- Zakaria L, Ning CH (2013) Endophytic *Fusarium* spp. from roots of lawn grass (*Axonopus compressus*). *Tropical Life Sciences Research* 24: 85–90.